ANNALS OF GEOPHYSICS, 66, 2023; doi:10.4401/ag-8882

SUPPLEMENT TO

CRUSTAL ANISOTROPY FROM THE BIREFRINGENCE OF P-TO-S CONVERTED WAVES: BIAS ASSOCIATED WITH P-WAVE ANISOTROPY

Jeffrey Park[1], Xiaoran Chen[2] and Vadim Levin[2]

[1] Department of Earth and Planetary Sciences, Yale University, New Haven CT, USA
[2] Department of Earth and Planetary Sciences, Rutgers University, Piscataway NJ, USA

Keywords: Seismic anisotropy; Receiver functions; Shear-wave splitting; Crustal structure; Moho discontinuity

This supplement presents receiver function estimates from synthetic seismogram simulations of P-wave coda for the anisotropic crustal models enumerated in Figure 1 and Figure 11 of the main text. We use synthetic P coda from 471 earthquake locations during 1997–2005, relative to GSN station RAYN (Ar Rayn, Saudi Arabia). The RF traces are migrated by a moving-window algorithm discussed in Park and Levin [2016b] for a target depth of 40 km, which is the Moho depth of the crustal models. Two figures per model are shown below. One plot displays back-azimuth sweeps of migrated radial and transverse receiver functions (RFs). A second plot displays the harmonic regression of the RFs with the linear combination of radial and transverse RFs predicted by first-order theory for hexagonal anisotropic models and dipping interfaces, as well as the conjugate ("Unmodelled") linear combination, see Park and Levin [2016a].

Several key features should be noted in the plots. First, the RFs for surface layers that contain anisotropy, particularly with a tilted axis of symmetry, have non-zero harmonic terms at the free surface. Such a feature is also found in Ps converted phases from a dipping interface between isotropic layers; it cannot be used to distinguish dipping layers from tilted-axis anisotropy. Second, note that the birefringence that Moho Ps phases suffer while travelling through anisotropic crust will generate a four-lobed term in the harmonic regression only for shear anisotropy (Backus parameter E), see Figure S10, not compressional (Backus parameter B), see Figure S12.

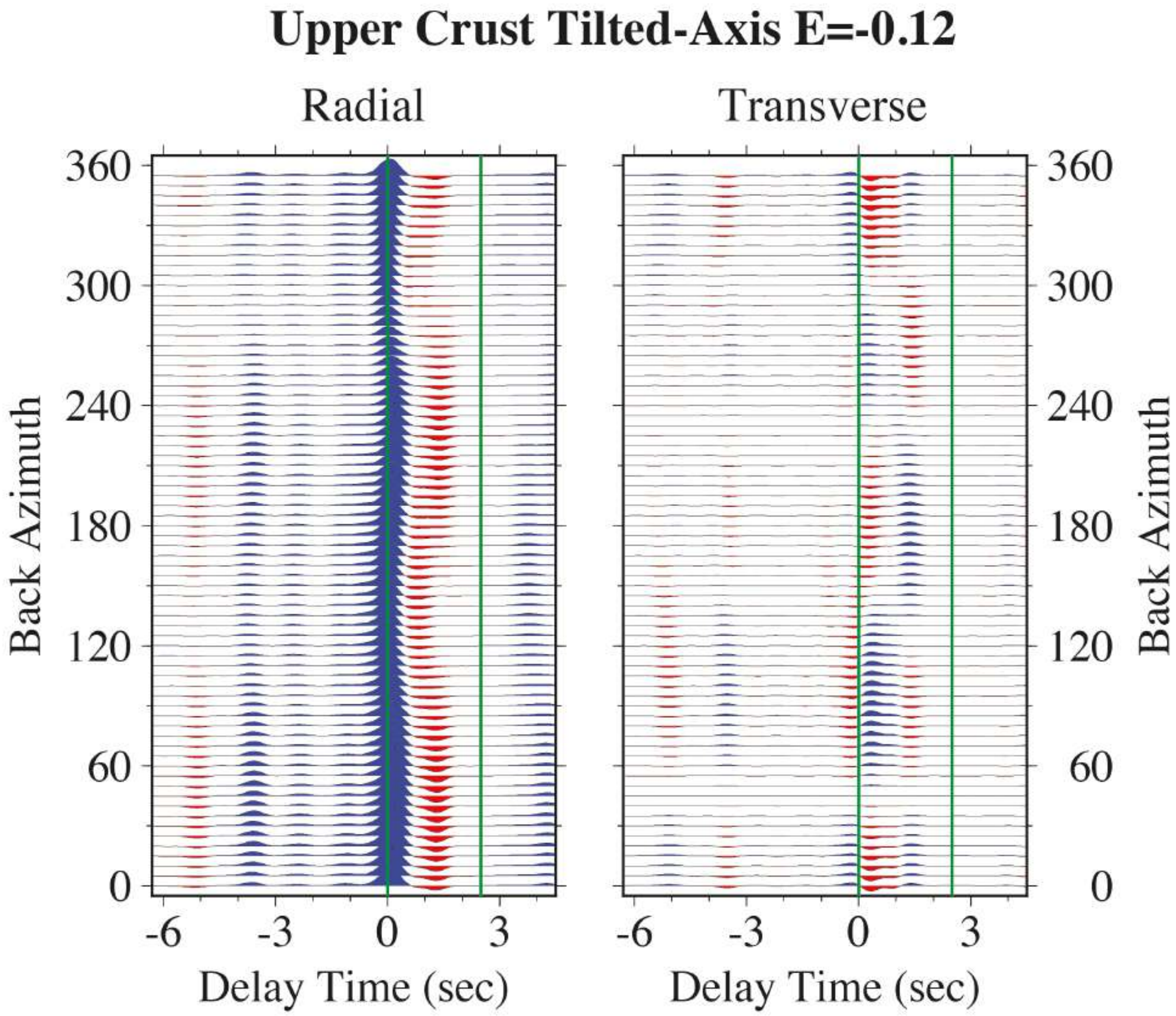

Figure S1. Back-azimuth receiver-function sweeps for synthetic seismograms in a 40-km crust with shear anisotropy E=-0.12 (12% peak-to-peak S anisotropy) with a slow symmetry axis with 45° tilt in the uppermost 10-km layer.

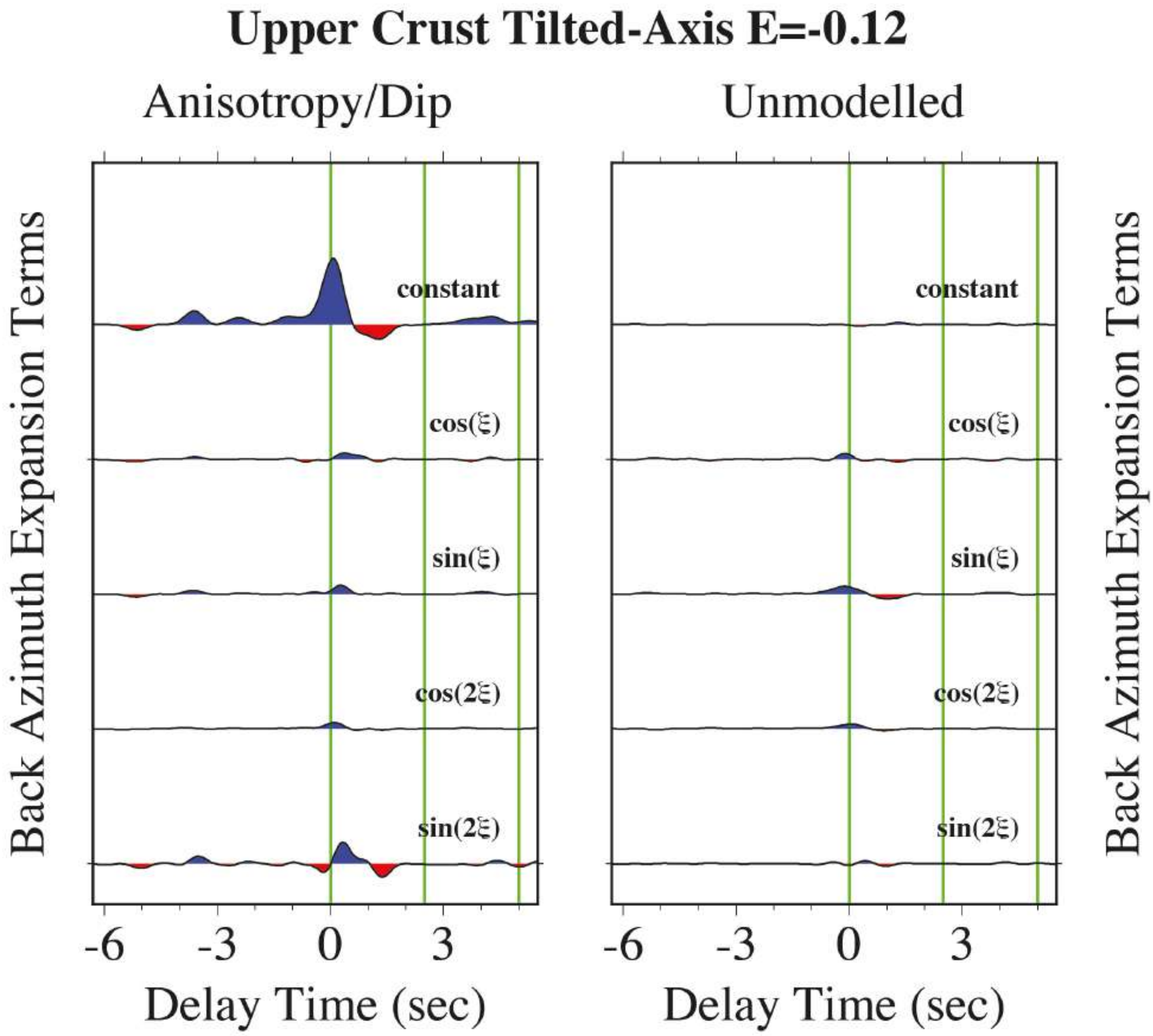

Figure S2. Harmonic terms of back azimuth ξ fit by least-squares in the frequency domain to receiver-functions estimated from synthetic seismograms in a 40-km crust with shear anisotropy E=-0.12 (12% peak-to-peak S anisotropy) with a slow symmetry axis with 45° tilt in the uppermost 10-km layer.

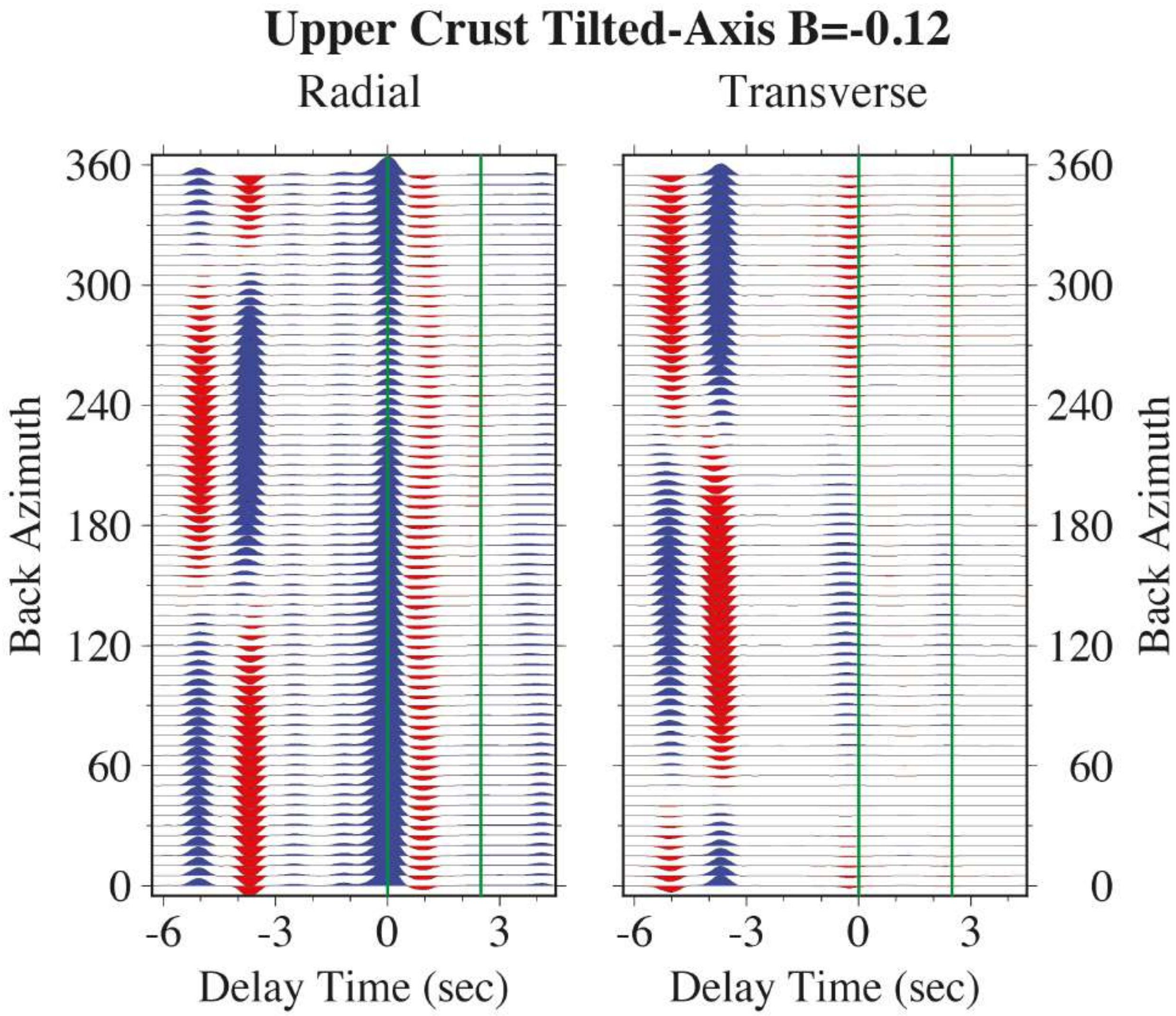

Figure S3. Back-azimuth receiver-function sweeps for synthetic seismograms in a 40-km crust with compressional anisotropy B=-0.12 (12% peak-to-peak P anisotropy) with a slow symmetry axis with 45° tilt in the uppermost 10-km layer.

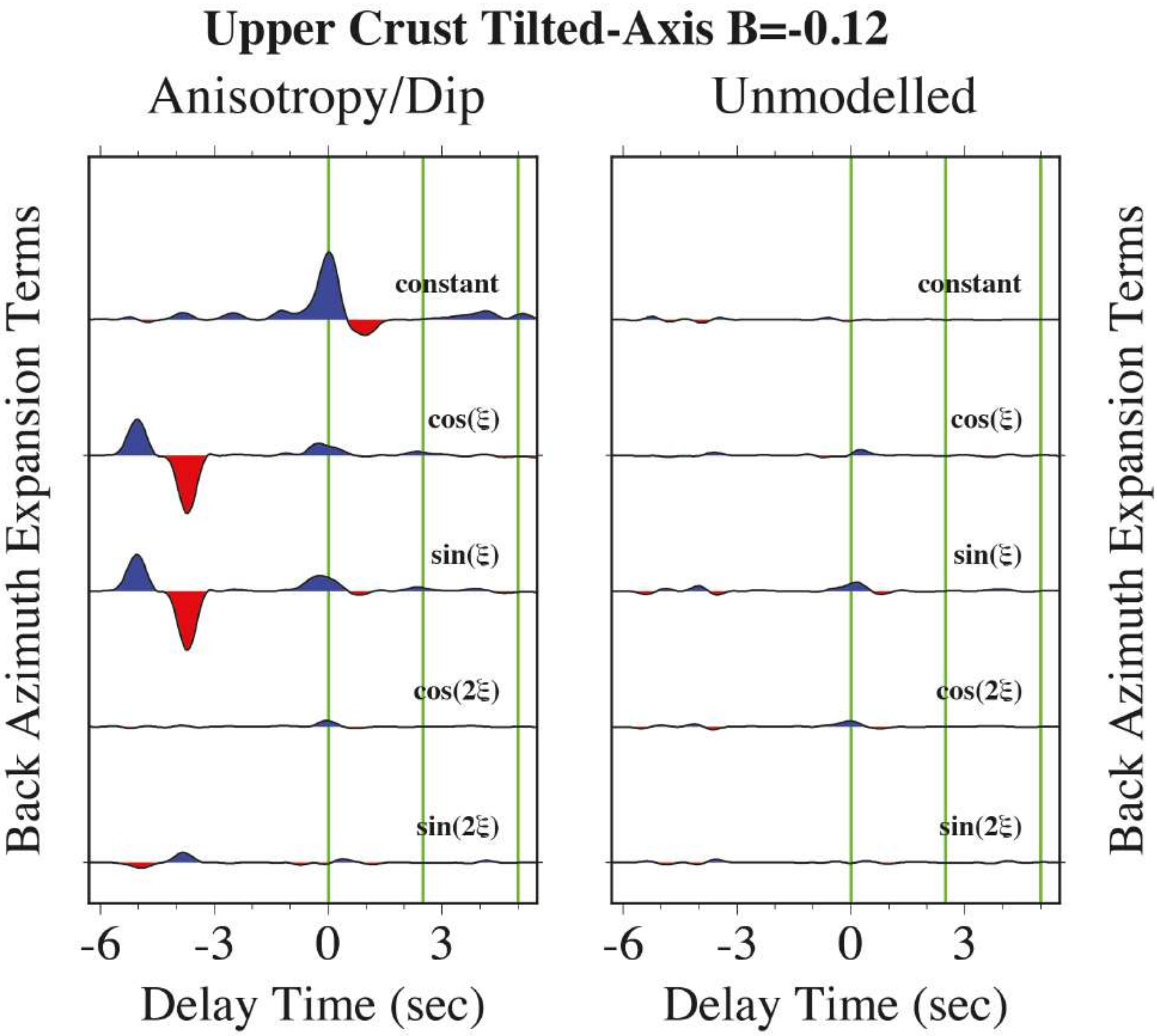

Figure S4. Harmonic terms of back azimuth ξ fit by least-squares in the frequency domain to receiver-functions estimated from synthetic seismograms in a 40-km crust with compressional anisotropy B=-0.12 (12% peak-to-peak P anisotropy) with a slow symmetry axis with 45° tilt in the uppermost 10-km layer.

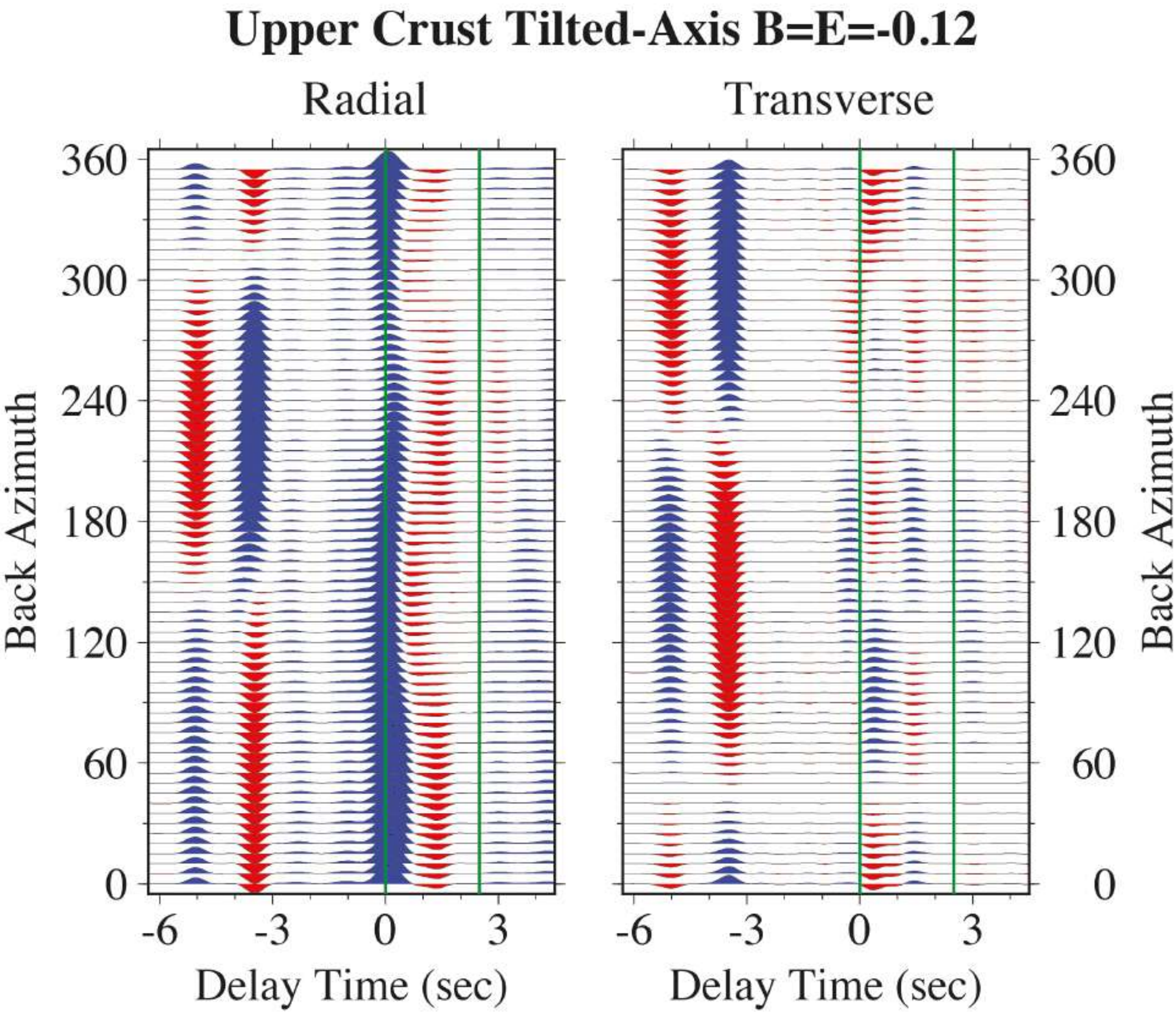

Figure S5. Back-azimuth receiver-function sweeps for synthetic seismograms in a 40-km crust with mixed anisotropy B=E=-0.12 (12% peak-to-peak P and S anisotropy) with a slow symmetry axis with 45° tilt in the uppermost 10-km layer.

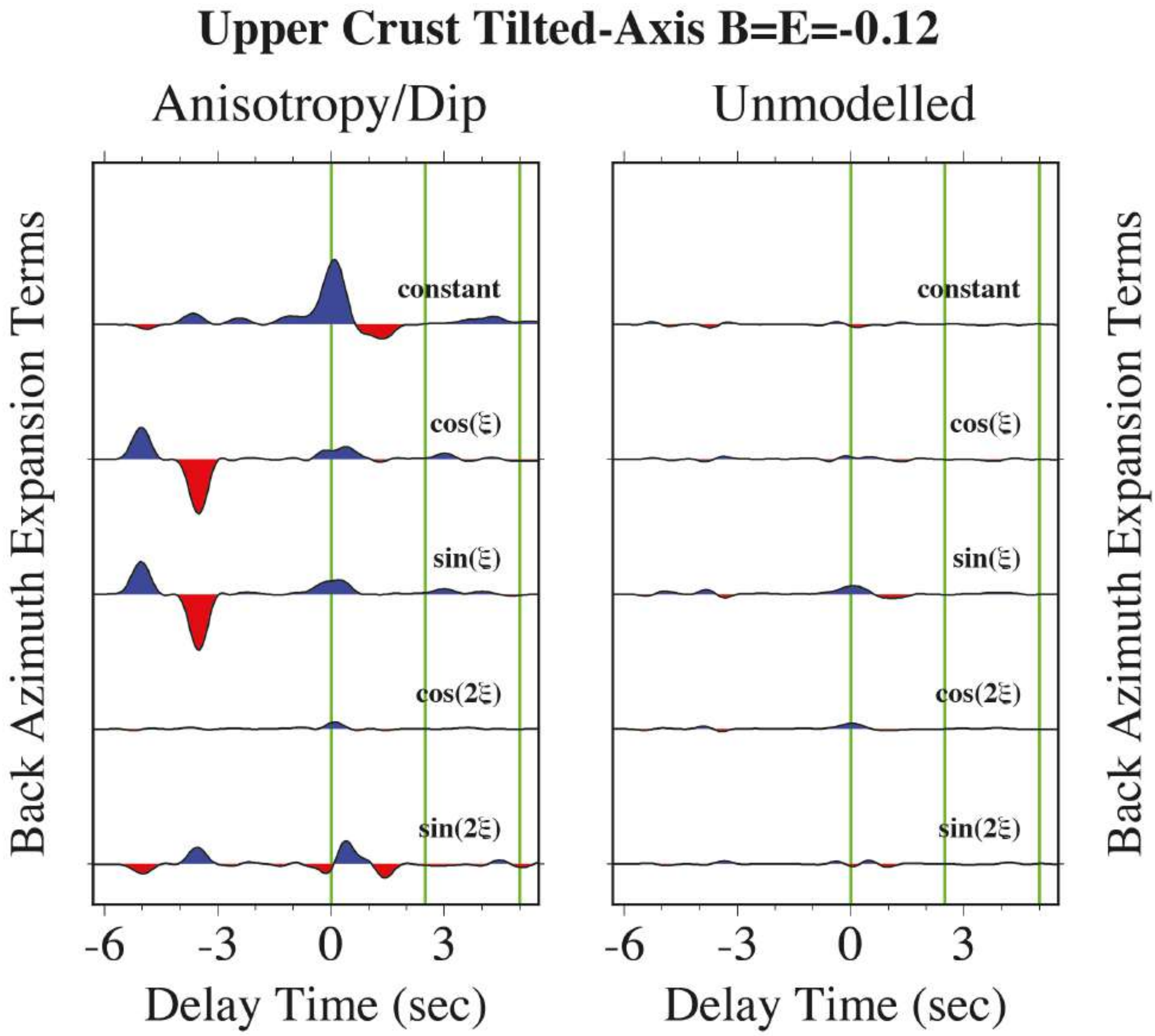

Figure S6. Harmonic terms of back azimuth ξ fit by least-squares in the frequency domain to receiver-functions estimated from synthetic seismograms in a 40-km crust with mixed anisotropy B=E=-0.12 (12% peak-to-peak P and S anisotropy) with a slow symmetry axis with 45° tilt in the uppermost 10-km layer.

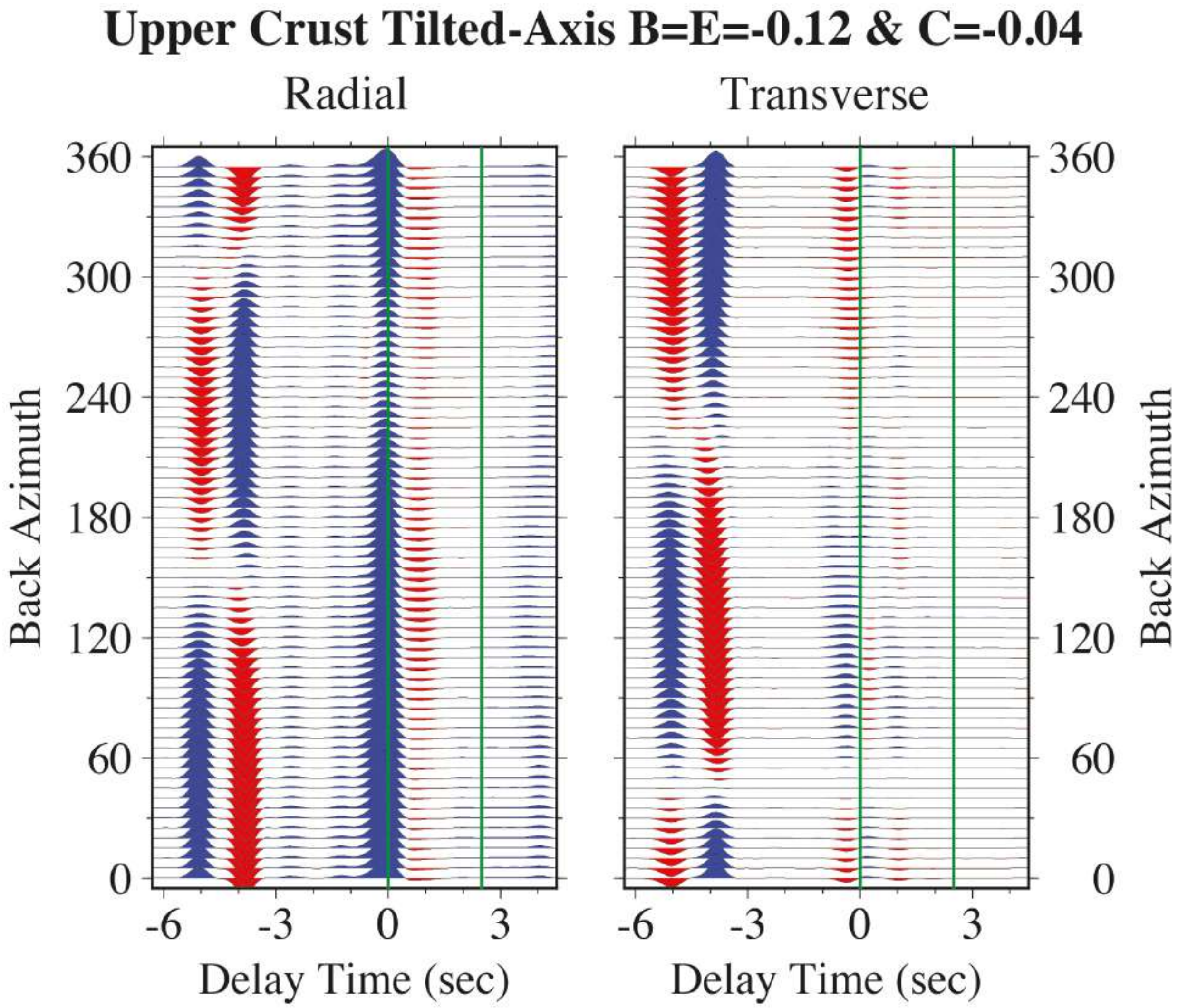

Figure S7. Back-azimuth receiver-function sweeps for synthetic seismograms in a 40-km crust with mixed anisotropy B=E=-0.12 and C=-0.04 with a slow symmetry axis with 45° tilt in the uppermost 10-km layer. This corresponds to 12% peak-to-peak elliptical P and S anisotropy, plus a cos 4ξ wavespeed variation consistent with Brownlee et al (2017).

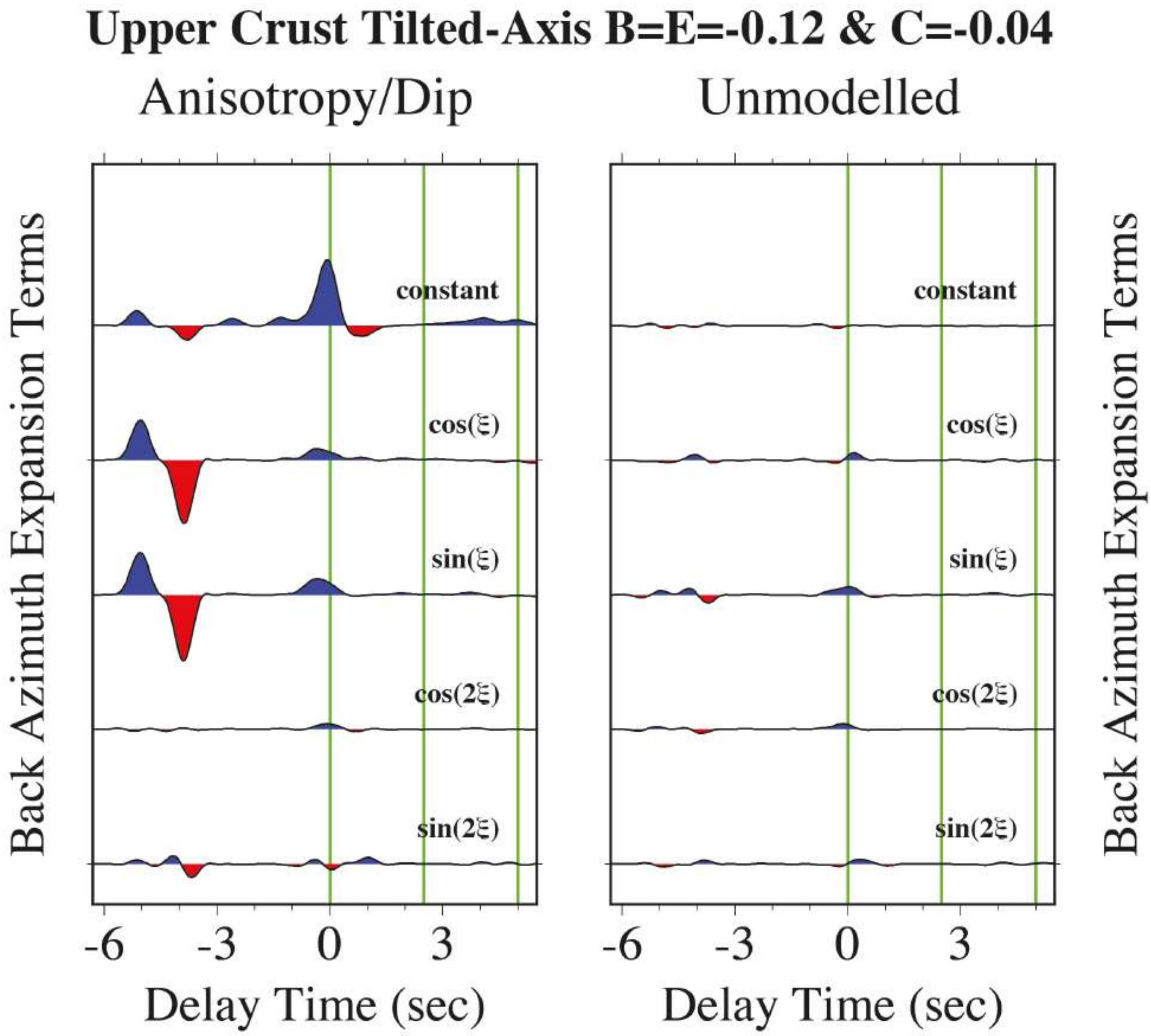

Figure S8. Harmonic terms of back azimuth ξ fit by least-squares in the frequency domain to receiver-functions estimated from synthetic seismograms in a 40-km crust with mixed anisotropy B=E=-0.12 and C=-0.04 with a slow symmetry axis with 45° tilt in the uppermost 10-km layer. This corresponds to 12% peak-to-peak elliptical P and S anisotropy, plus a cos 4ξ wavespeed variation consistent with Brownlee et al (2017).

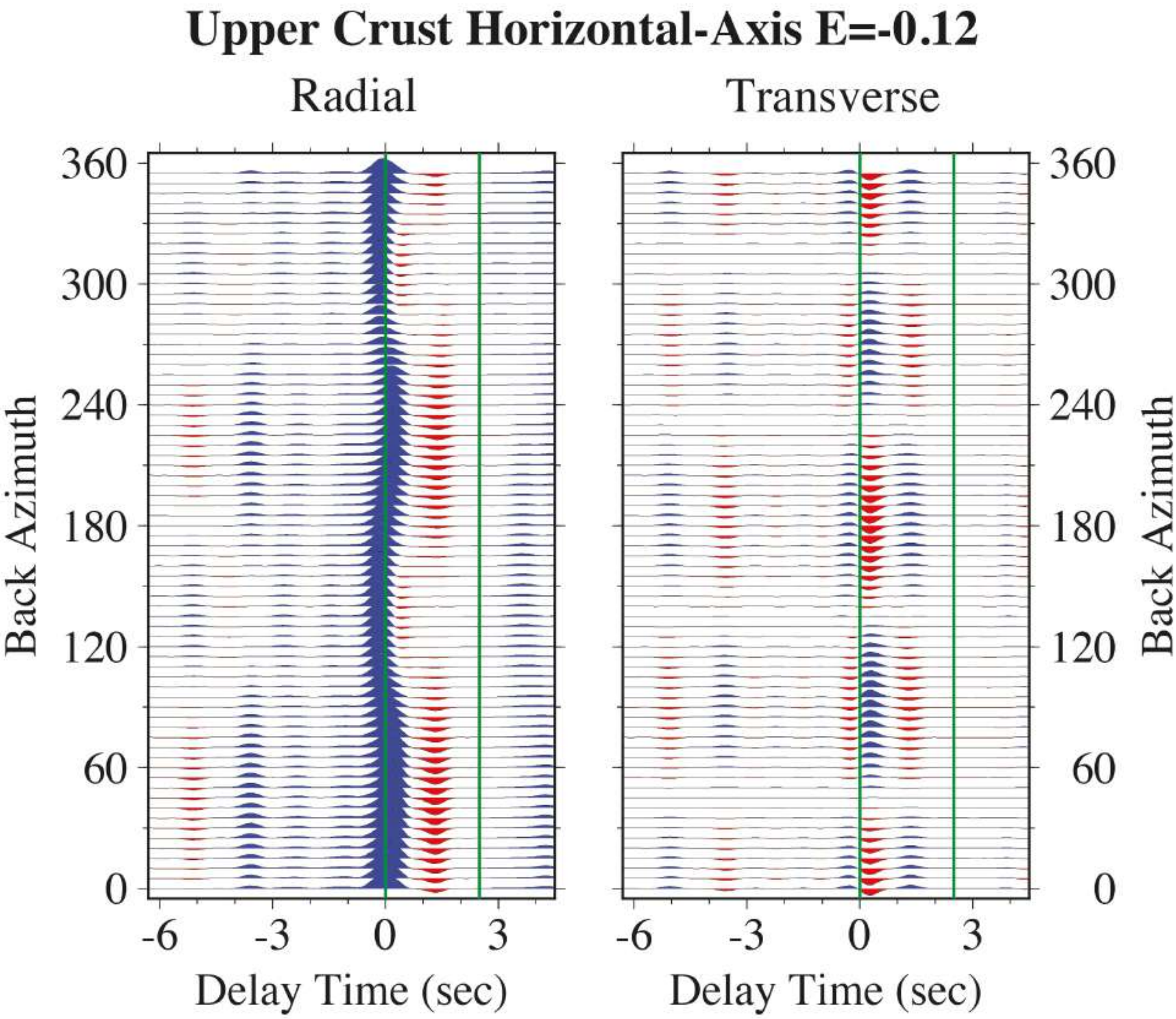

Figure S9. Back-azimuth receiver-function sweeps for synthetic seismograms in a 40-km crust with shear anisotropy E=-0.12 (12% peak-to-peak S anisotropy) with a horizontal slow symmetry axis in the uppermost 10-km layer.

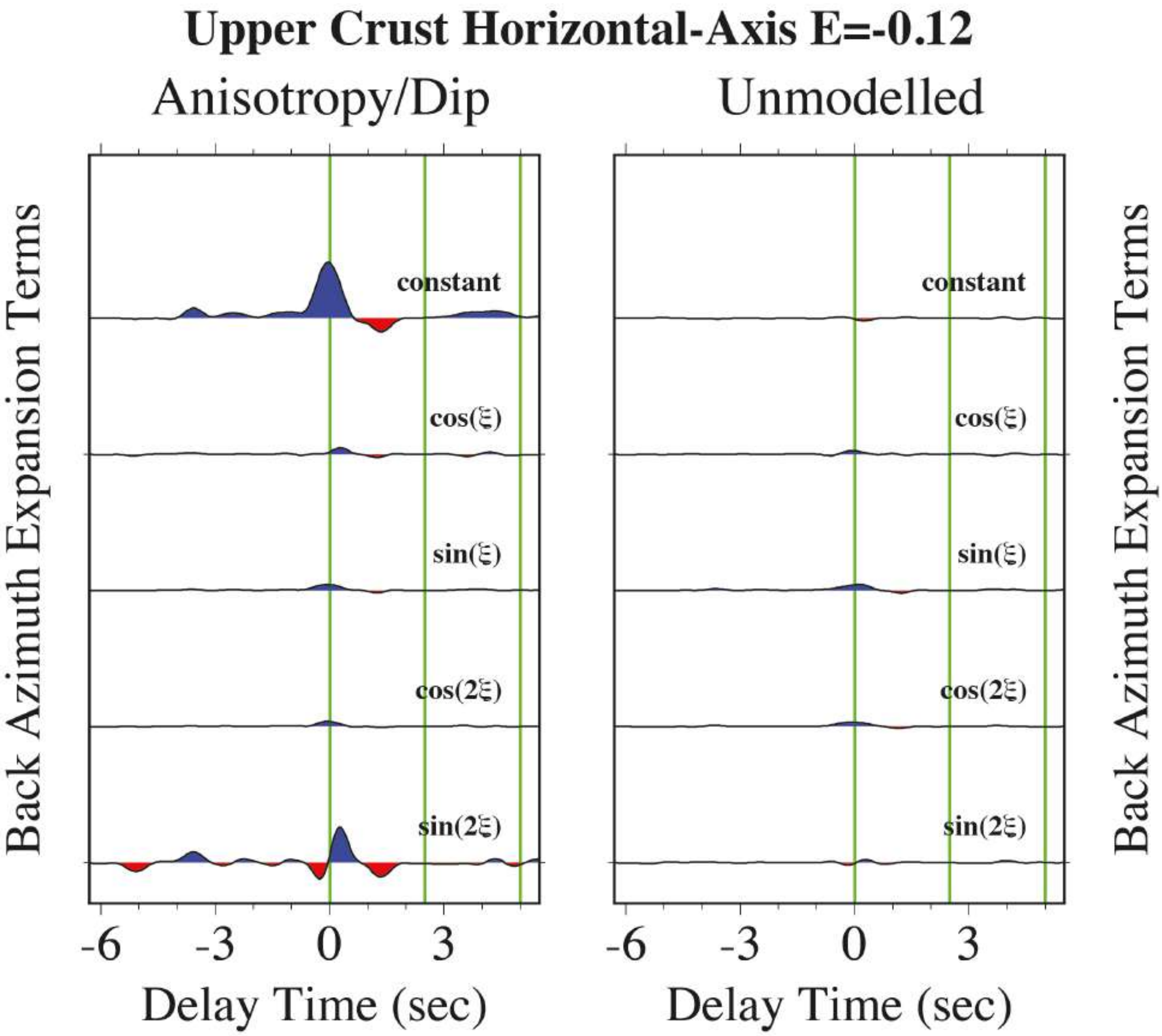

Figure S10. Harmonic terms of back azimuth ξ fit by least-squares in the frequency domain to receiver-functions estimated from synthetic seismograms in a 40-km crust with shear anisotropy E=-0.12 (12% peak-to-peak S anisotropy) with a horizontal slow symmetry axis in the uppermost 10-km layer.

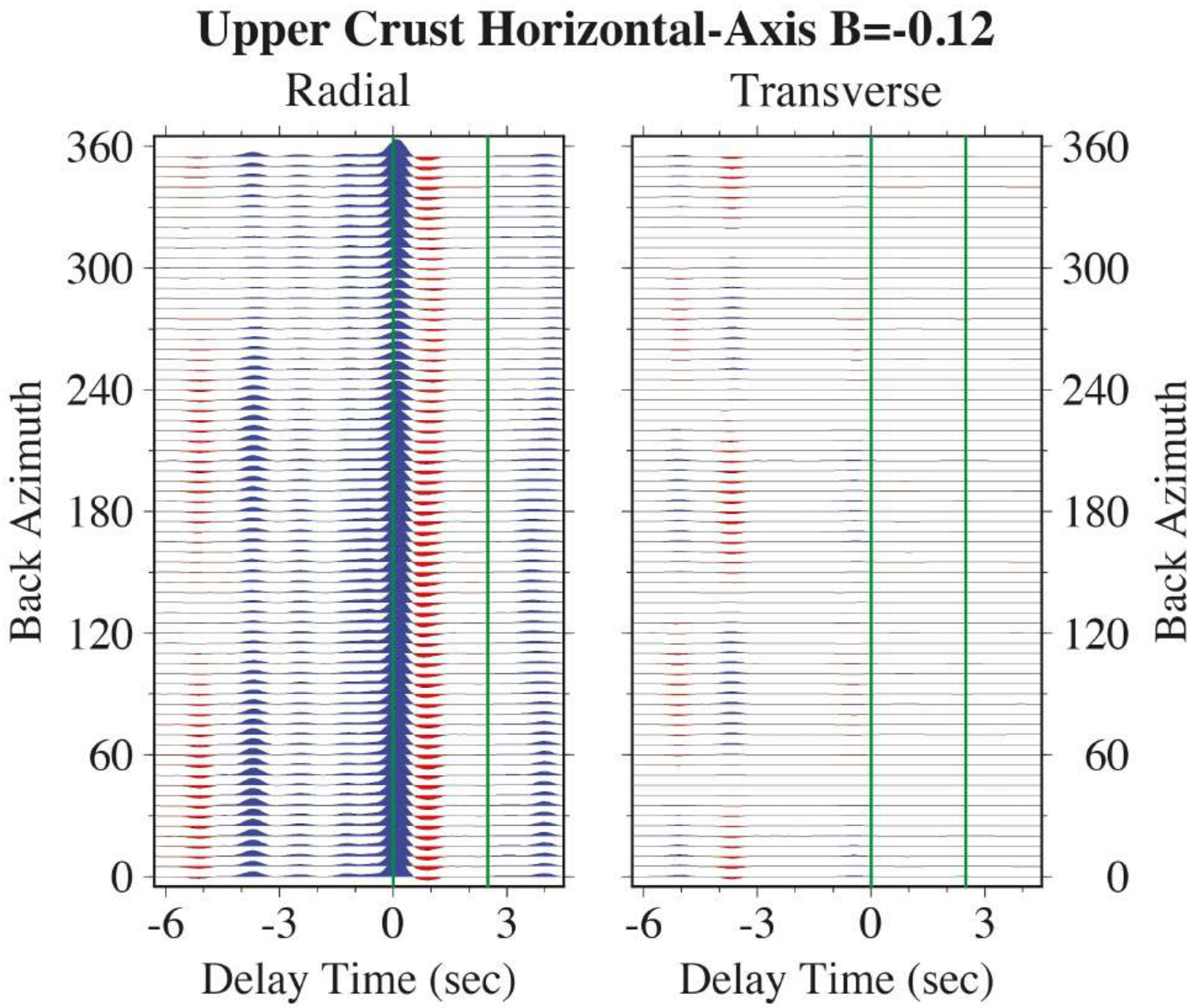

Figure S11. Back-azimuth receiver-function sweeps for synthetic seismograms in a 40-km crust with compressional anisotropy B=-0.12 (12% peak-to-peak P anisotropy) with a horizontal slow symmetry axis in the uppermost 10-km layer.

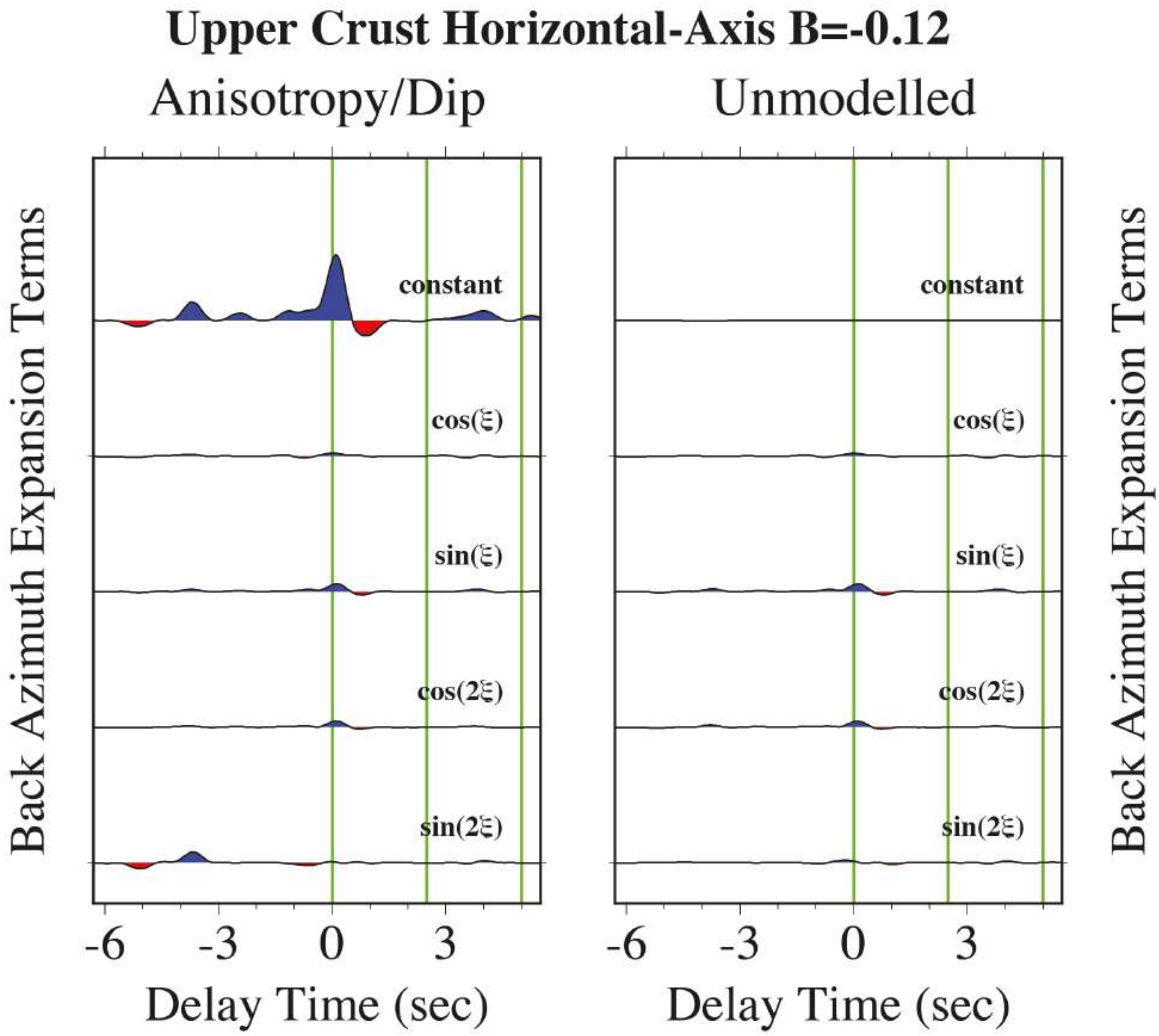

Figure S12. Harmonic terms of back azimuth ξ fit by least-squares in the frequency domain to receiver-functions estimated from synthetic seismograms in a 40-km crust with compressional anisotropy B=-0.12 (12% peak-to-peak P anisotropy) with a horizontal slow symmetry axis in the uppermost 10-km layer.

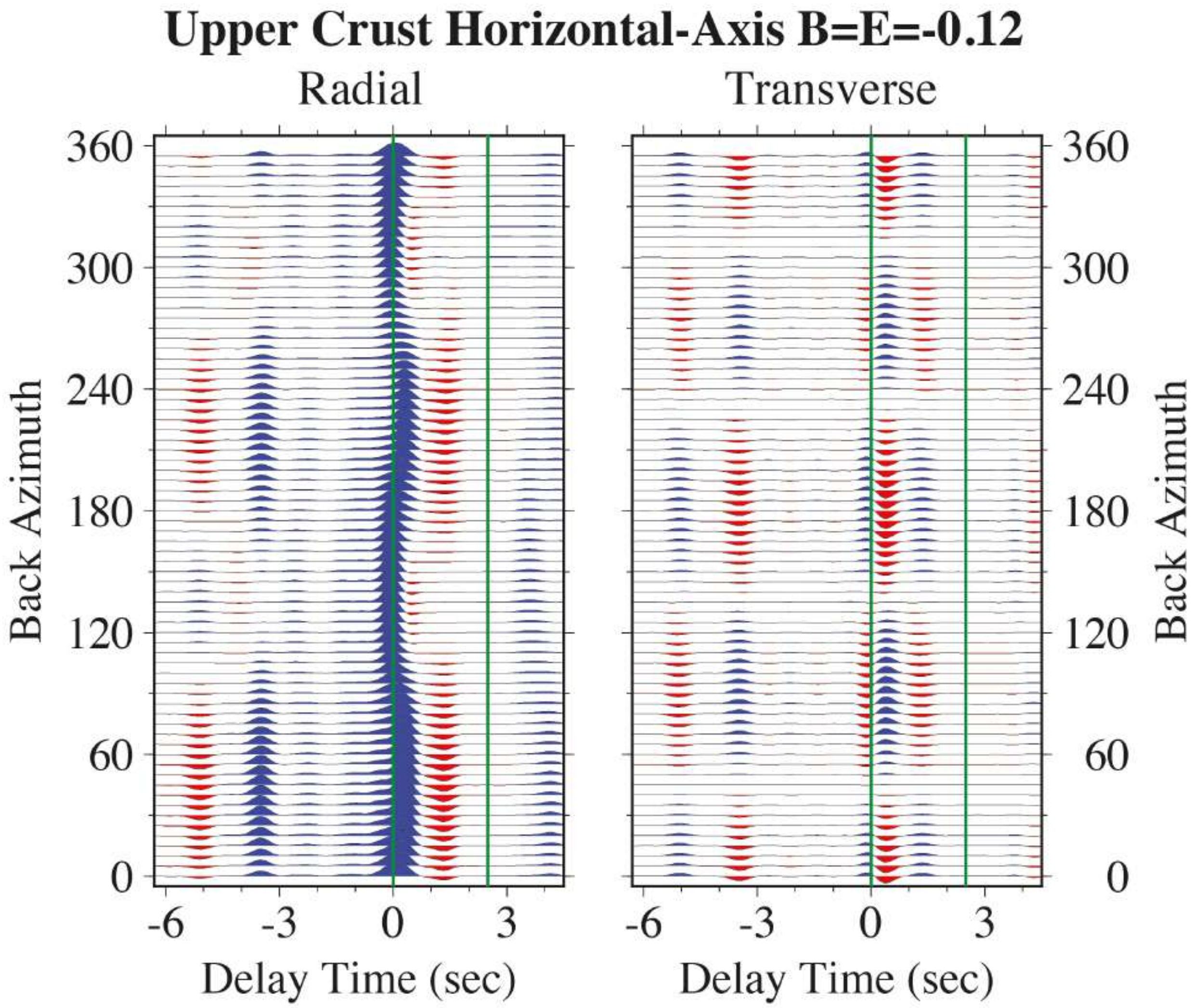

Figure S13. Back-azimuth receiver-function sweeps for synthetic seismograms in a 40-km crust with mixed anisotropy B=E=-0.12 (12% peak-to-peak P and S anisotropy) with a horizontal slow symmetry axis in the uppermost 10-km layer.

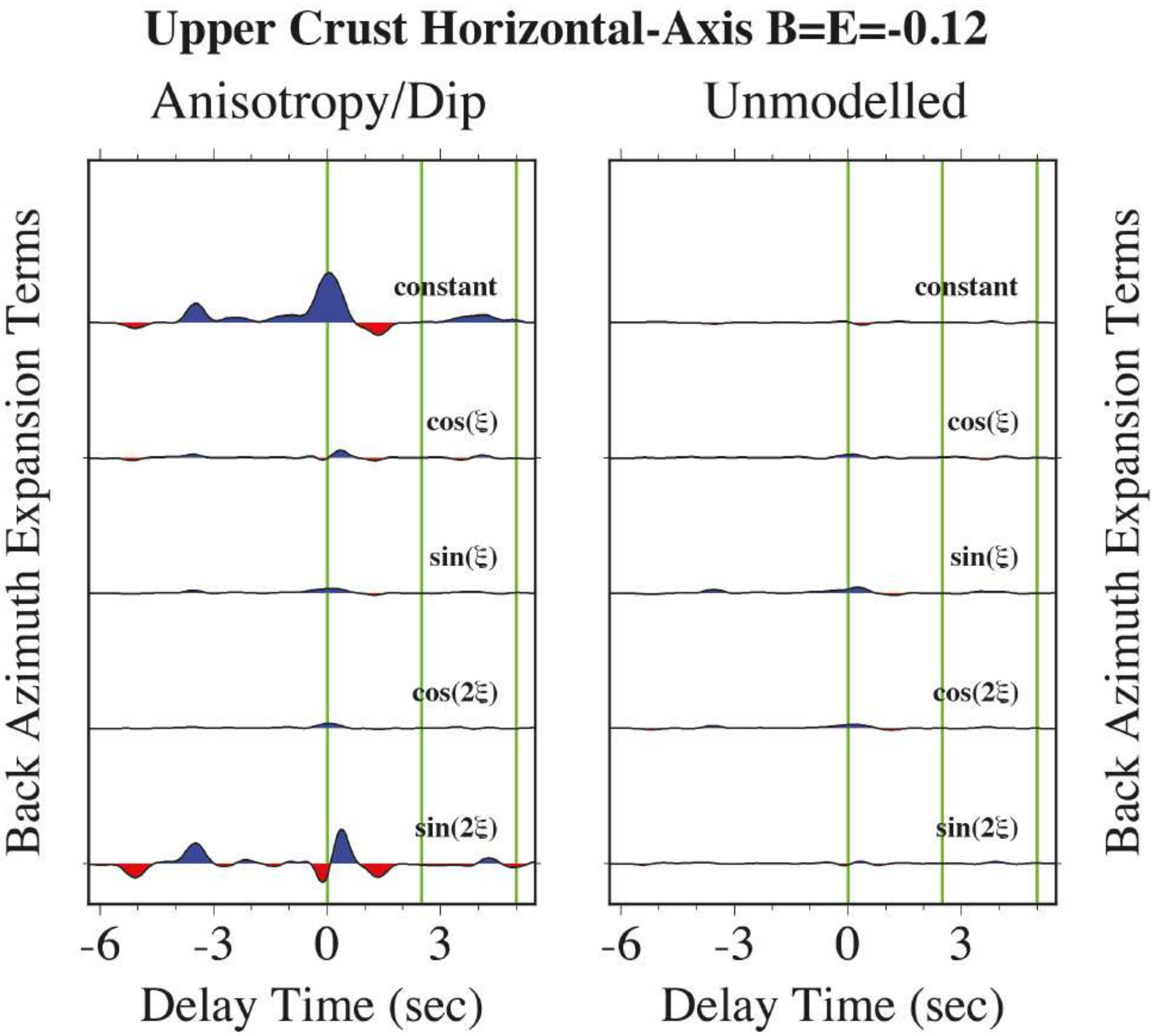

Figure S14. Harmonic terms of back azimuth ξ fit by least-squares in the frequency domain to receiver-functions estimated from synthetic seismograms in a 40-km crust with mixed anisotropy B=E=-0.12 (12% peak-to-peak P and S anisotropy) with a horizontal slow symmetry axis in the uppermost 10-km layer.

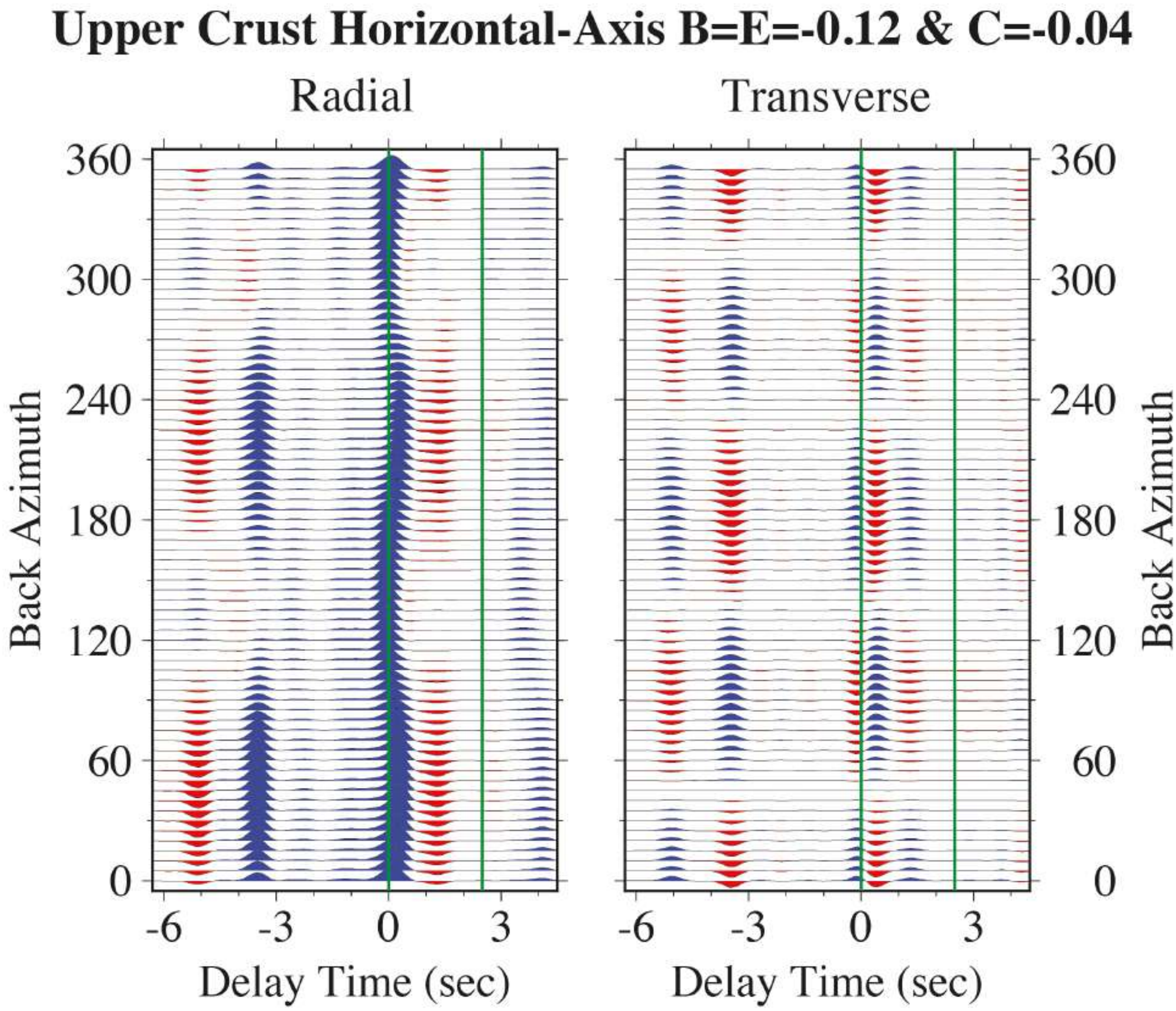

Figure S15. Back-azimuth receiver-function sweeps for synthetic seismograms in a 40-km crust with mixed anisotropy B=E=-0.12 and C=-0.04 with a horizontal slow symmetry axis in the uppermost 10-km layer. This corresponds to 12% peak-to-peak elliptical P and S anisotropy, plus a cos 4ξ wavespeed variation consistent with Brownlee et al (2017).

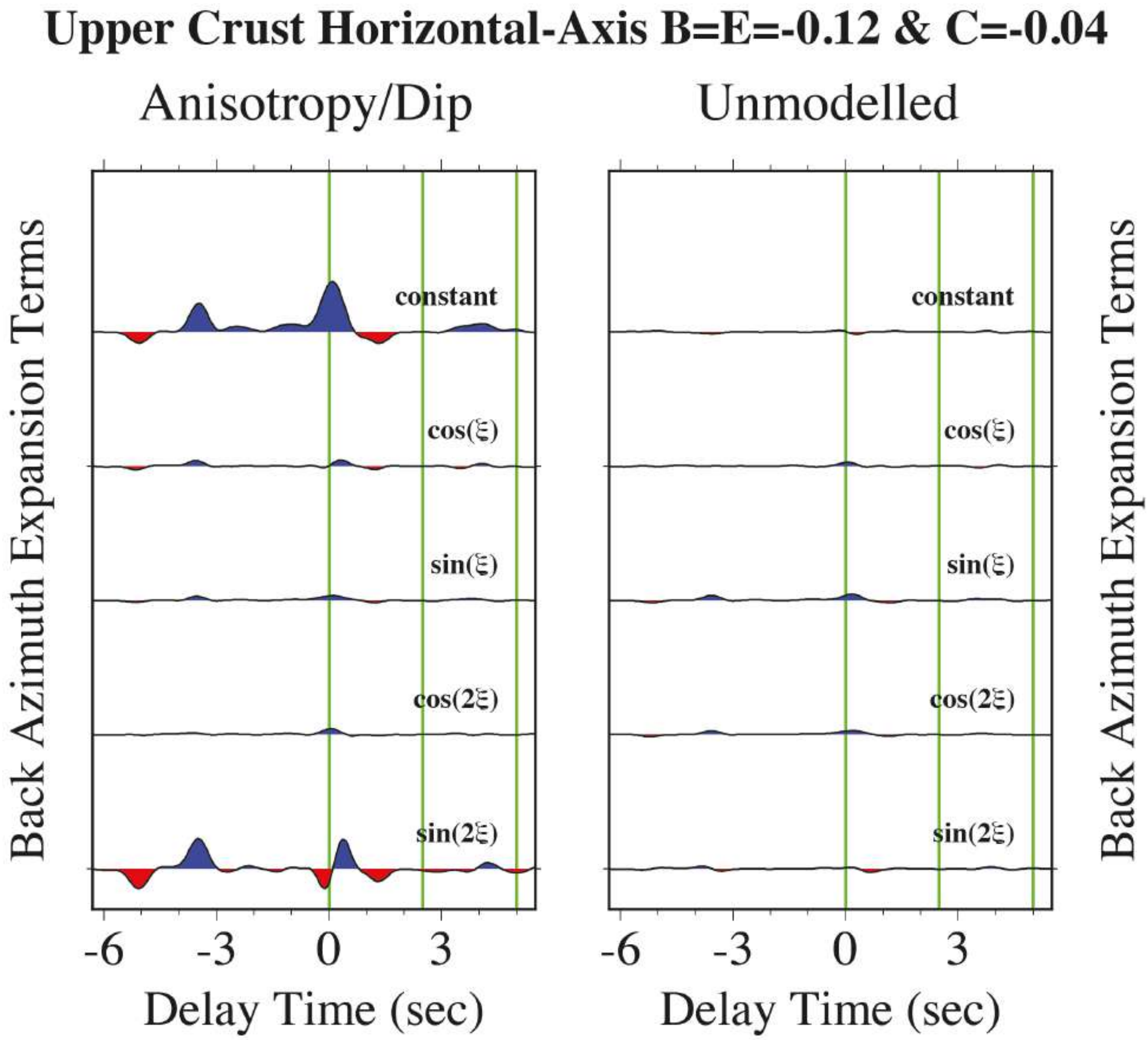

Figure S16. Harmonic terms of back azimuth ξ fit by least-squares in the frequency domain to receiver-functions estimated from synthetic seismograms in a 40-km crust with mixed anisotropy B=E=-0.12 and C=-0.04 with a horizontal slow symmetry axis in the uppermost 10-km layer. This corresponds to 12% peak-to-peak elliptical P and S anisotropy, plus a cos 4ξ wavespeed variation consistent with Brownlee et al (2017).

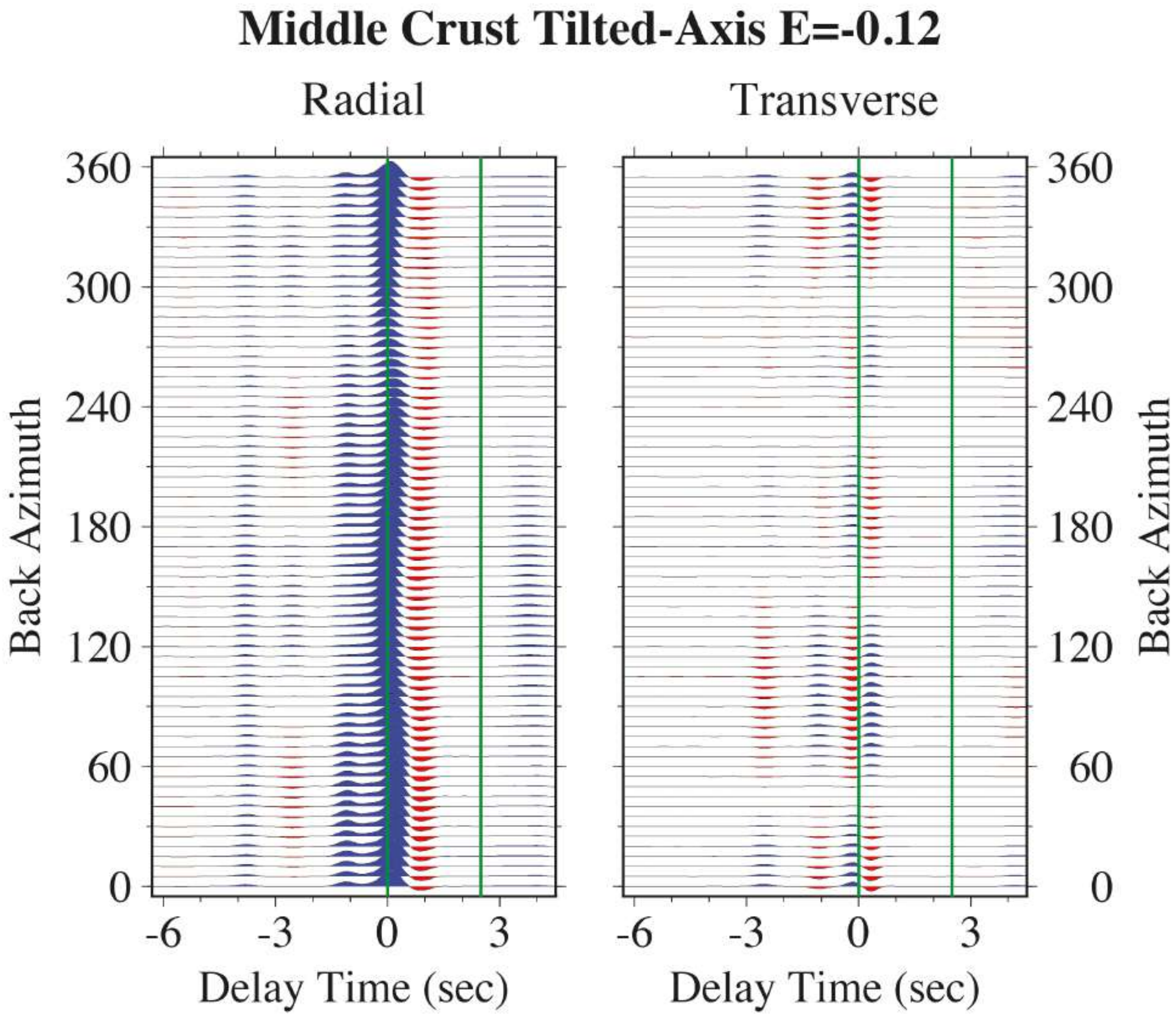

Figure S17. Back-azimuth receiver-function sweeps for synthetic seismograms in a 40-km crust with shear anisotropy E=-0.12 (12% peak-to-peak S anisotropy) with a slow symmetry axis with 45° tilt in a mid-crustal layer at 20-30-km depth.

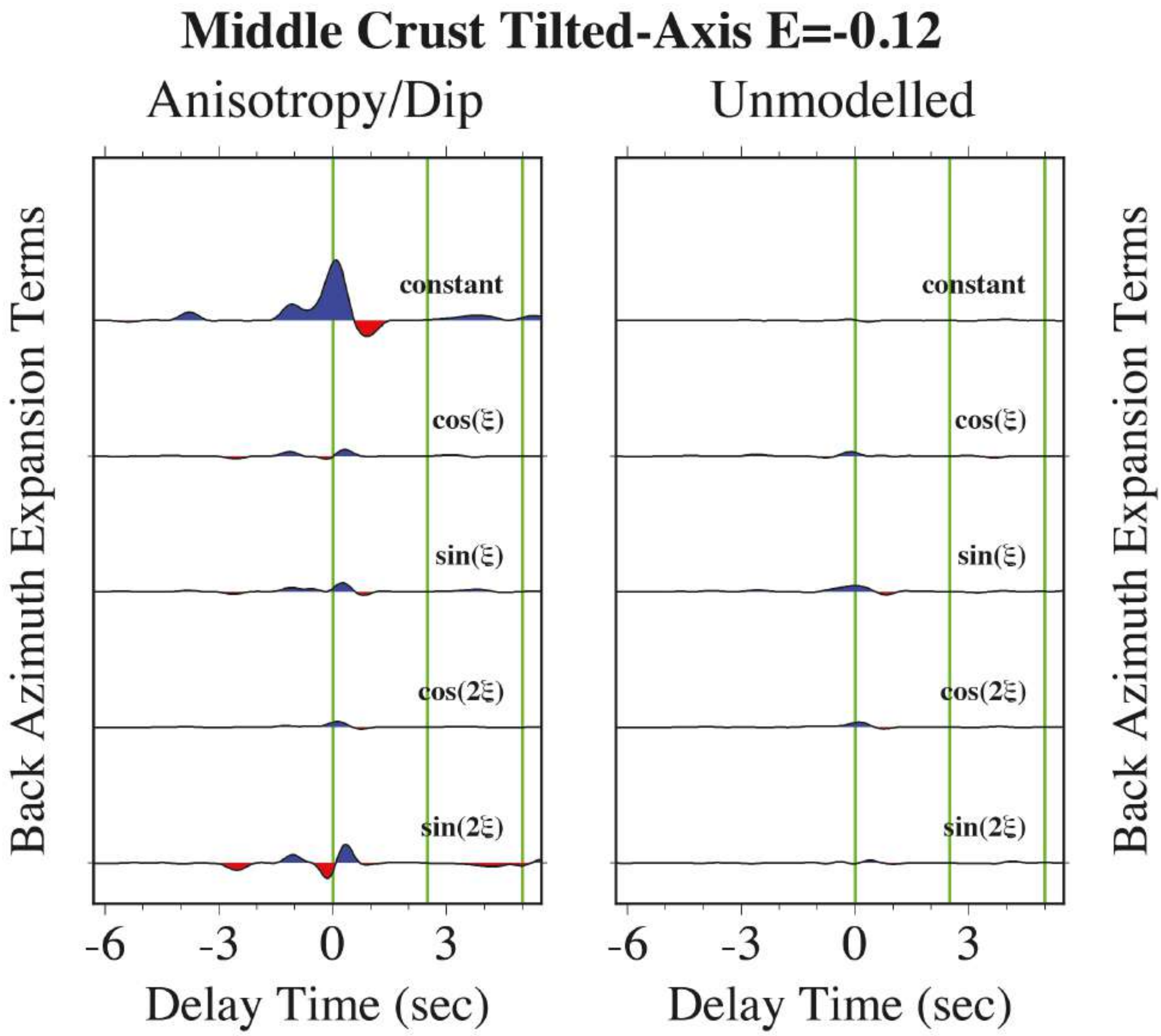

Figure S18. Harmonic terms of back azimuth ξ fit by least-squares in the frequency domain to receiver-functions estimated from synthetic seismograms in a 40-km crust with shear anisotropy E=-0.12 (12% peak-to-peak S anisotropy) with a slow symmetry axis with 45° tilt in a mid-crustal layer at 20-30-km depth.

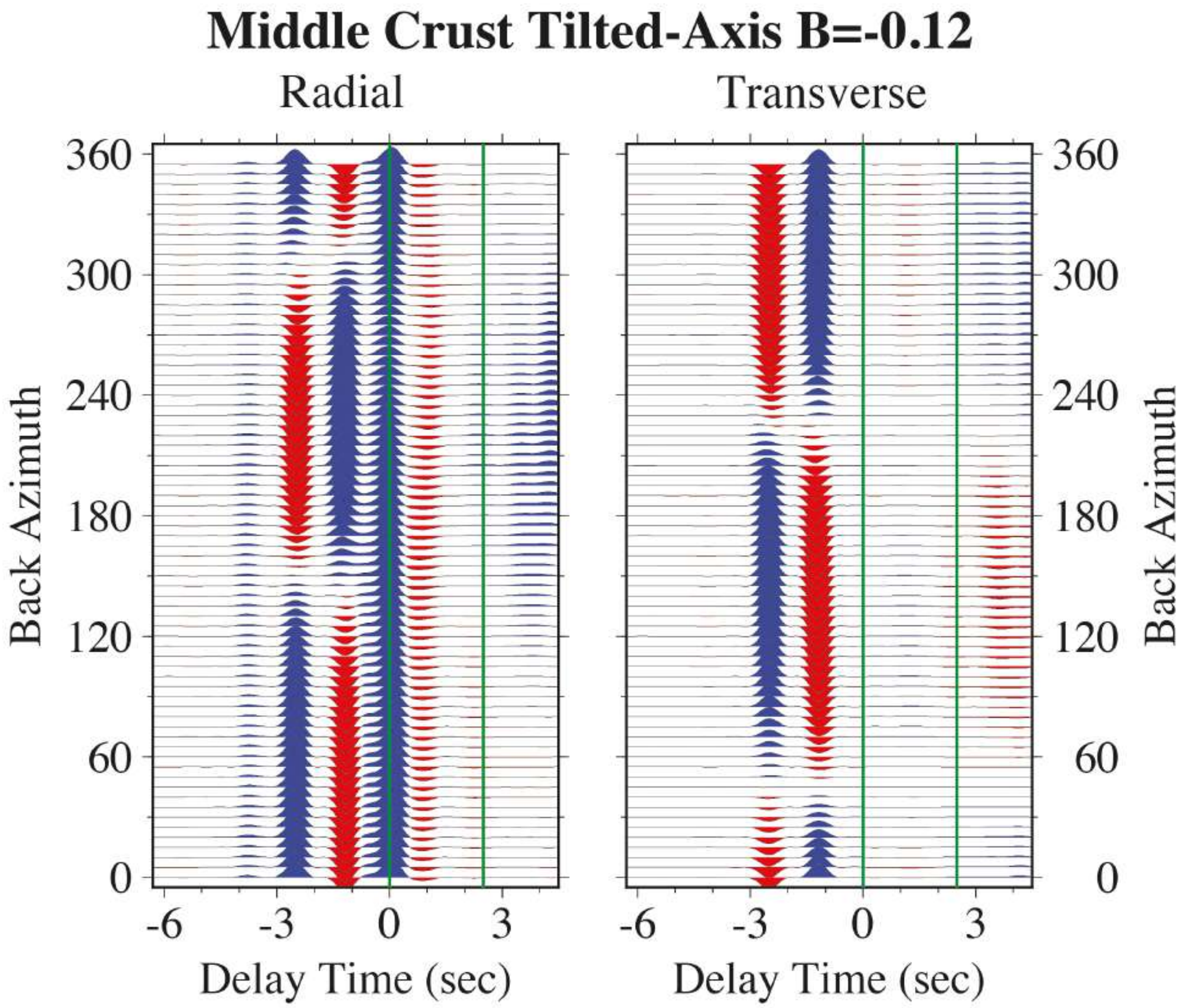

Figure S19. Back-azimuth receiver-function sweeps for synthetic seismograms in a 40-km crust with compressional anisotropy B=-0.12 (12% peak-to-peak P anisotropy) with a slow symmetry axis with 45° tilt in a mid-crustal layer at 20-30-km depth.

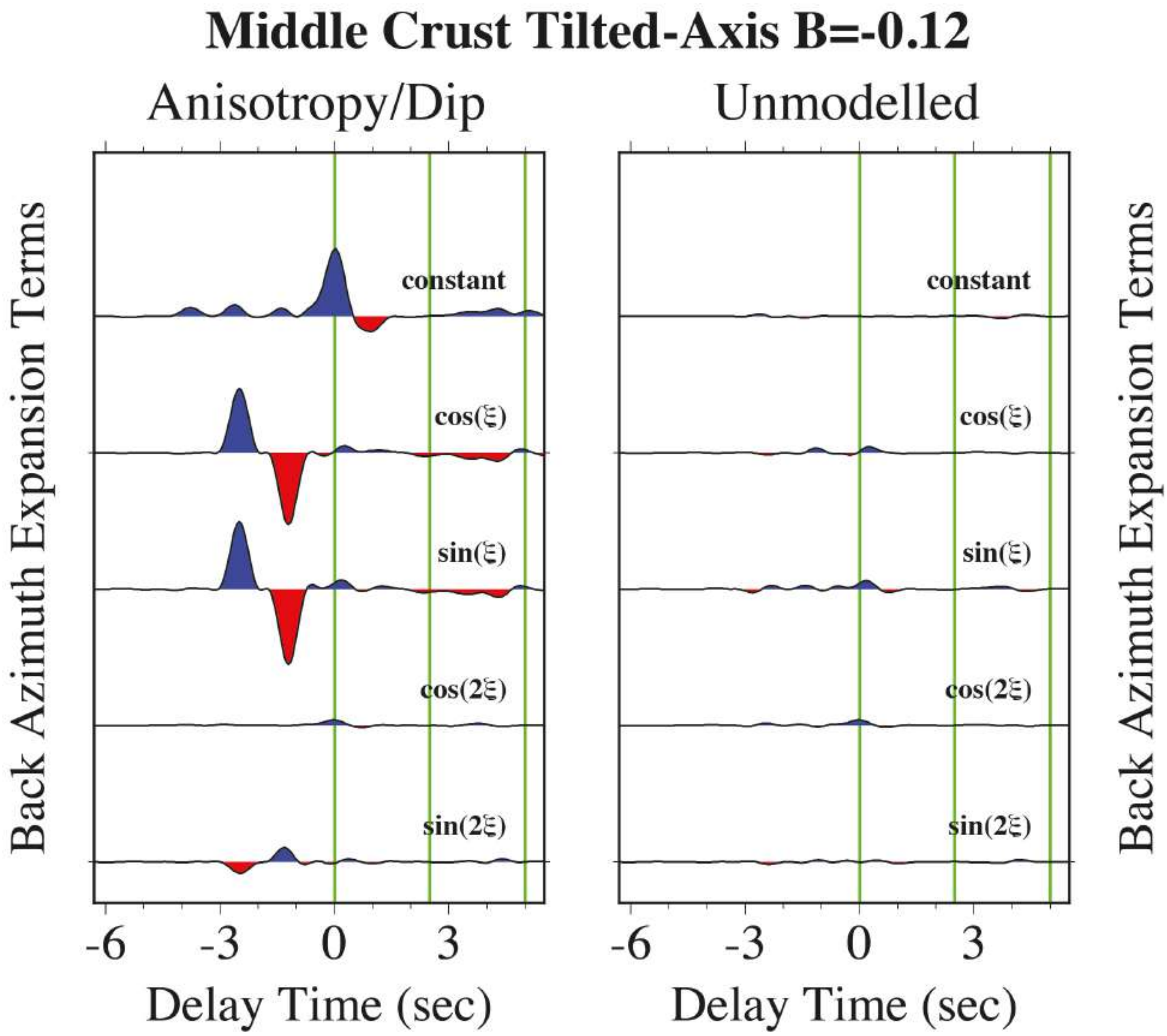

Figure S20. Harmonic terms of back azimuth ξ fit by least-squares in the frequency domain to receiver-functions estimated from synthetic seismograms in a 40-km crust with compressional anisotropy B=-0.12 (12% peak-to-peak P anisotropy) with a slow symmetry axis with 45° tilt in a mid-crustal layer at 20-30-km depth.

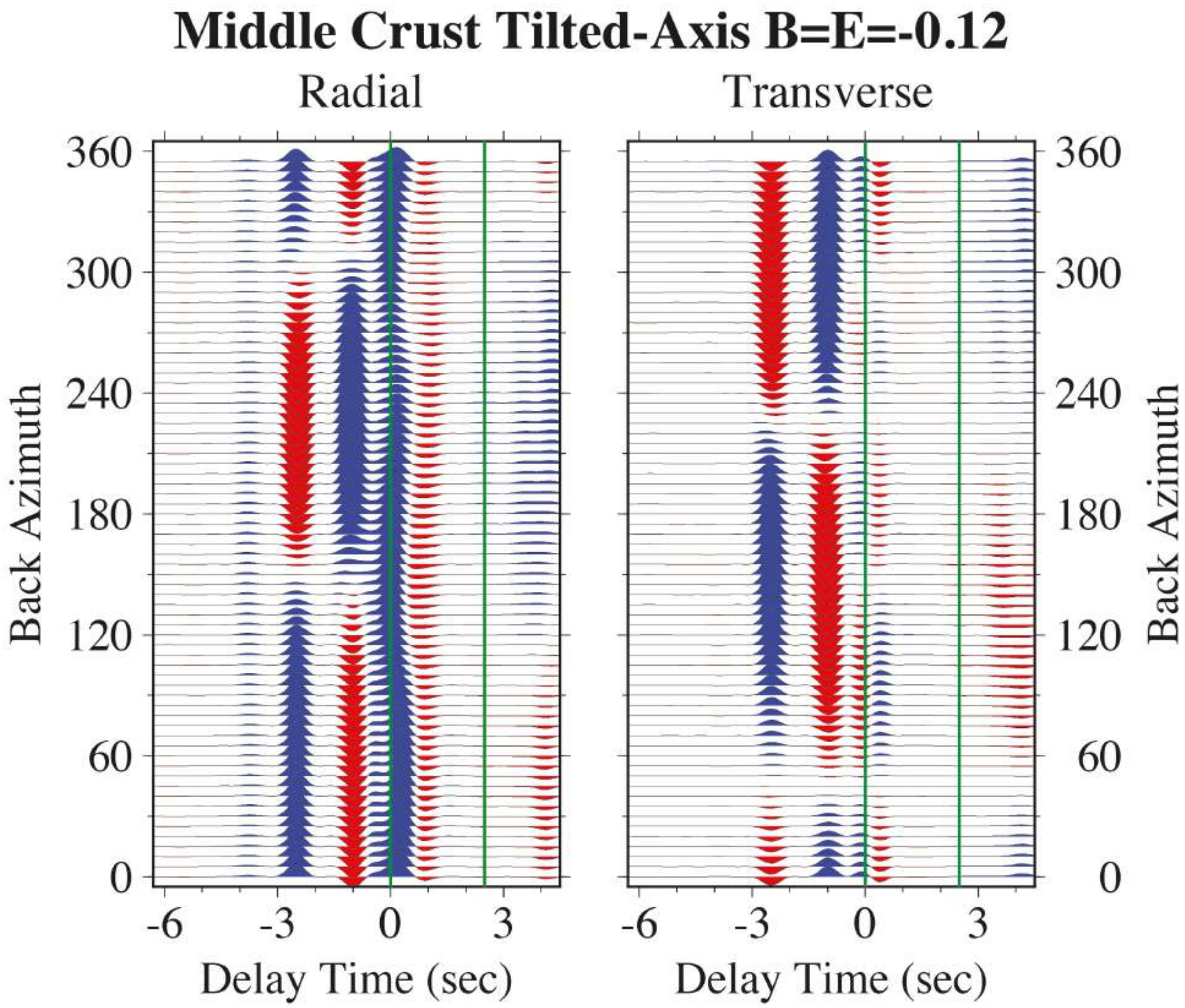

Figure S21. Back-azimuth receiver-function sweeps for synthetic seismograms in a 40-km crust with mixed anisotropy B=E=-0.12 (12% peak-to-peak P and S anisotropy) with a slow symmetry axis with 45° tilt in a mid-crustal layer at 20-30-km depth.

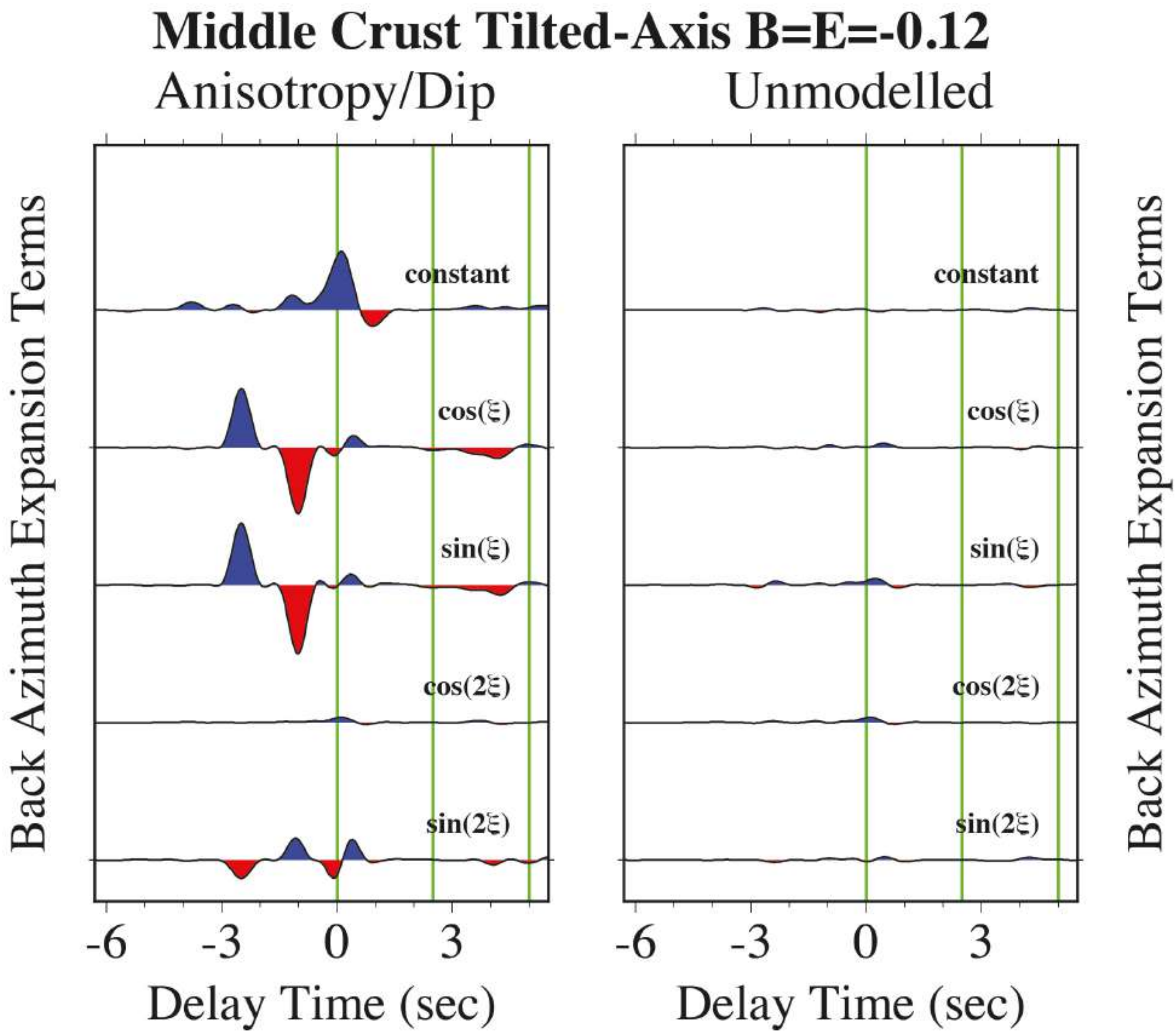

Figure S22. Harmonic terms of back azimuth ξ fit by least-squares in the frequency domain to receiver-functions estimated from synthetic seismograms in a 40-km crust with mixed anisotropy B=E=-0.12 (12% peak-to-peak P and S anisotropy) with a slow symmetry axis with 45° tilt in a mid-crustal layer at 20-30-km depth.

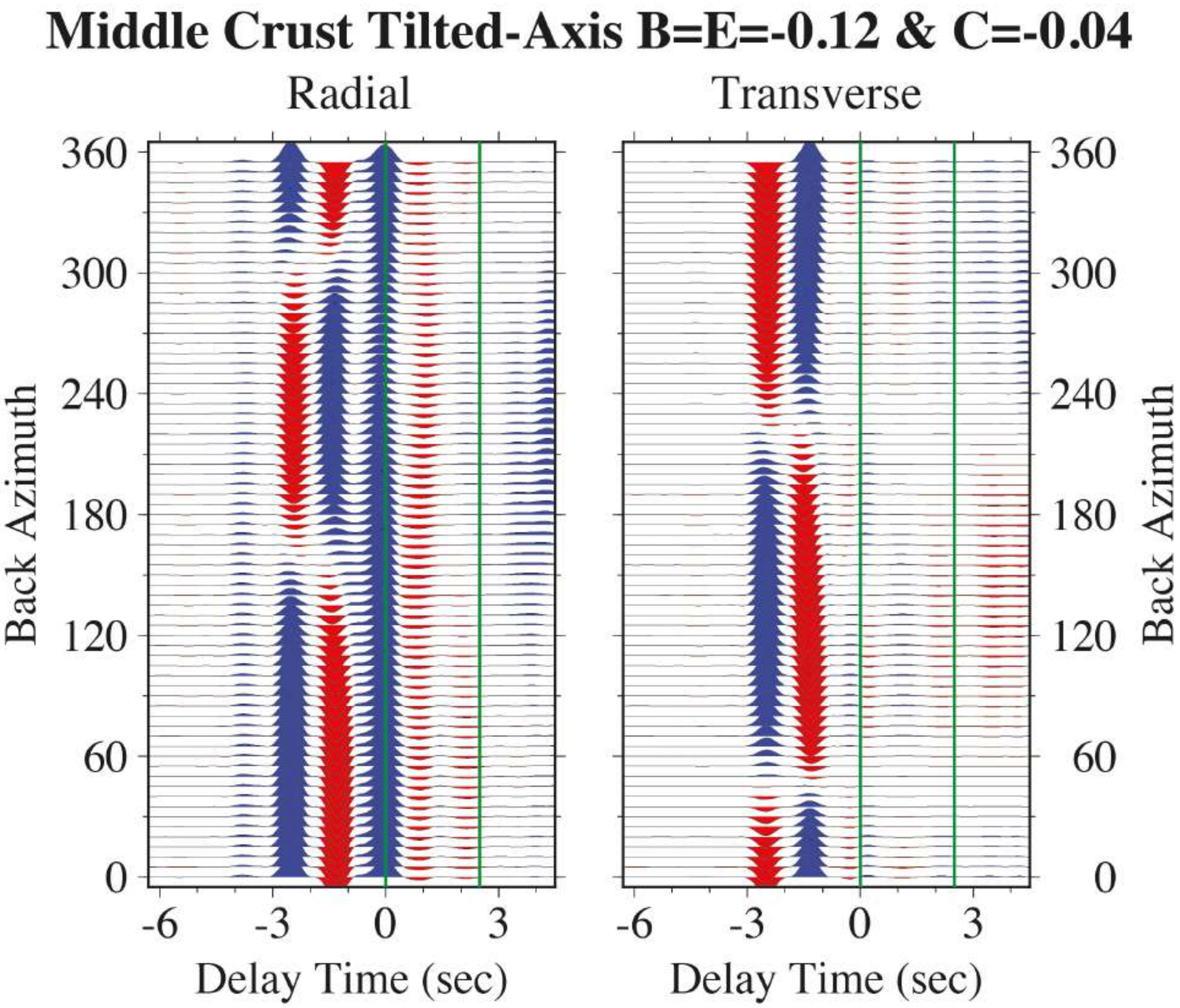

Figure S23. Back-azimuth receiver-function sweeps for synthetic seismograms in a 40-km crust with mixed anisotropy B=E=-0.12 and C=-0.04 with a slow symmetry axis with 45° tilt in a mid-crustal layer at 20-30-km depth. This corresponds to 12% peak-to-peak elliptical P and S anisotropy, plus a cos 4ξ wavespeed variation consistent with Brownlee et al (2017).

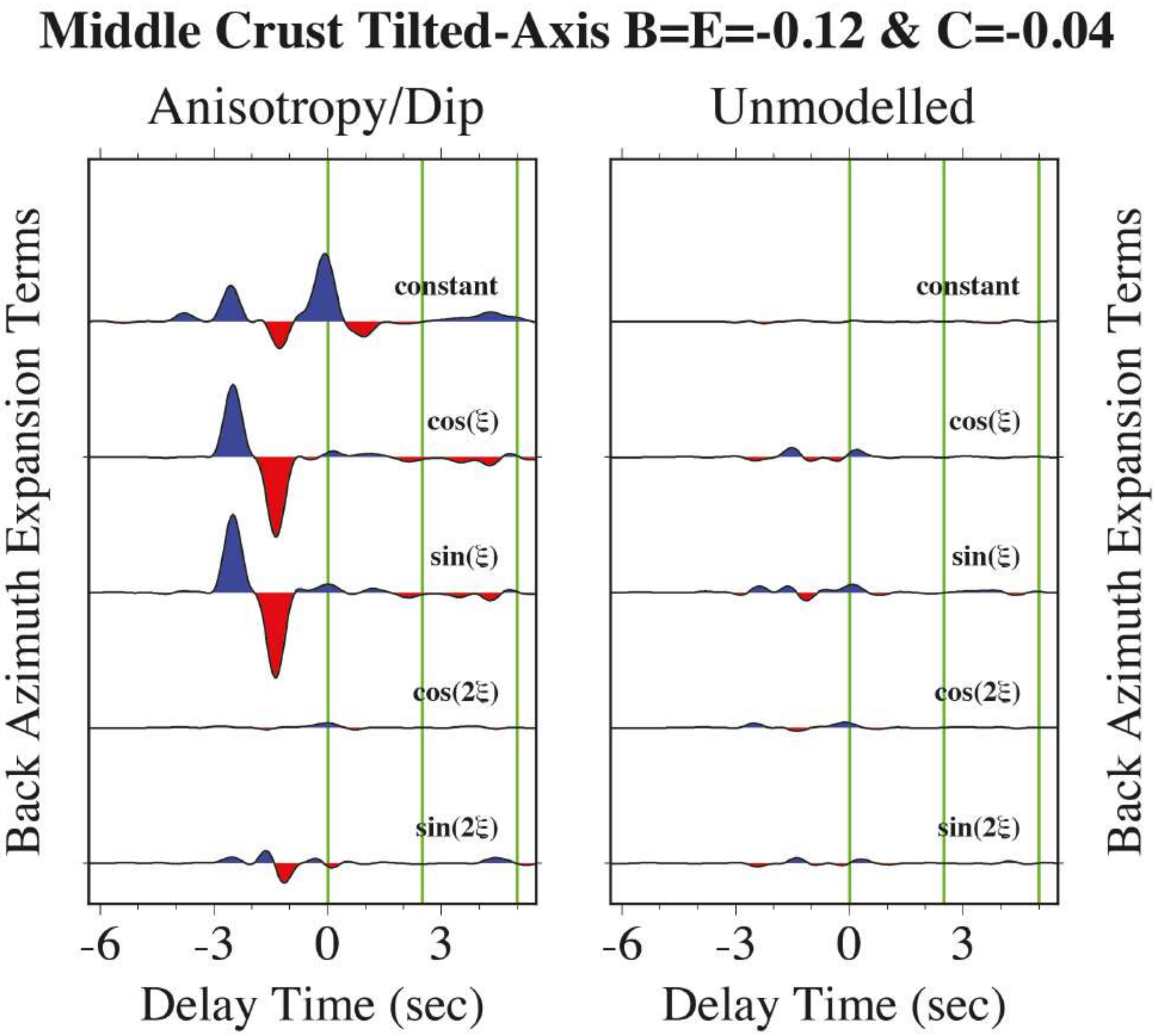

Figure S24. Harmonic terms of back azimuth ξ fit by least-squares in the frequency domain to receiver-functions estimated from synthetic seismograms in a 40-km crust with mixed anisotropy B=E=-0.12 and C=-0.04 with a slow symmetry axis with 45° tilt in a mid-crustal layer at 20-30-km depth. This corresponds to 12% peak-to-peak elliptical P and S anisotropy, plus a cos 4ξ wavespeed variation consistent with Brownlee et al (2017).

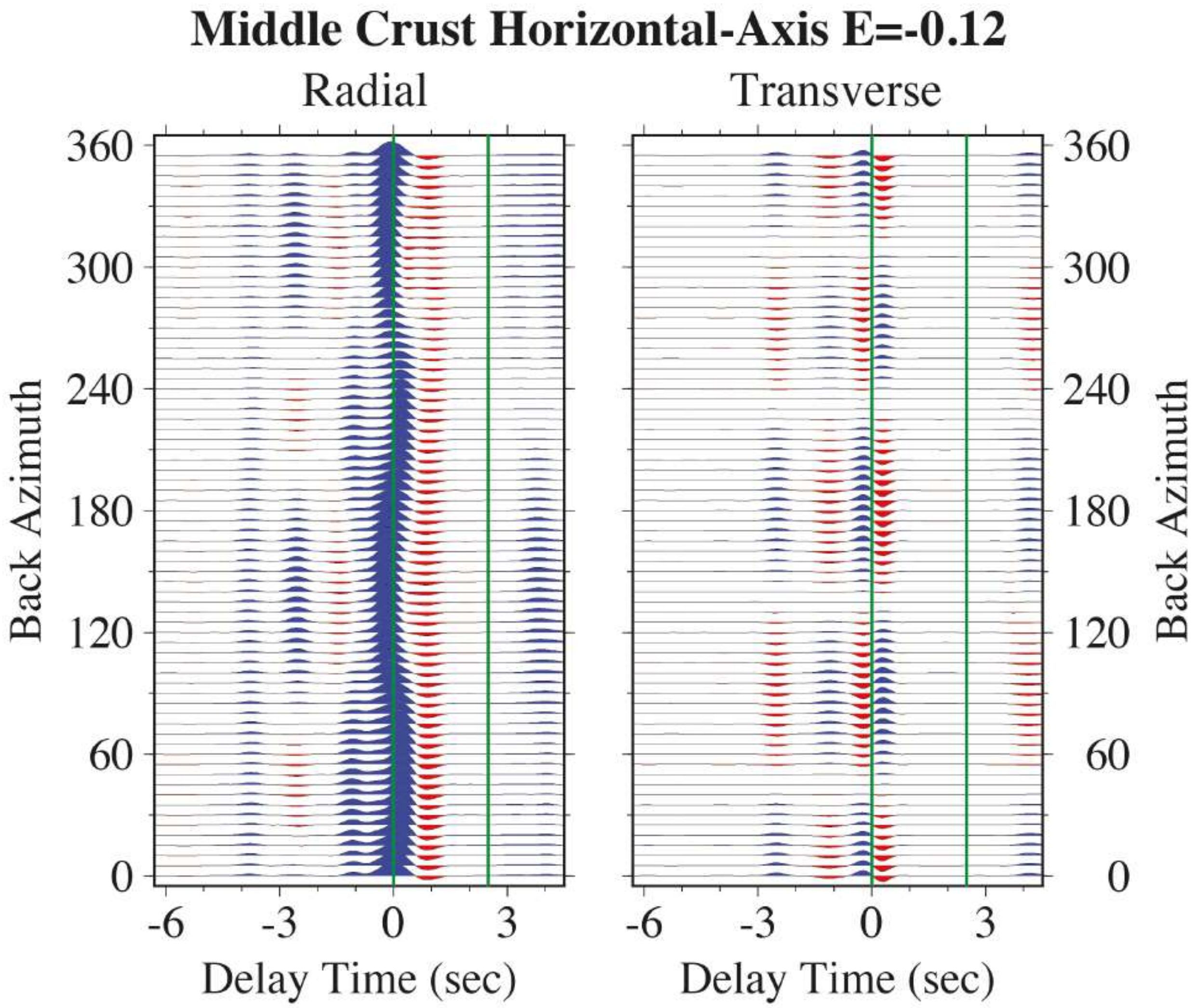

Figure S25. Back-azimuth receiver-function sweeps for synthetic seismograms in a 40-km crust with shear anisotropy E=-0.12 (12% peak-to-peak S anisotropy) with a horizontal slow symmetry axis in a mid-crustal layer at 20-30-km depth.

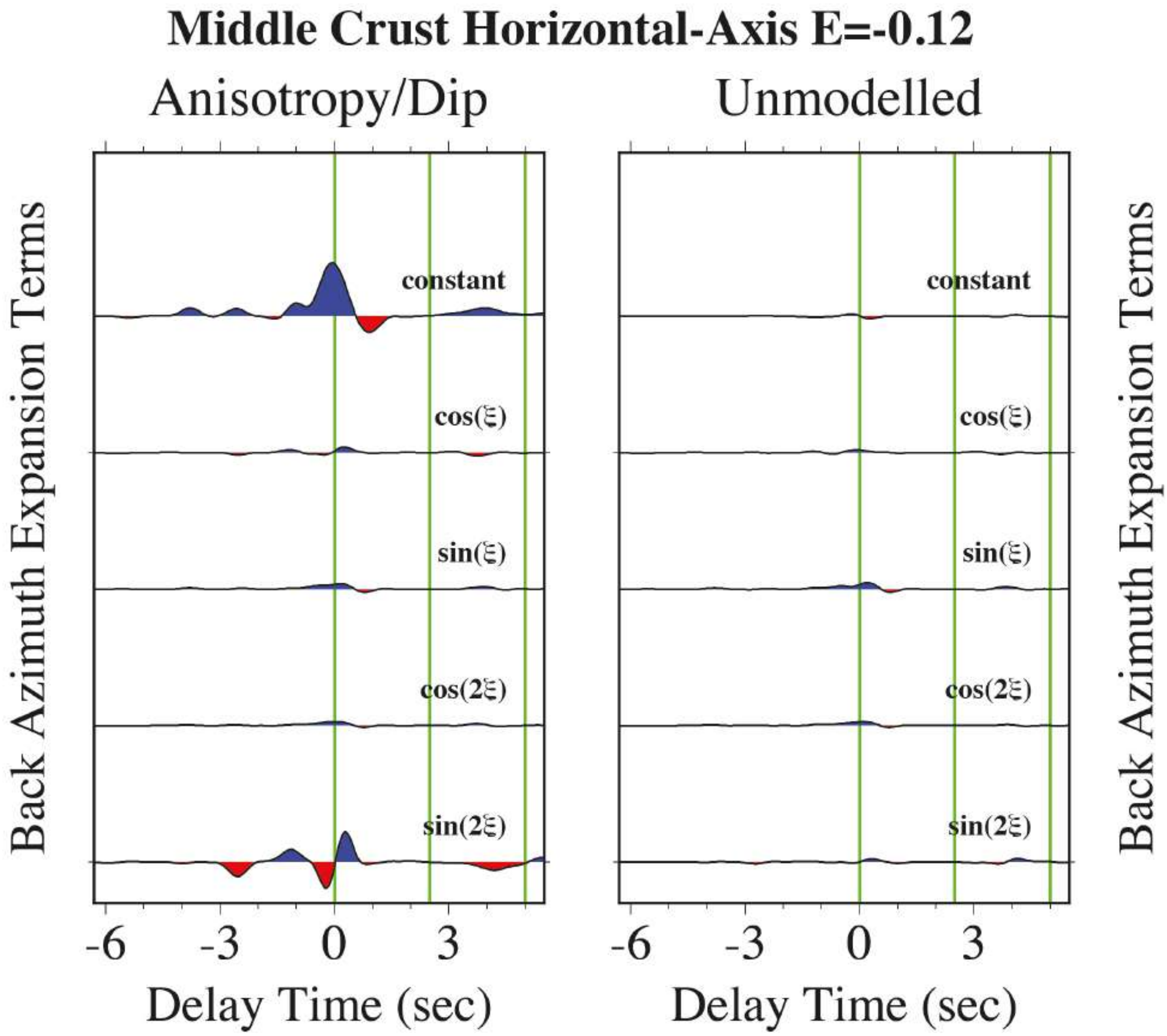

Figure S26. Harmonic terms of back azimuth ξ fit by least-squares in the frequency domain to receiver-functions estimated from synthetic seismograms in a 40-km crust with shear anisotropy E=-0.12 (12% peak-to-peak S anisotropy) with a horizontal slow symmetry axis in a mid-crustal layer at 20-30-km depth.

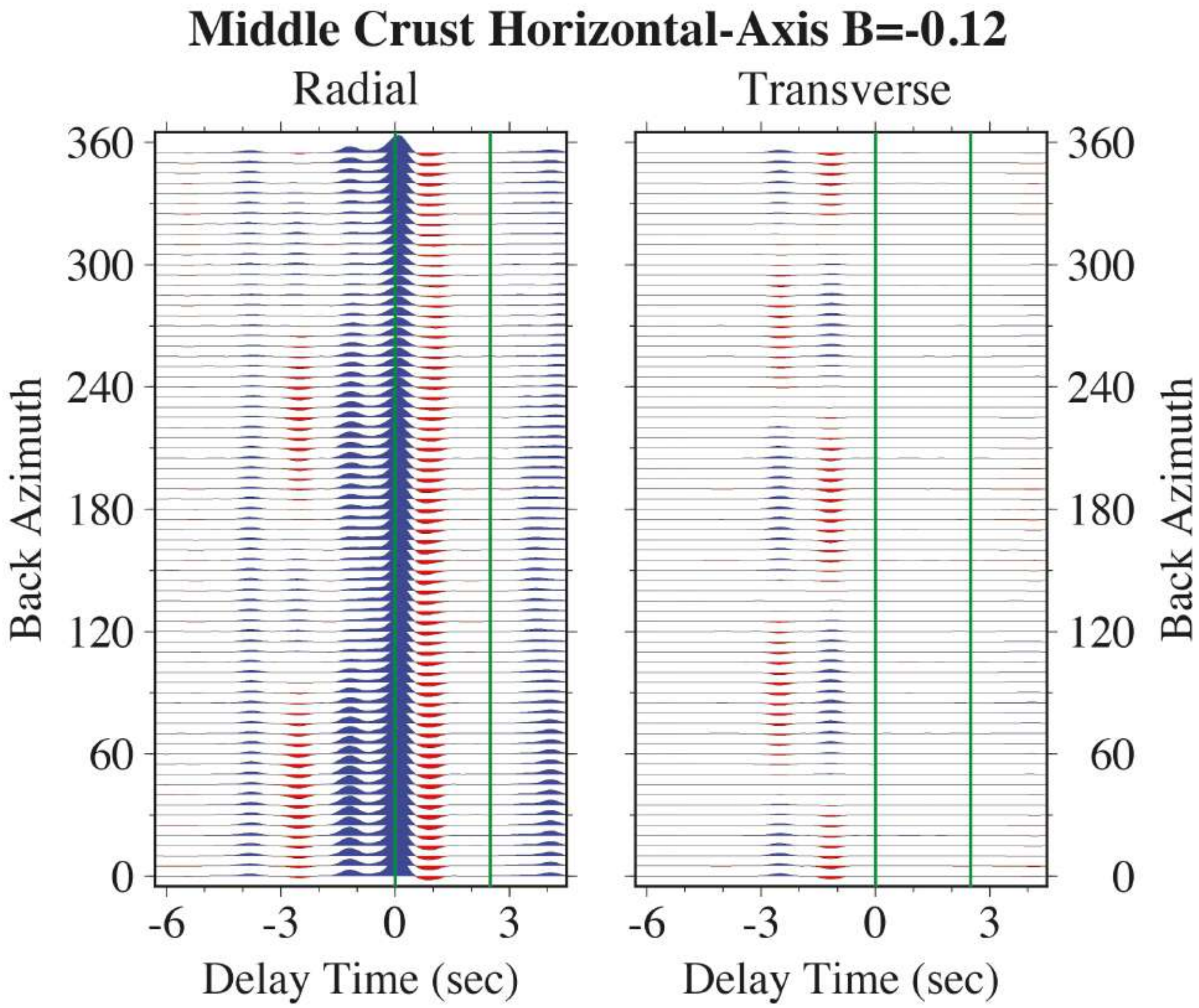

Figure S27. Back-azimuth receiver-function sweeps for synthetic seismograms in a 40-km crust with compressional anisotropy B=-0.12 (12% peak-to-peak P anisotropy) with a horizontal slow symmetry axis in a mid-crustal layer at 20-30-km depth.

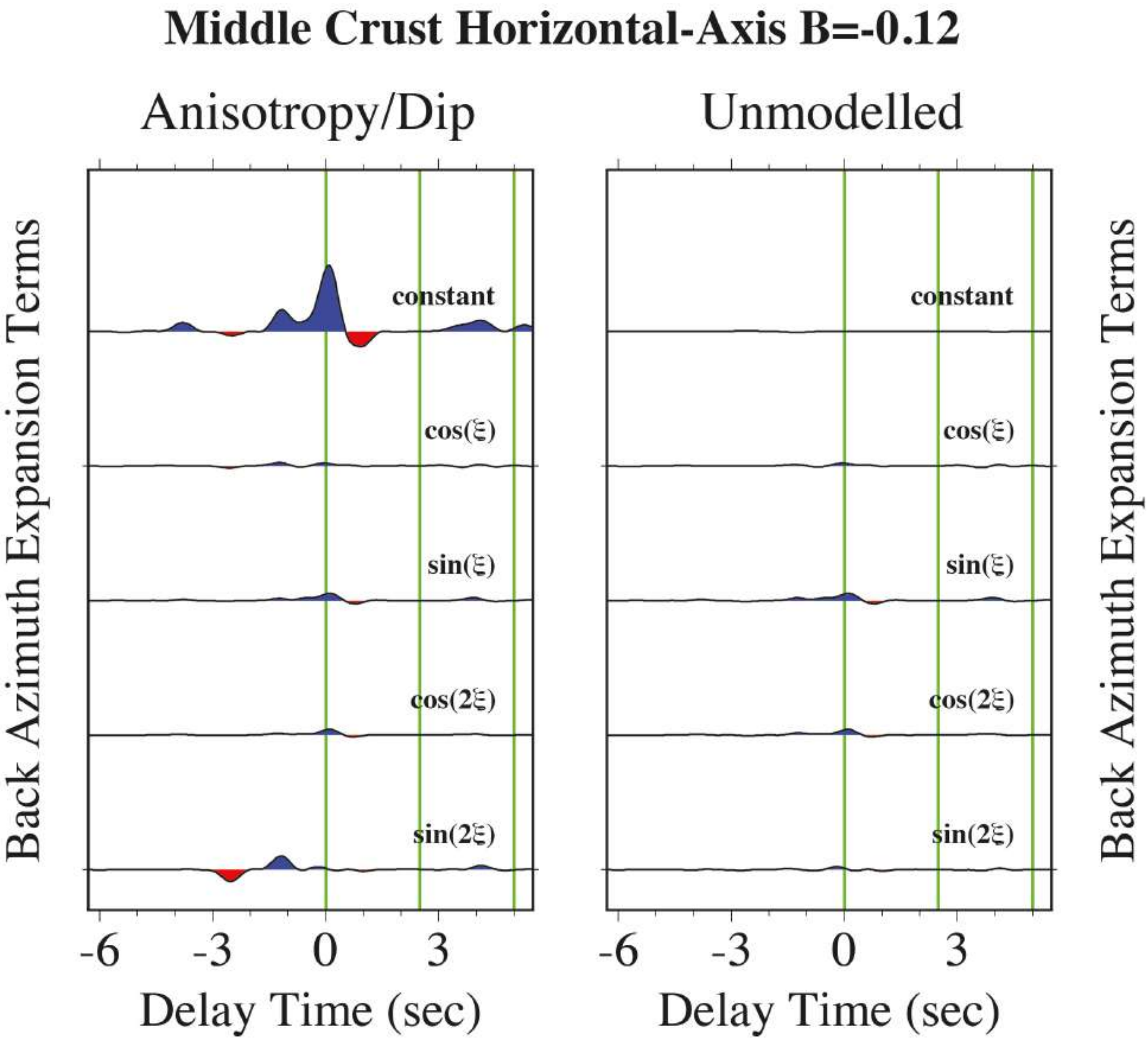

Figure S28. Harmonic terms of back azimuth ξ fit by least-squares in the frequency domain to receiver-functions estimated from synthetic seismograms in a 40-km crust with compressional anisotropy B=-0.12 (12% peak-to-peak P anisotropy) with a horizontal slow symmetry axis in a mid-crustal layer at 20-30-km depth.

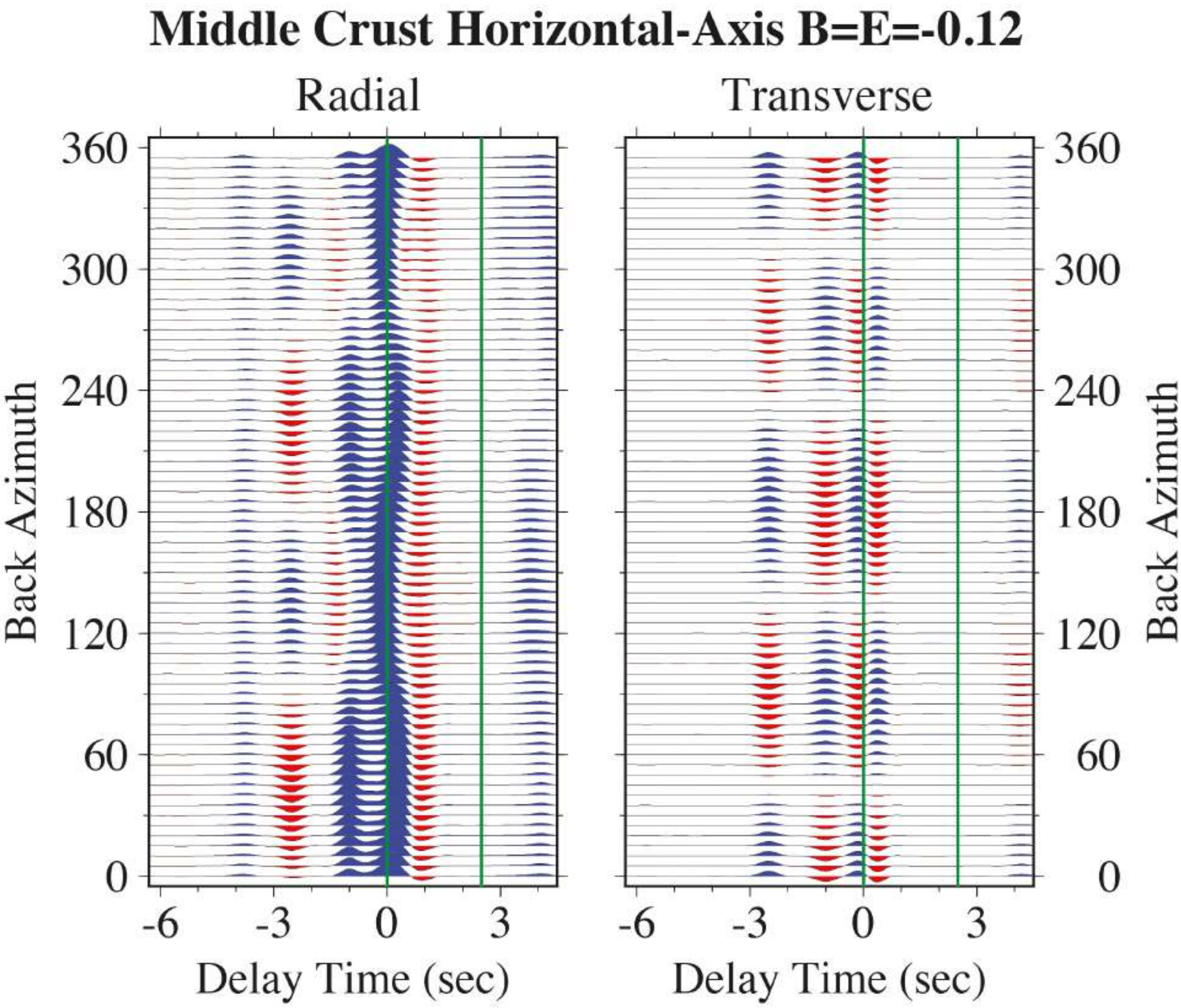

Figure S29. Back-azimuth receiver-function sweeps for synthetic seismograms in a 40-km crust with mixed anisotropy B=E=-0.12 (12% peak-to-peak P and S anisotropy) with a horizontal slow symmetry axis in a mid-crustal layer at 20-30-km depth.

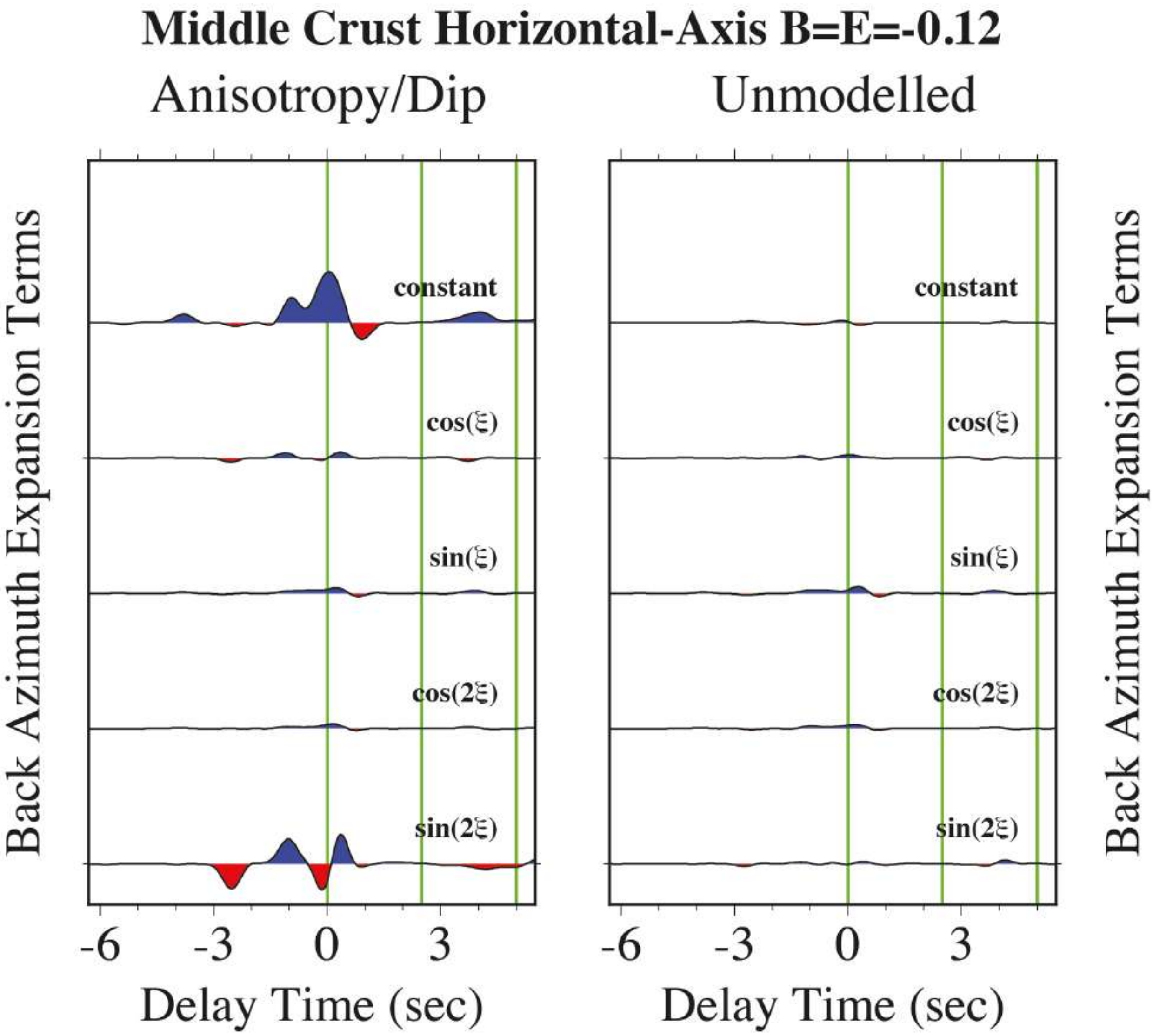

Figure S30. Harmonic terms of back azimuth ξ fit by least-squares in the frequency domain to receiver-functions estimated from synthetic seismograms in a 40-km crust with mixed anisotropy B=E=-0.12 (12% peak-to-peak P and S anisotropy) with a horizontal slow symmetry axis in a mid-crustal layer at 20-30-km depth.

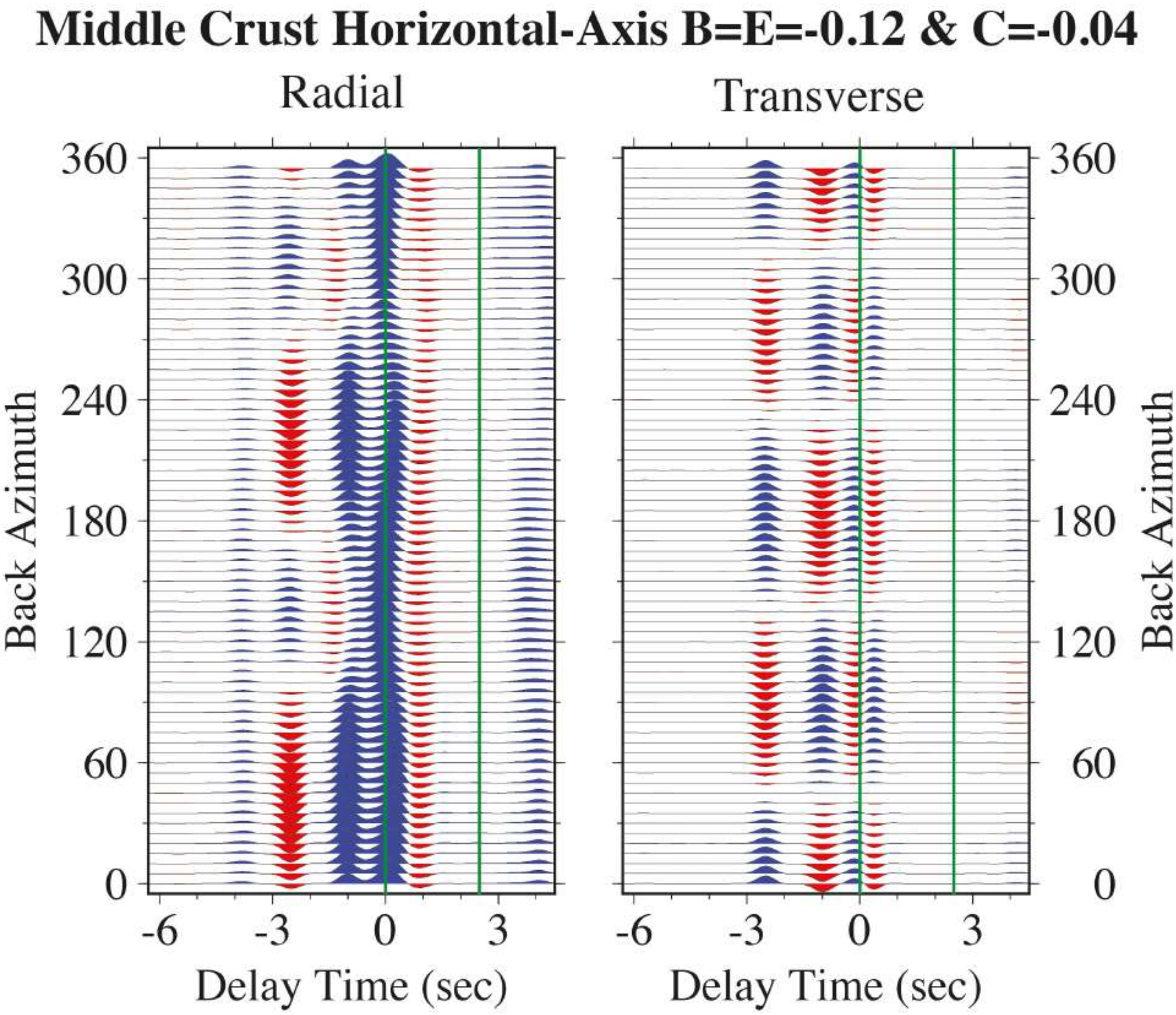

Figure S31. Back-azimuth receiver-function sweeps for synthetic seismograms in a 40-km crust with mixed anisotropy B=E=-0.12 and C=-0.04 with a horizontal slow symmetry axis in a mid-crustal layer at 20-30-km depth. This corresponds to 12% peak-to-peak elliptical P and S anisotropy, plus a cos 4ξ wavespeed variation consistent with Brownlee et al (2017).

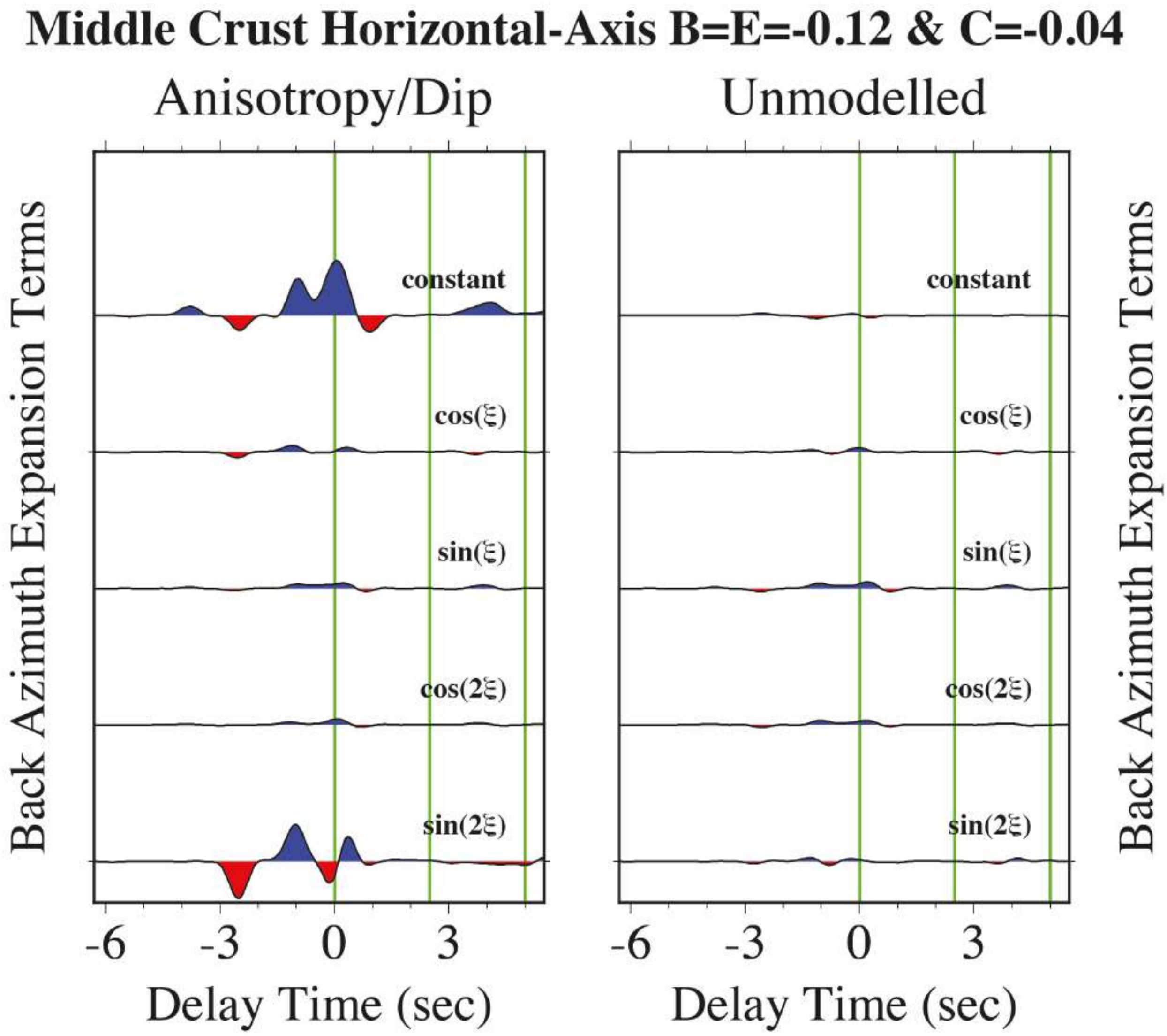

Figure S32. Harmonic terms of back azimuth ξ fit by least-squares in the frequency domain to receiver-functions estimated from synthetic seismograms in a 40-km crust with mixed anisotropy B=E=-0.12 and C=-0.04 with a horizontal slow symmetry axis in a mid-crustal layer at 20-30-km depth. This corresponds to 12% peak-to-peak elliptical P and S anisotropy, plus a cos 4ξ wavespeed variation consistent with Brownlee et al (2017).

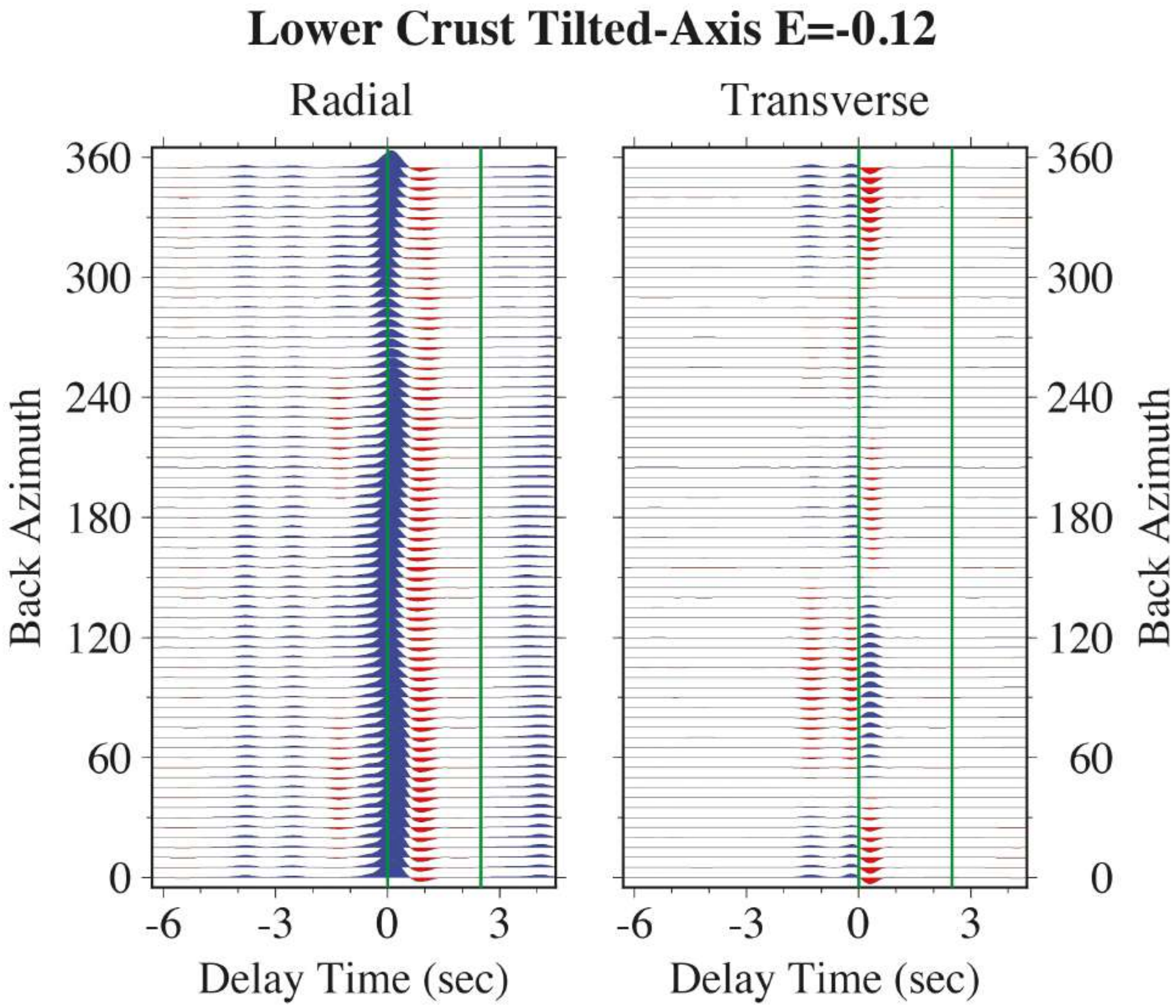

Figure S33. Back-azimuth receiver-function sweeps for synthetic seismograms in a 40-km crust with shear anisotropy E=-0.12 (12% peak-to-peak S anisotropy) with a slow symmetry axis with 45° tilt in a lower-crustal layer at 30-40-km depth.

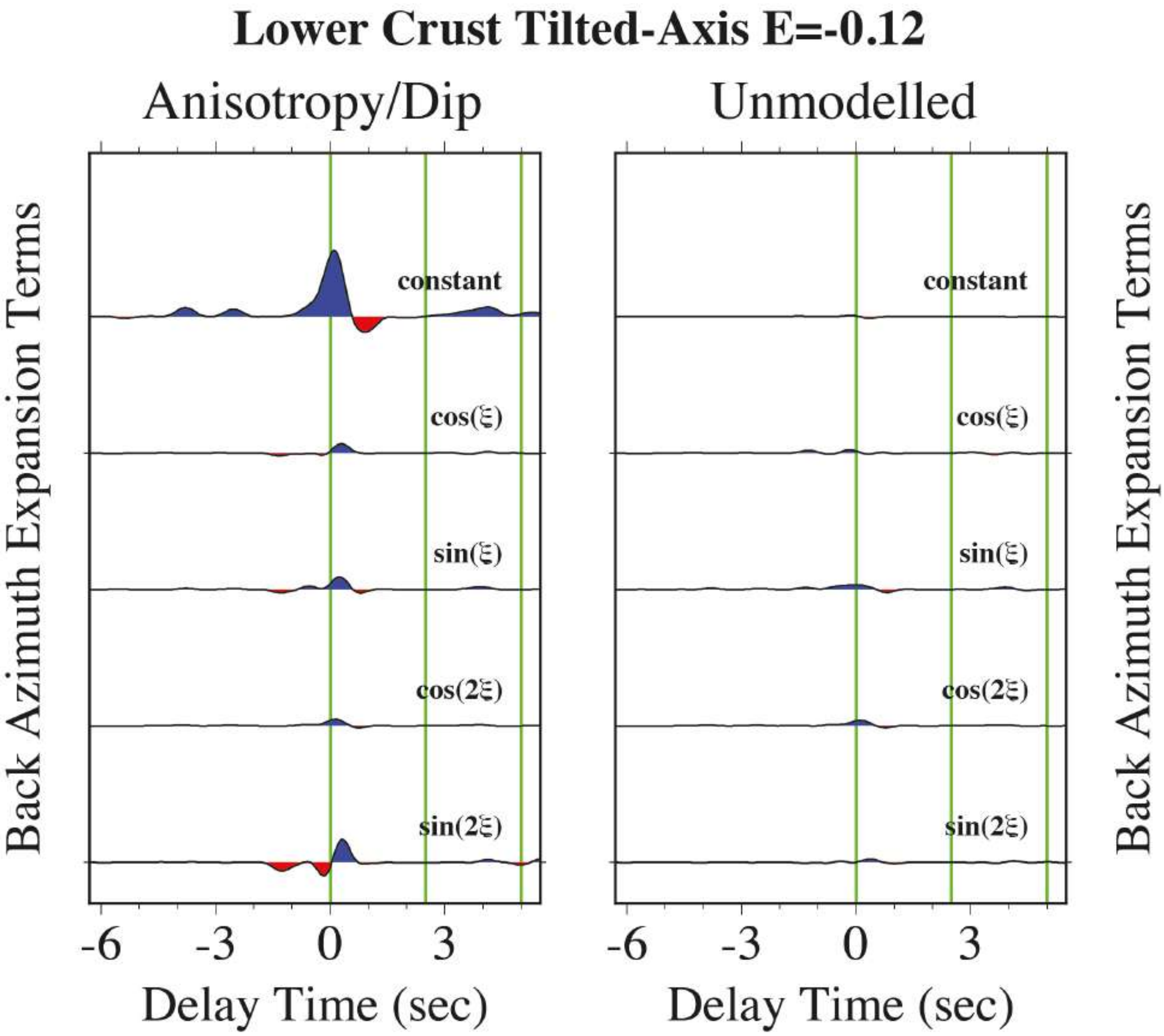

Figure S34. Harmonic terms of back azimuth ξ fit by least-squares in the frequency domain to receiver-functions estimated from synthetic seismograms in a 40-km crust with shear anisotropy E=-0.12 (12% peak-to-peak S anisotropy) with a slow symmetry axis with 45° tilt in a lower-crustal layer at 30-40-km depth.

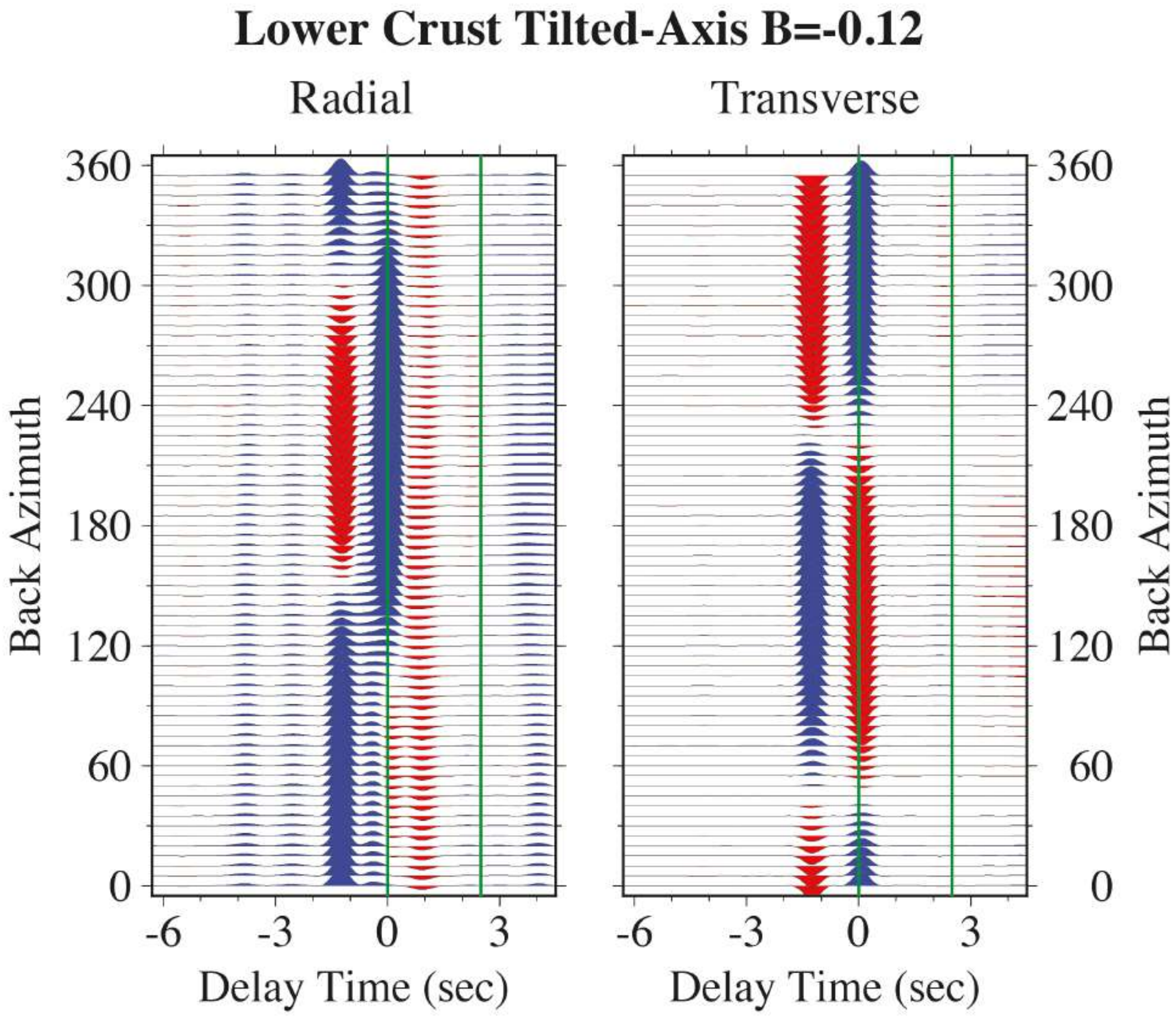

Figure S35. Back-azimuth receiver-function sweeps for synthetic seismograms in a 40-km crust with compressional anisotropy B=-0.12 (12% peak-to-peak P anisotropy) with a slow symmetry axis with 45° tilt in a lower-crustal layer at 30-40-km depth.

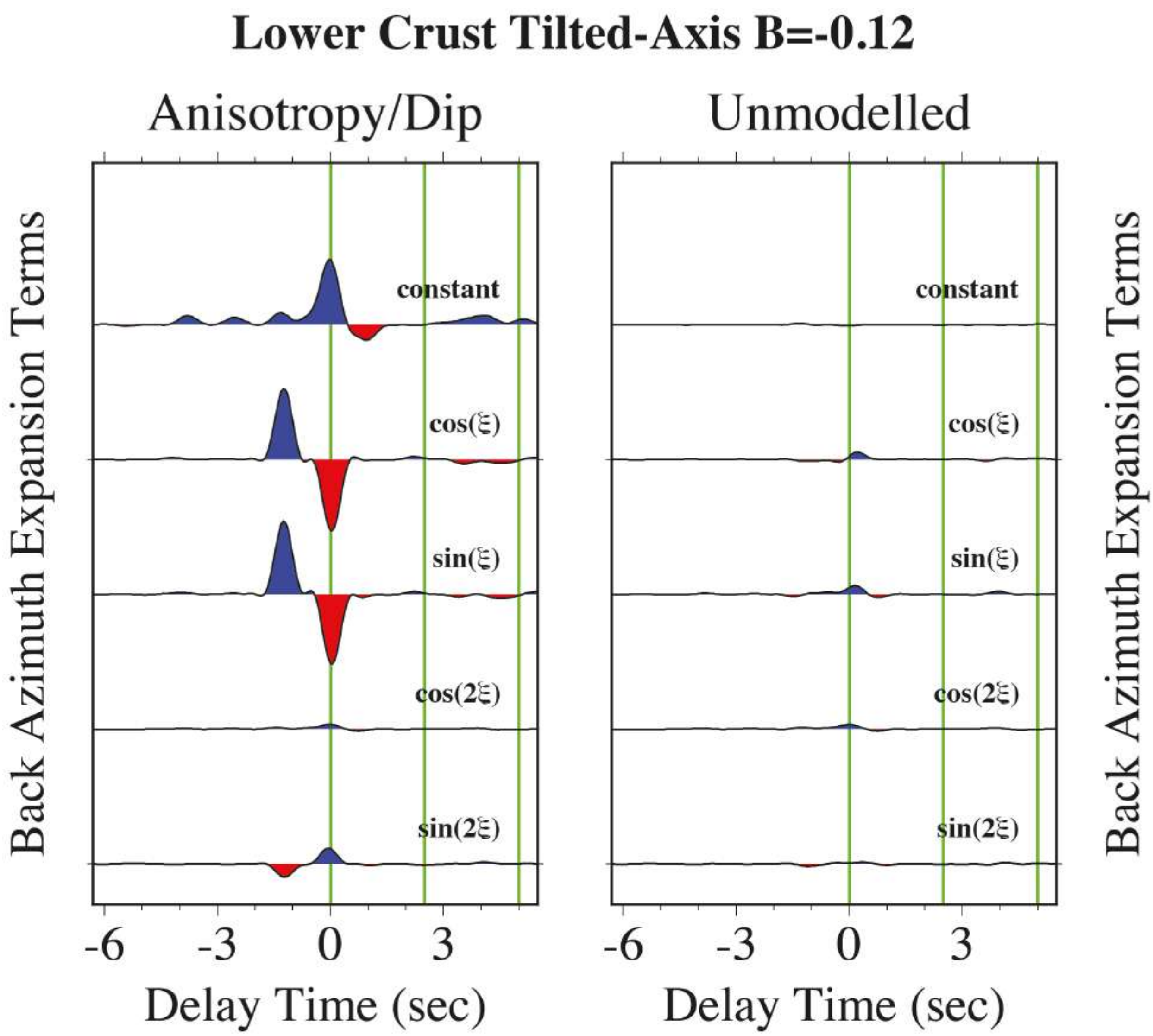

Figure S36. Harmonic terms of back azimuth ξ fit by least-squares in the frequency domain to receiver-functions estimated from synthetic seismograms in a 40-km crust with compressional anisotropy B=-0.12 (12% peak-to-peak P anisotropy) with a slow symmetry axis with 45° tilt in a lower-crustal layer at 30-40-km depth.

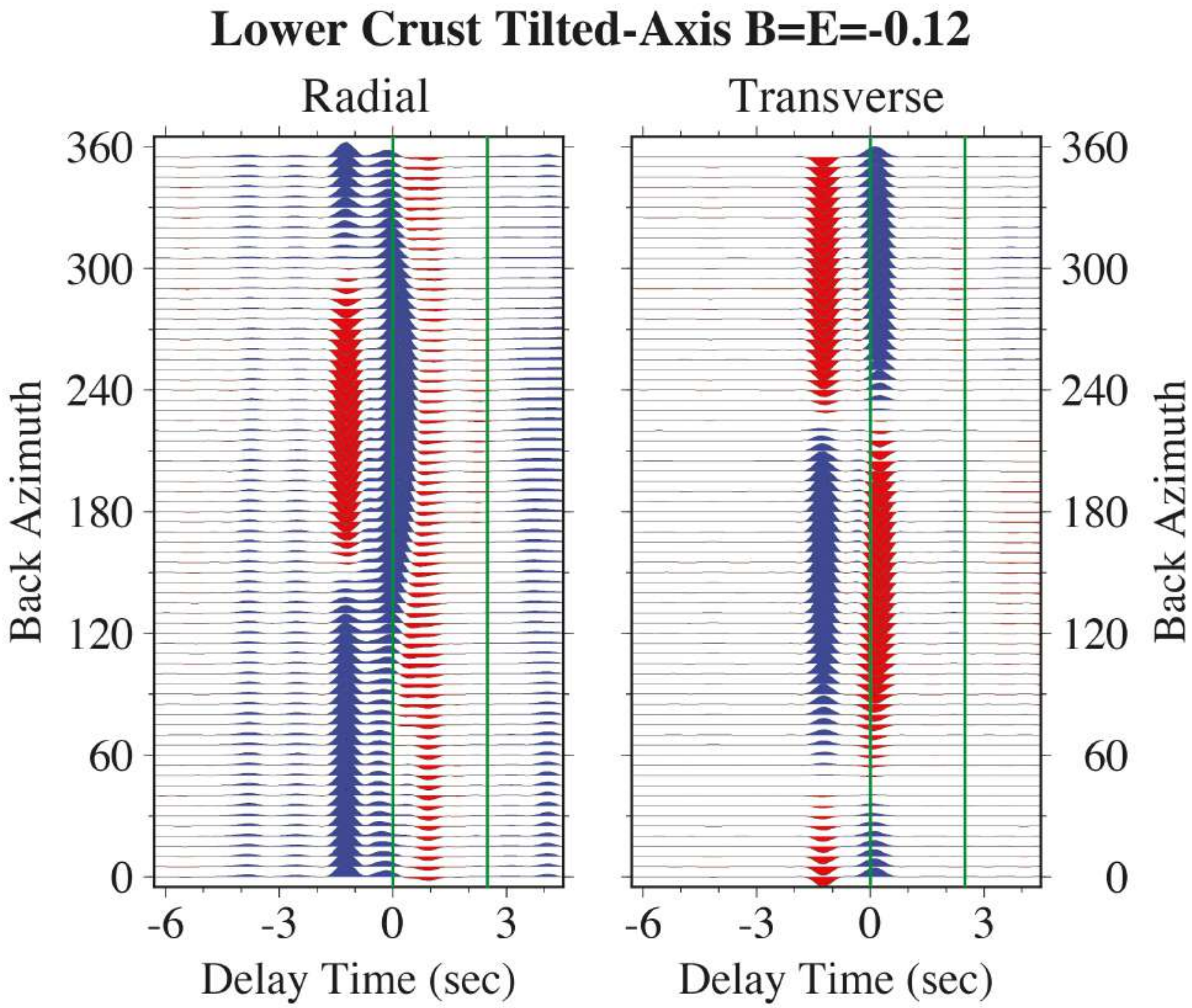

Figure S37. Back-azimuth receiver-function sweeps for synthetic seismograms in a 40-km crust with mixed anisotropy B=E=-0.12 (12% peak-to-peak P and S anisotropy) with a slow symmetry axis with 45° tilt in a lower-crustal layer at 30-40-km depth.

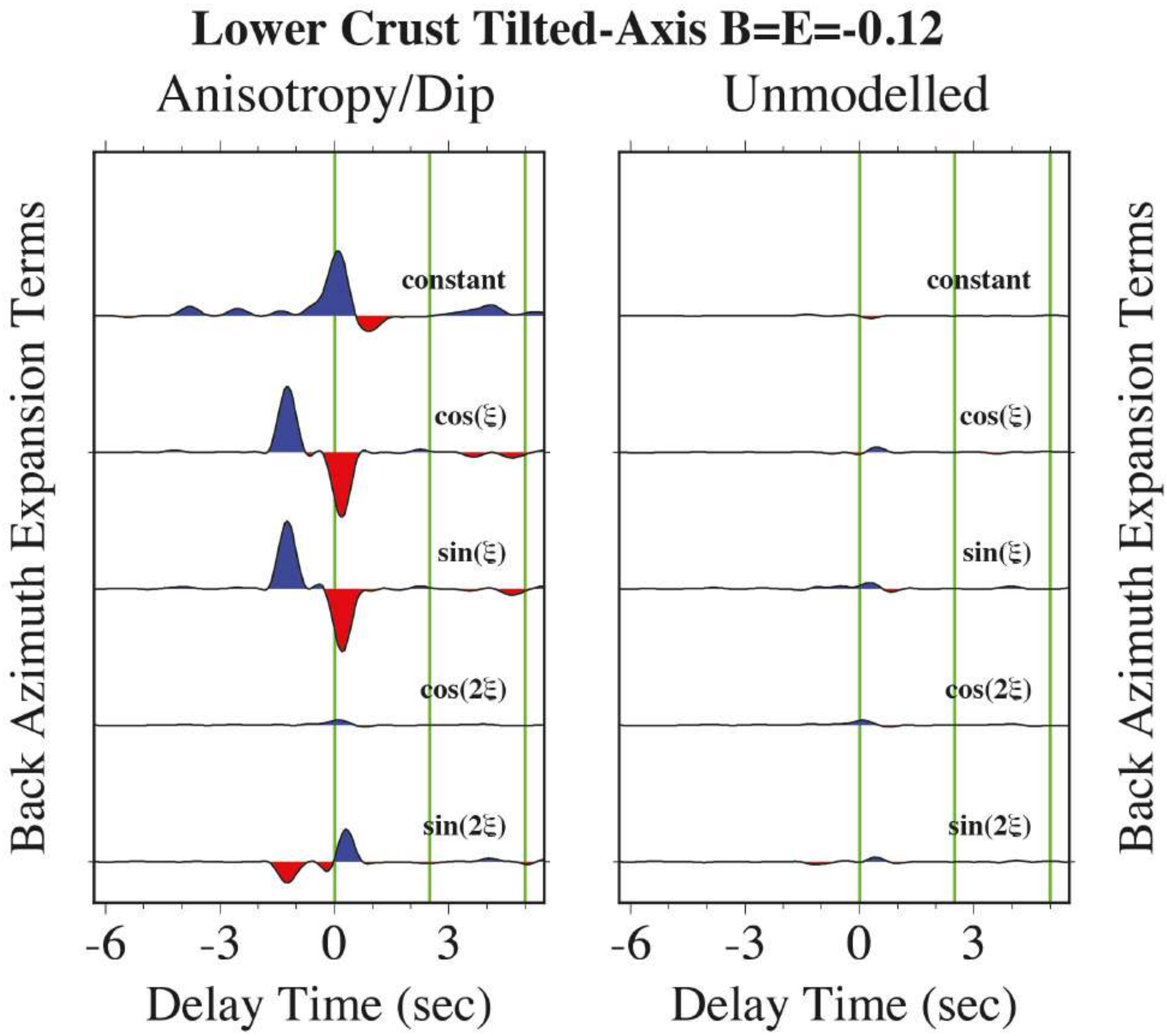

Figure S38. Harmonic terms of back azimuth ξ fit by least-squares in the frequency domain to receiver-functions estimated from synthetic seismograms in a 40-km crust with mixed anisotropy B=E=-0.12 (12% peak-to-peak P and S anisotropy) with a slow symmetry axis with 45° tilt in a lower-crustal layer at 30-40-km depth.

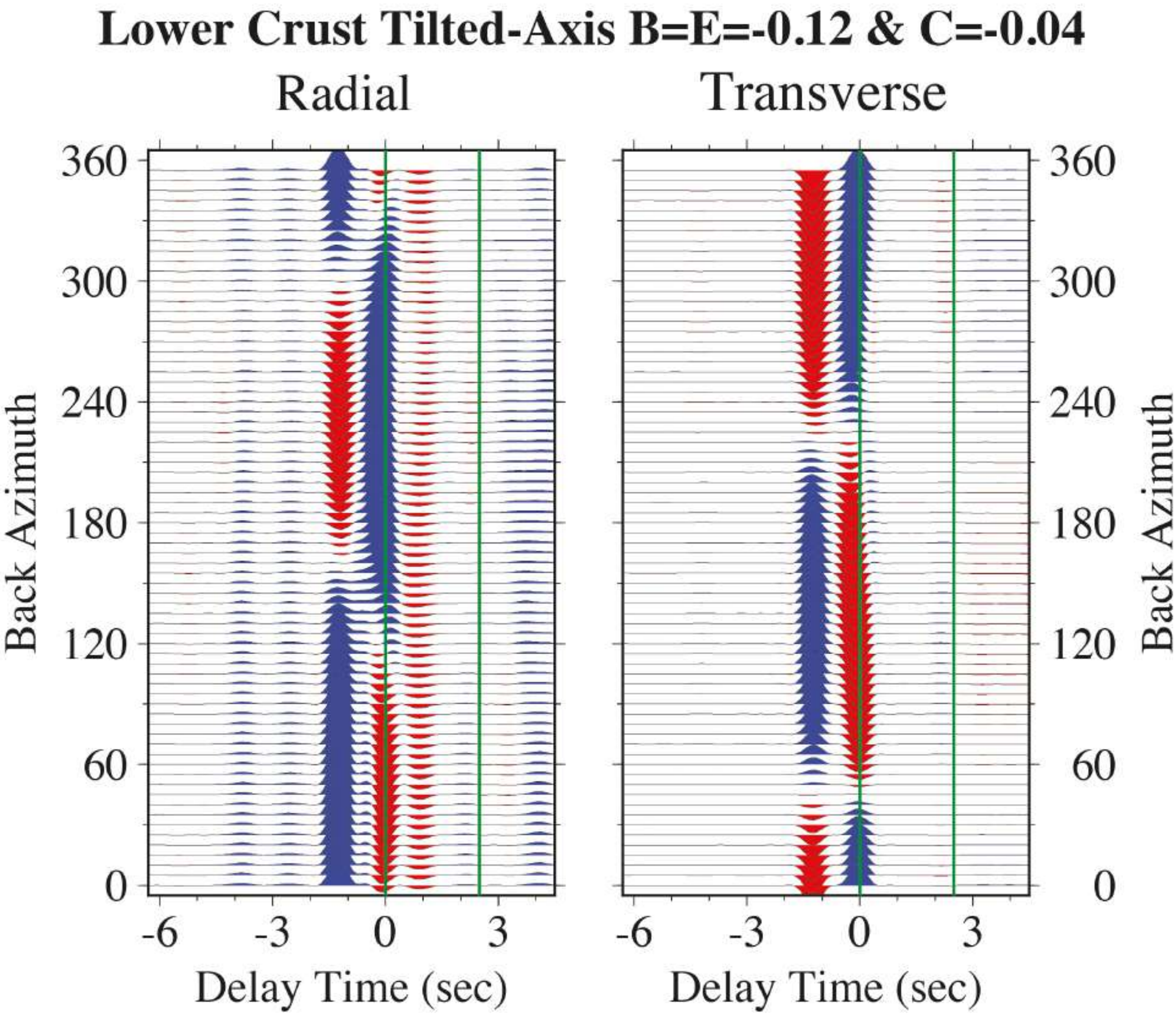

Figure S39. Back-azimuth receiver-function sweeps for synthetic seismograms in a 40-km crust with mixed anisotropy B=E=-0.12 and C=-0.04 with a slow symmetry axis with 45° tilt in a lower-crustal layer at 30-40-km depth. This corresponds to 12% peak-to-peak elliptical P and S anisotropy, plus a cos 4ξ wavespeed variation consistent with Brownlee et al (2017).

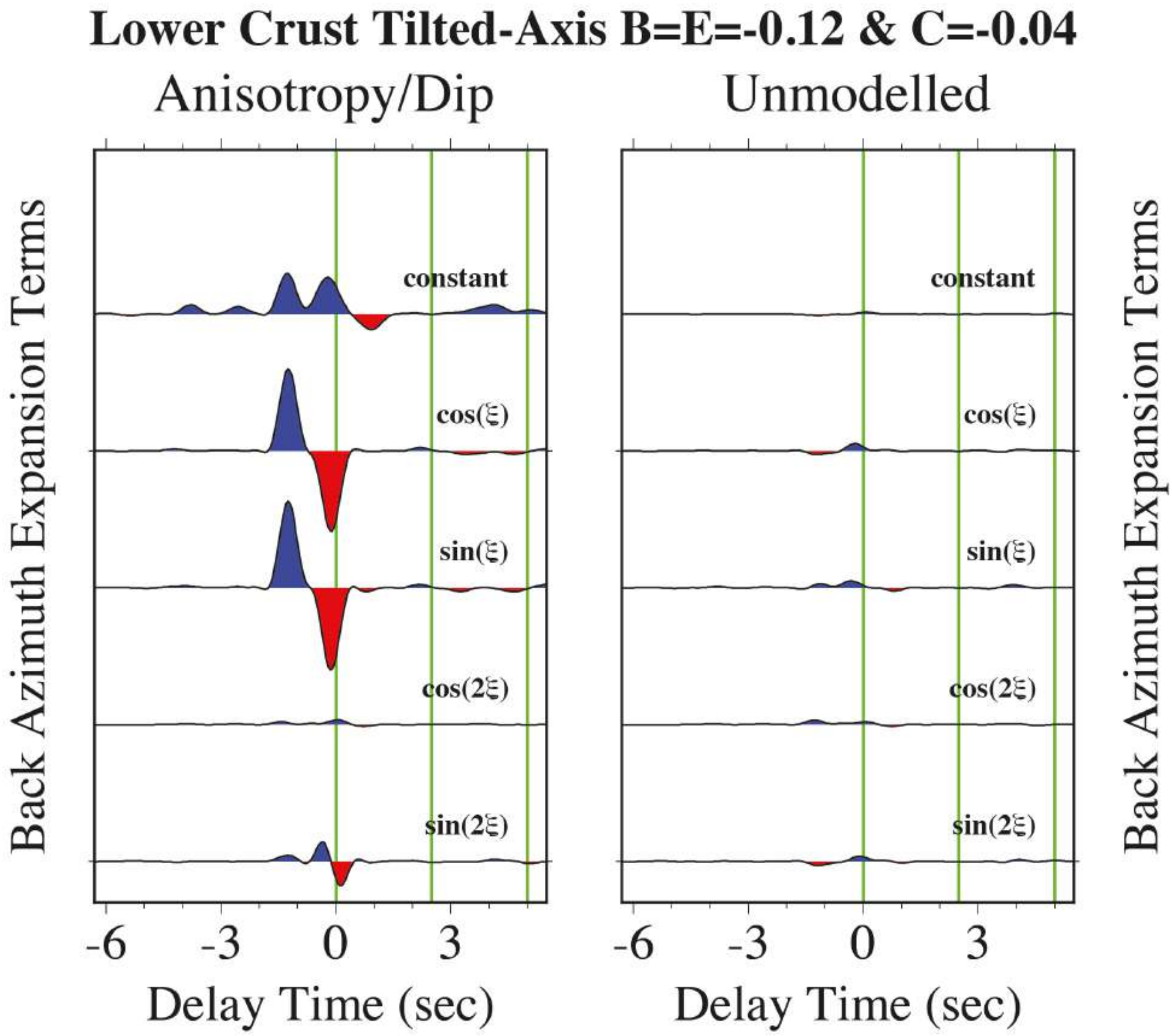

Figure S40. Harmonic terms of back azimuth ξ fit by least-squares in the frequency domain to receiver-functions estimated from synthetic seismograms in a 40-km crust with mixed anisotropy B=E=-0.12 and C=-0.04 with a slow symmetry axis with 45° tilt in a lower-crustal layer at 30-40-km depth. This corresponds to 12% peak-to-peak elliptical P and S anisotropy, plus a cos 4ξ wavespeed variation consistent with Brownlee et al (2017).

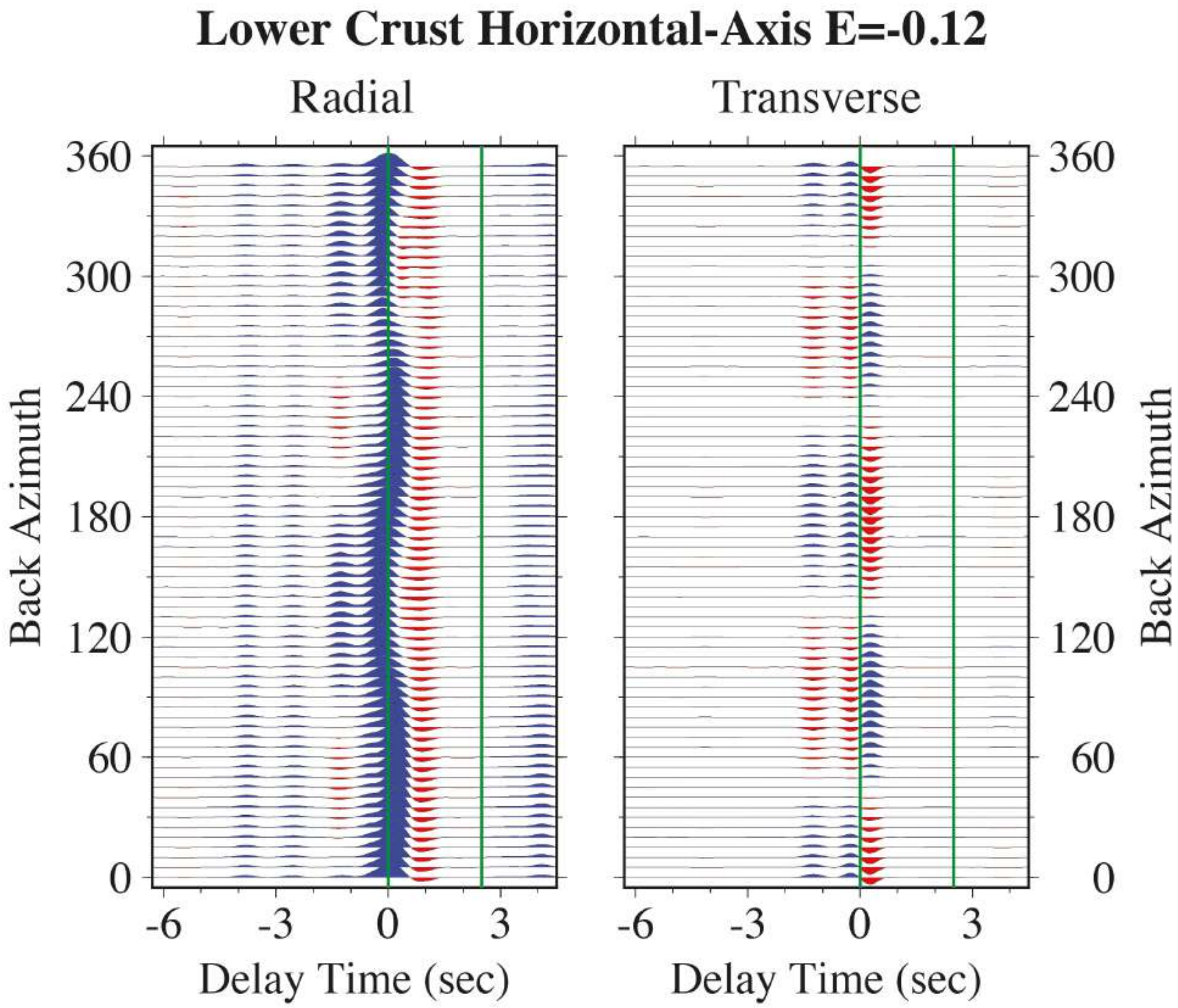

Figure S41. Back-azimuth receiver-function sweeps for synthetic seismograms in a 40-km crust with shear anisotropy E=-0.12 (12% peak-to-peak S anisotropy) with a horizontal slow symmetry axis in a lower-crustal layer at 30-40-km depth.

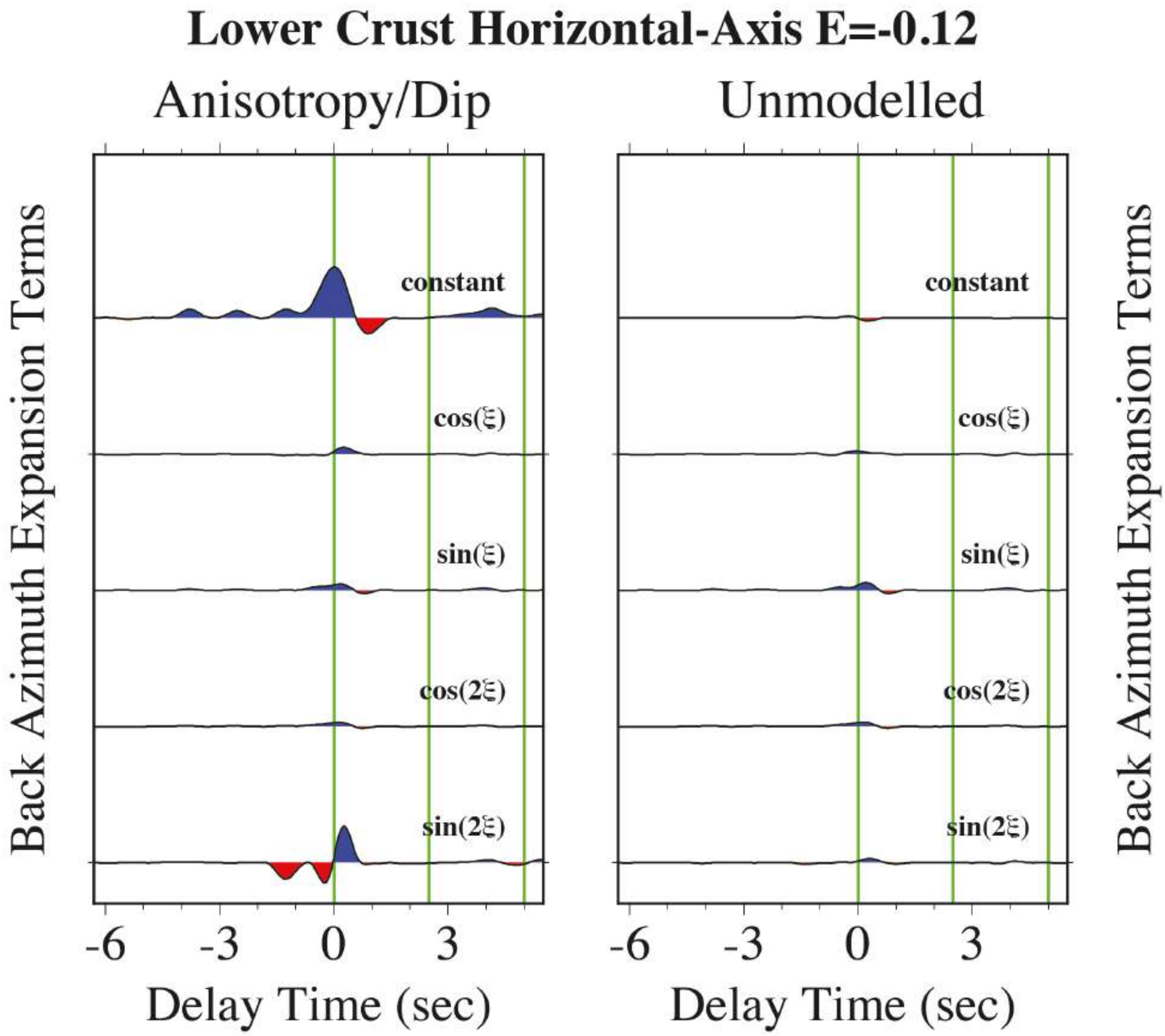

Figure S42. Harmonic terms of back azimuth ξ fit by least-squares in the frequency domain to receiver-functions estimated from synthetic seismograms in a 40-km crust with shear anisotropy E=-0.12 (12% peak-to-peak S anisotropy) with a horizontal slow symmetry axis in a lower-crustal layer at 30-40-km depth.

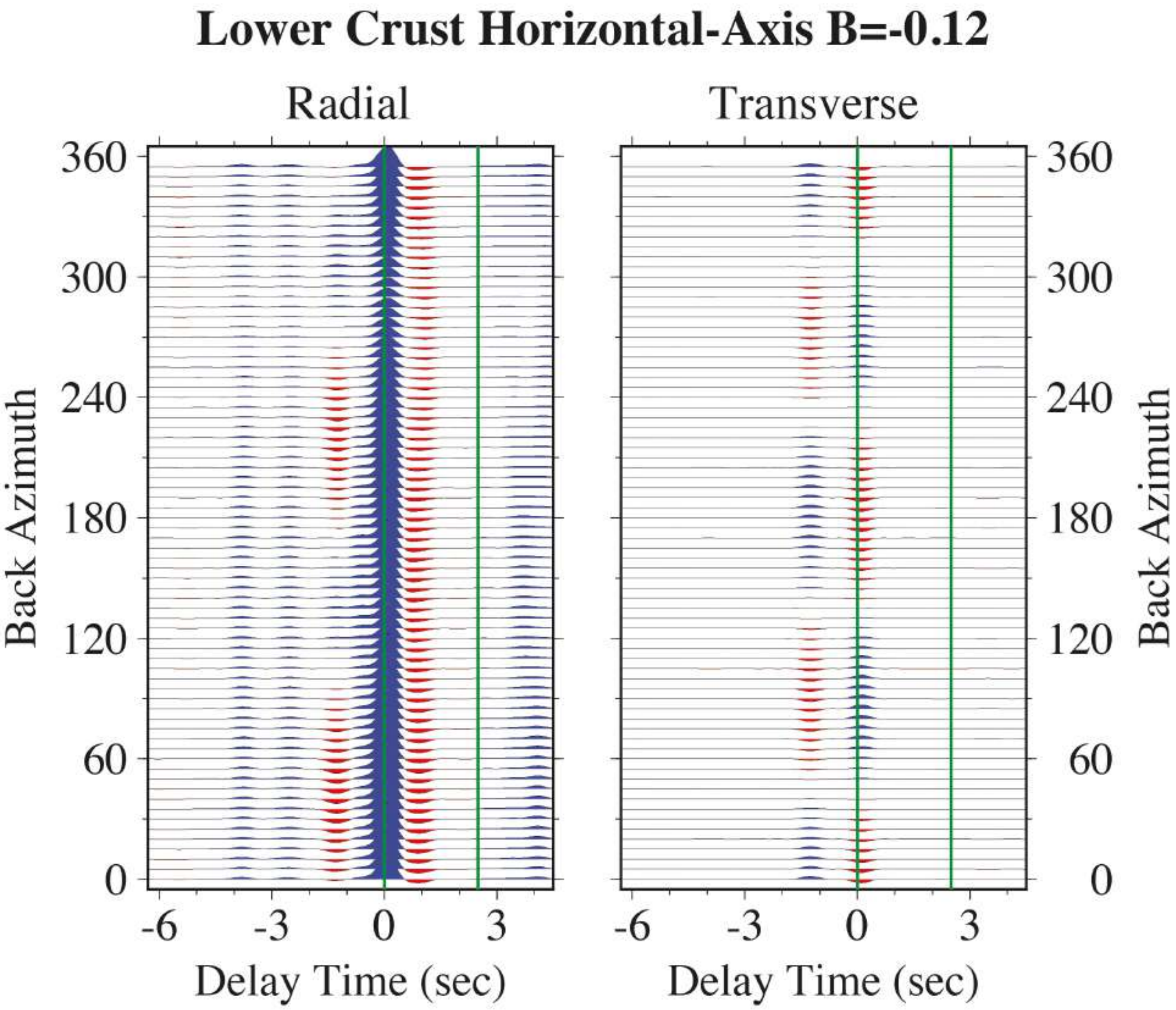

Figure S43. Back-azimuth receiver-function sweeps for synthetic seismograms in a 40-km crust with compressional anisotropy B=-0.12 (12% peak-to-peak P anisotropy) with a horizontal slow symmetry axis in a lower-crustal layer at 30-40-km depth.

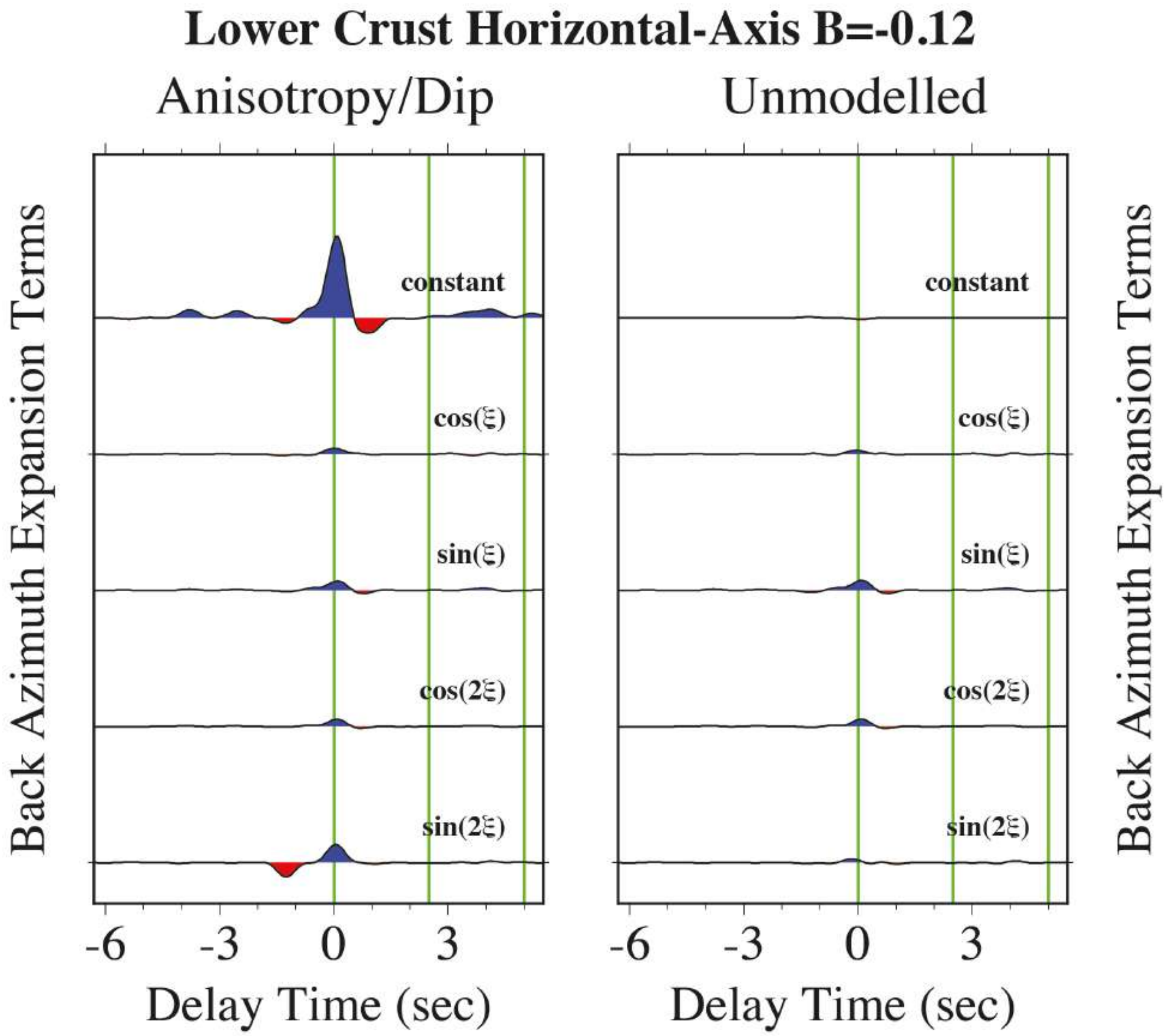

Figure S44. Harmonic terms of back azimuth ξ fit by least-squares in the frequency domain to receiver-functions estimated from synthetic seismograms in a 40-km crust with compressional anisotropy B=-0.12 (12% peak-to-peak P anisotropy) with a horizontal slow symmetry axis in a lower-crustal layer at 30-40-km depth.

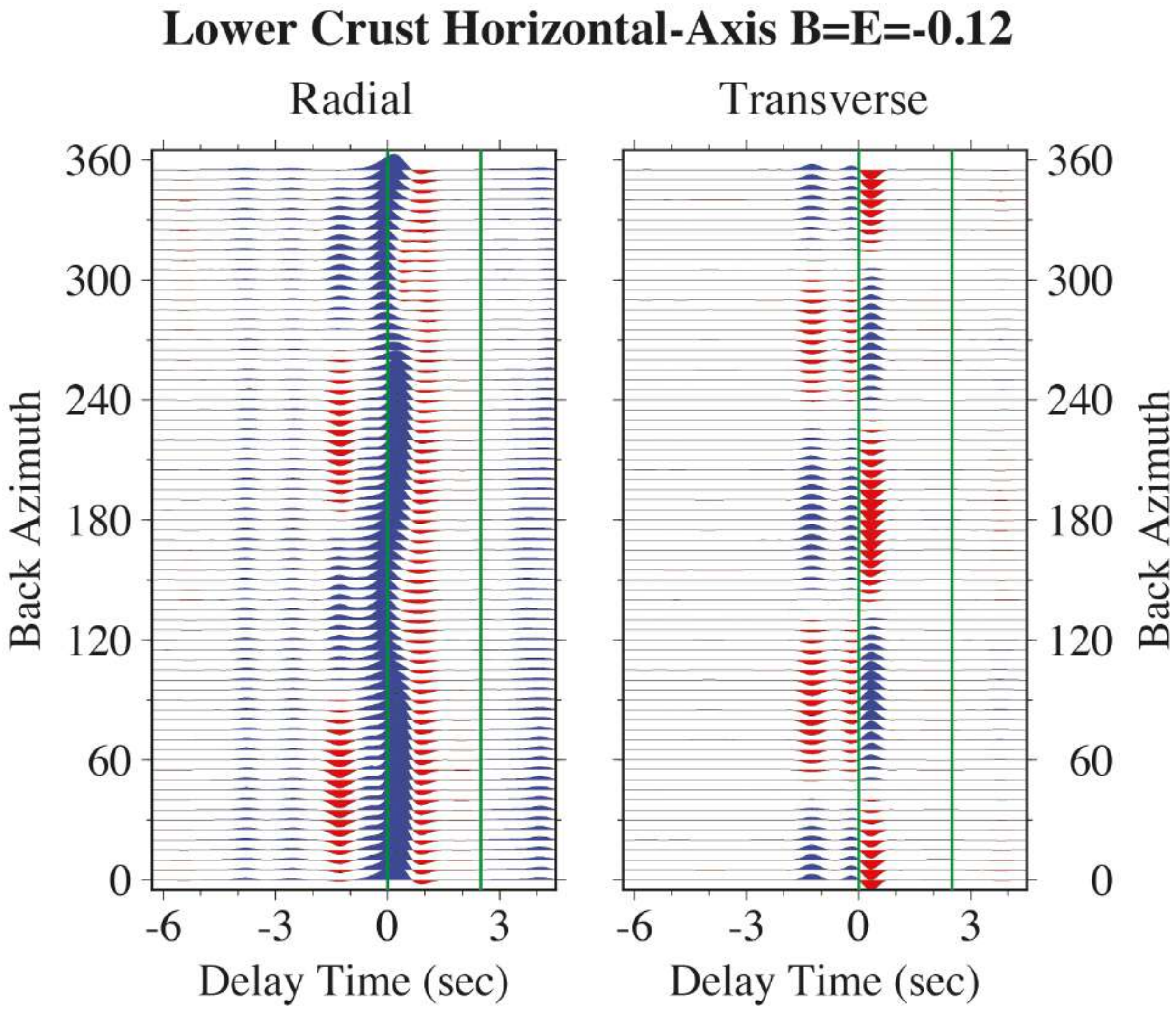

Figure S45. Back-azimuth receiver-function sweeps for synthetic seismograms in a 40-km crust with mixed anisotropy B=E=-0.12 (12% peak-to-peak P and S anisotropy) with a horizontal slow symmetry axis in a lower-crustal layer at 30-40-km depth.

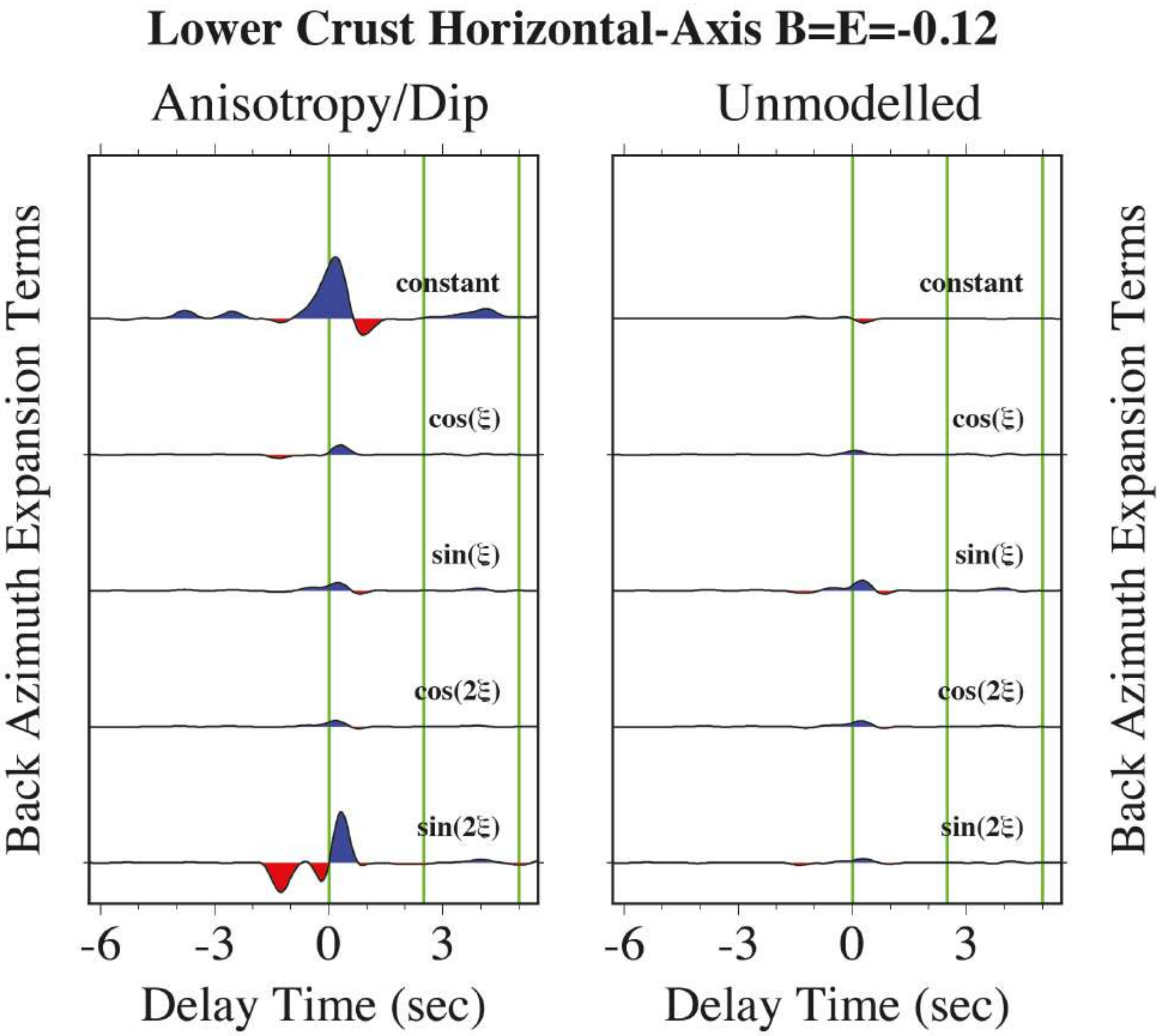

Figure S46. Harmonic terms of back azimuth ξ fit by least-squares in the frequency domain to receiver-functions estimated from synthetic seismograms in a 40-km crust with mixed anisotropy B=E=-0.12 (12% peak-to-peak P and S anisotropy) with a horizontal slow symmetry axis in a lower-crustal layer at 30-40-km depth.

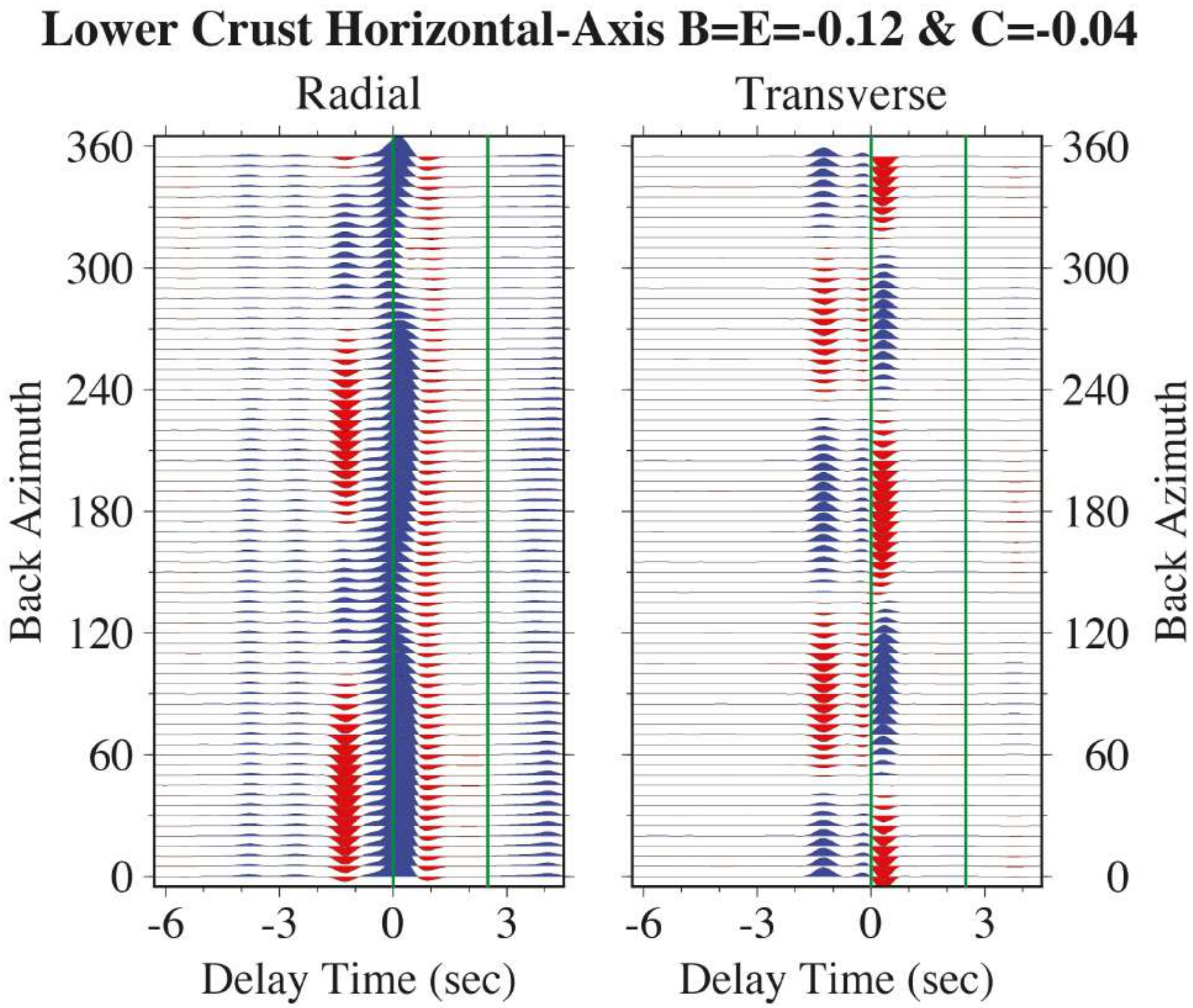

Figure S47. Back-azimuth receiver-function sweeps for synthetic seismograms in a 40-km crust with mixed anisotropy B=E=-0.12 and C=-0.04 with a horizontal slow symmetry axis in a lower-crustal layer at 30-40-km depth. This corresponds to 12% peak-to-peak elliptical P and S anisotropy, plus a cos 4ξ wavespeed variation consistent with Brownlee et al (2017).

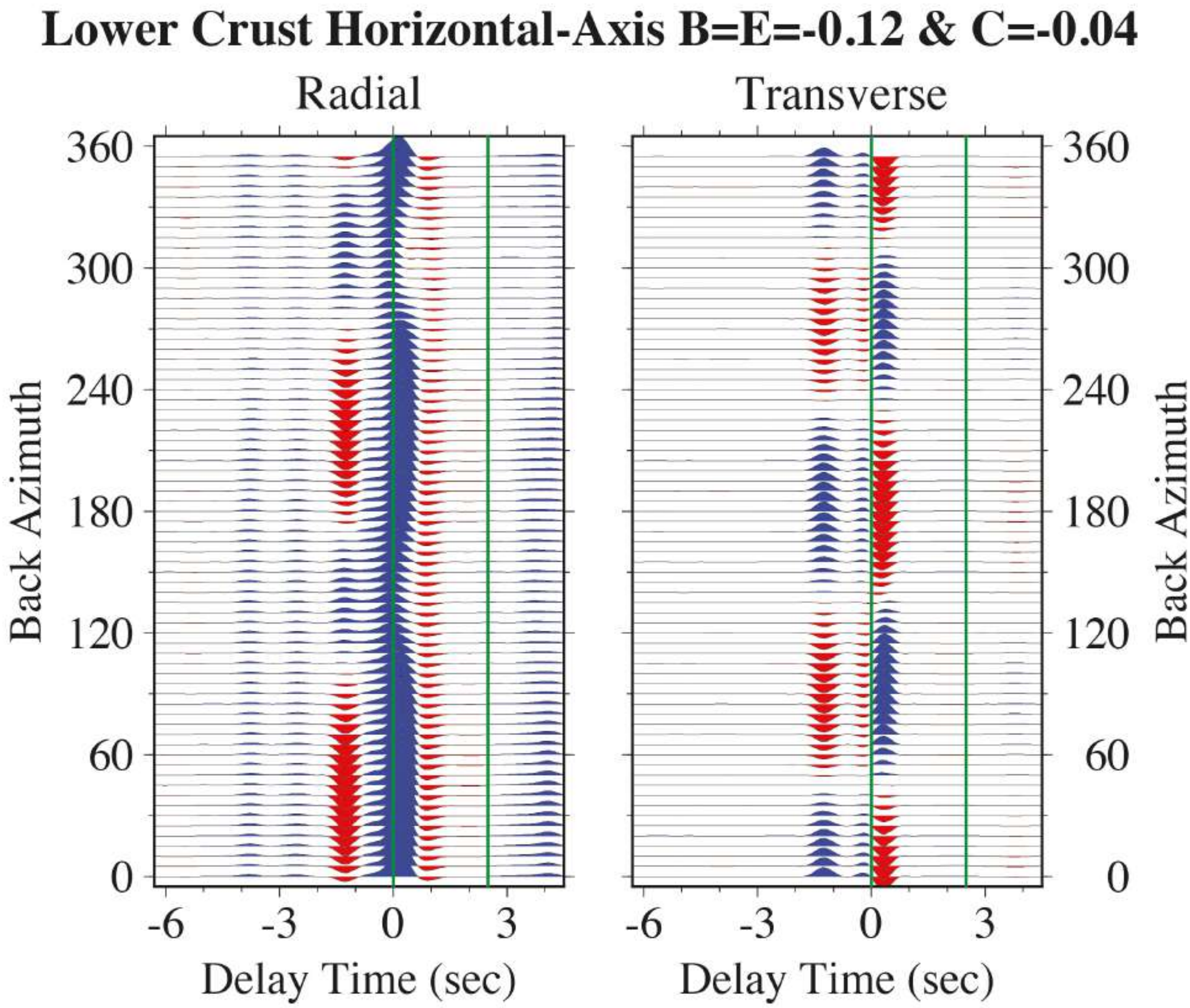

Figure S48. Harmonic terms of back azimuth ξ fit by least-squares in the frequency domain to receiver-functions estimated from synthetic seismograms in a 40-km crust with mixed anisotropy B=E=-0.12 and C=-0.04 with a horizontal slow symmetry axis in a lower-crustal layer at 30-40-km depth. This corresponds to 12% peak-to-peak elliptical P and S anisotropy, plus a cos 4ξ wavespeed variation consistent with Brownlee et al (2017).

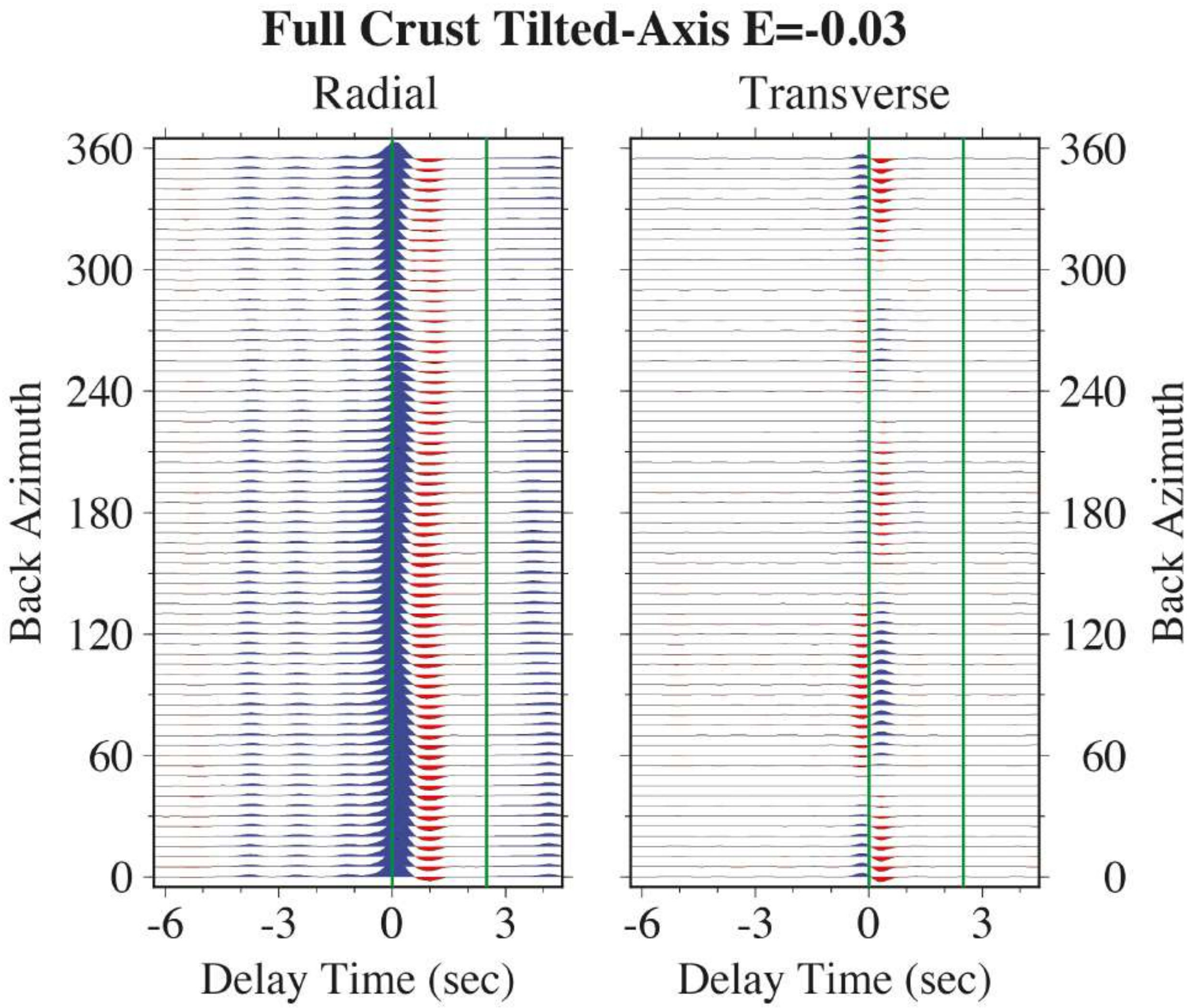

Figure S49. Back-azimuth receiver-function sweeps for synthetic seismograms in a 40-km crust with shear anisotropy E=-0.03 (3% peak-to-peak S anisotropy) with a slow symmetry axis with 45° tilt in the full 40-km crust.

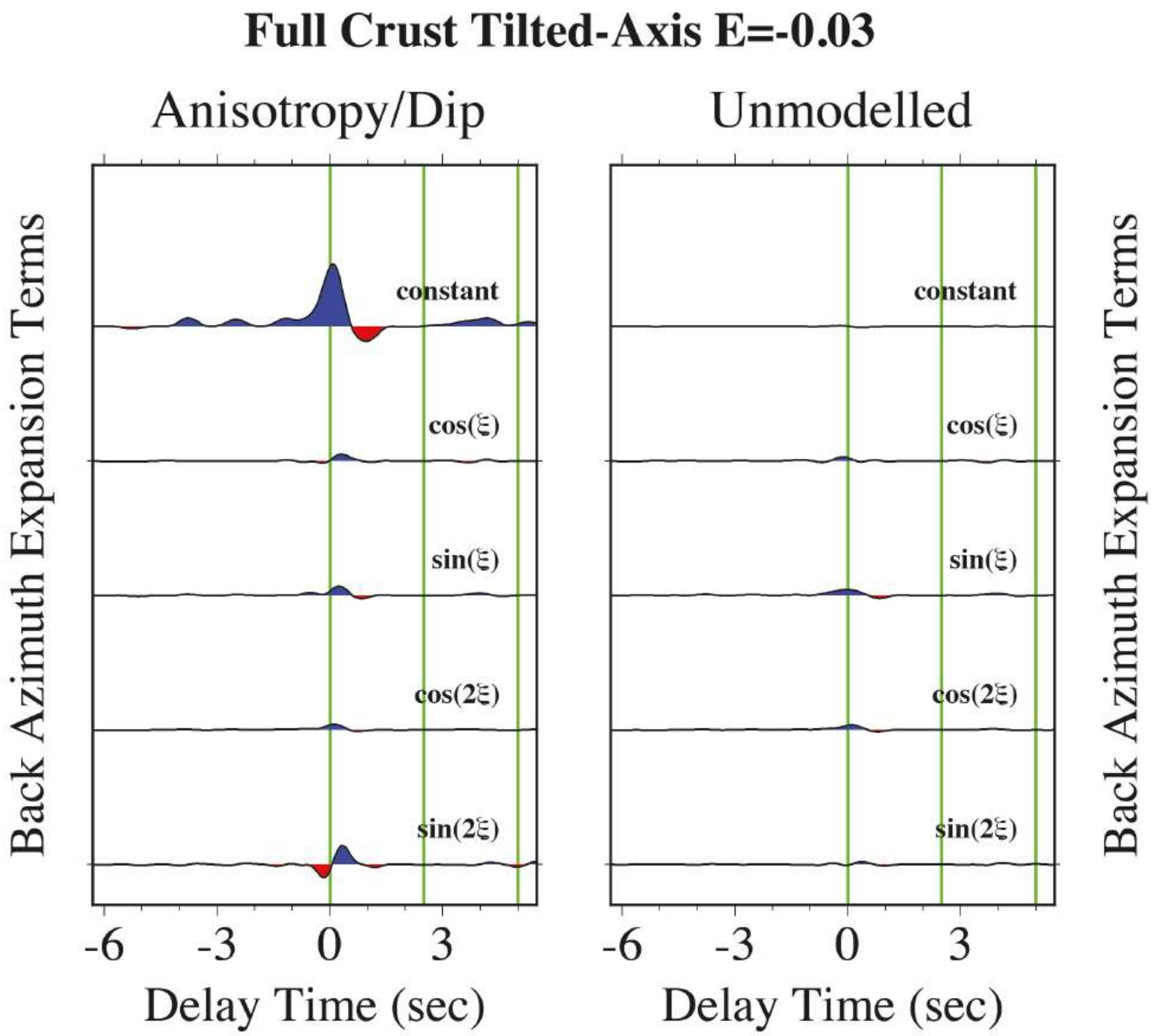

Figure S50. Harmonic terms of back azimuth ξ fit by least-squares in the frequency domain to receiver-functions estimated from synthetic seismograms in a 40-km crust with shear anisotropy E=-0.03 (3% peak-to-peak S anisotropy) with a slow symmetry axis with 45° tilt in the full 40-km crust.

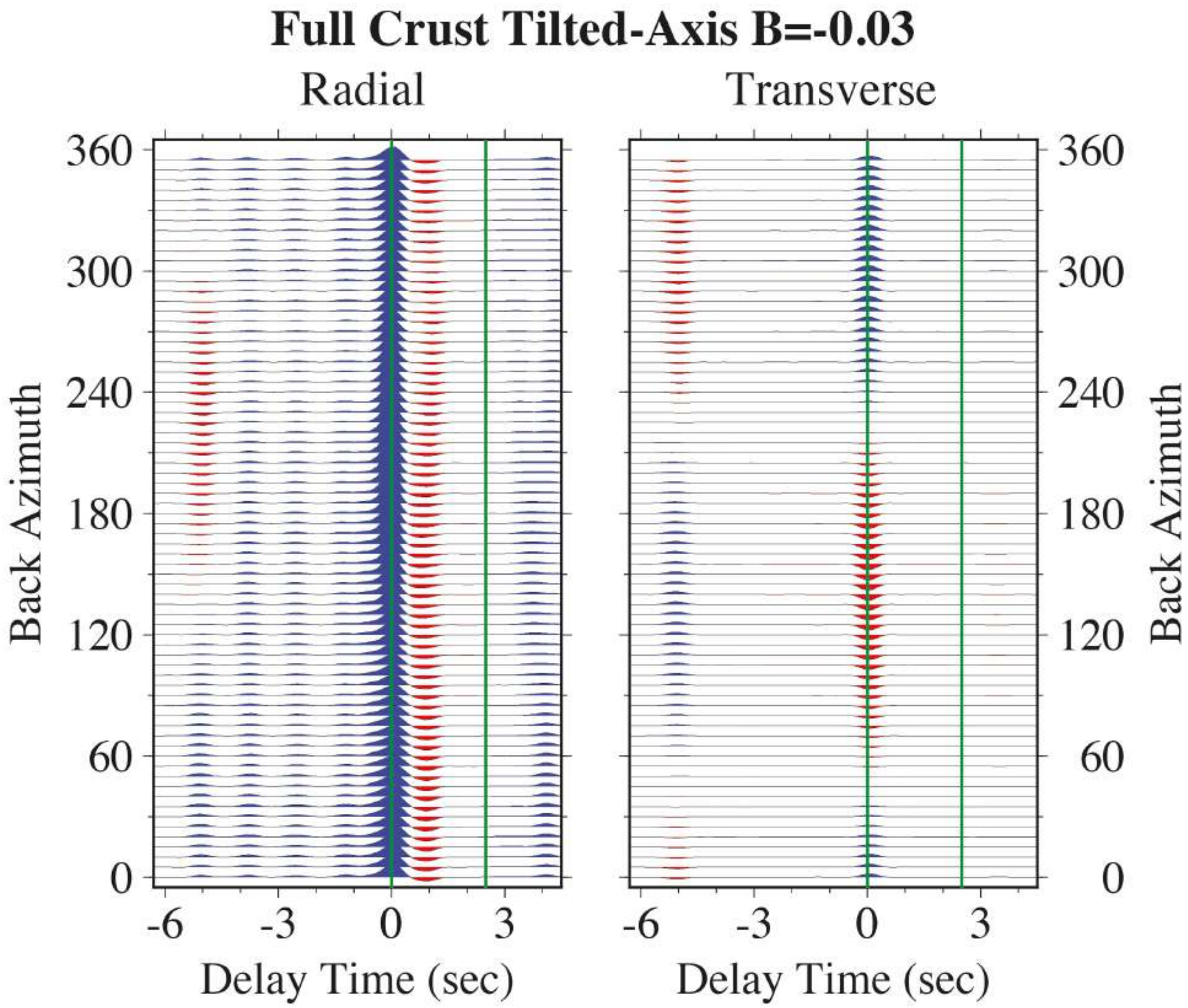

Figure S51. Back-azimuth receiver-function sweeps for synthetic seismograms in a 40-km crust with compressional anisotropy B=-0.03 (3% peak-to-peak P anisotropy) with a slow symmetry axis with 45° tilt in the full 40-km crust.

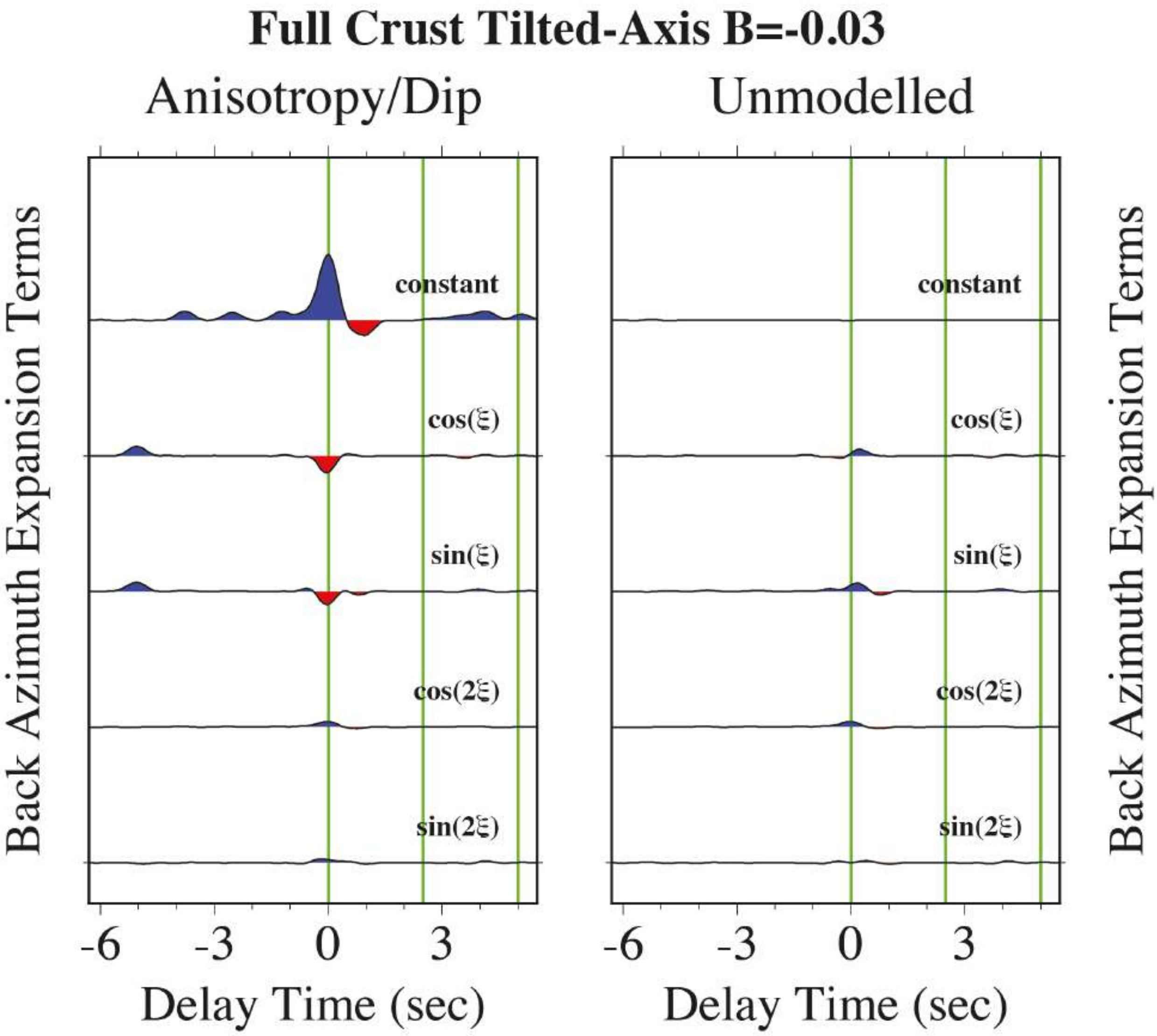

Figure S52. Harmonic terms of back azimuth ξ fit by least-squares in the frequency domain to receiver-functions estimated from synthetic seismograms in a 40-km crust with compressional anisotropy B=-0.03 (3% peak-to-peak P anisotropy) with a slow symmetry axis with 45° tilt in the full 40-km crust.

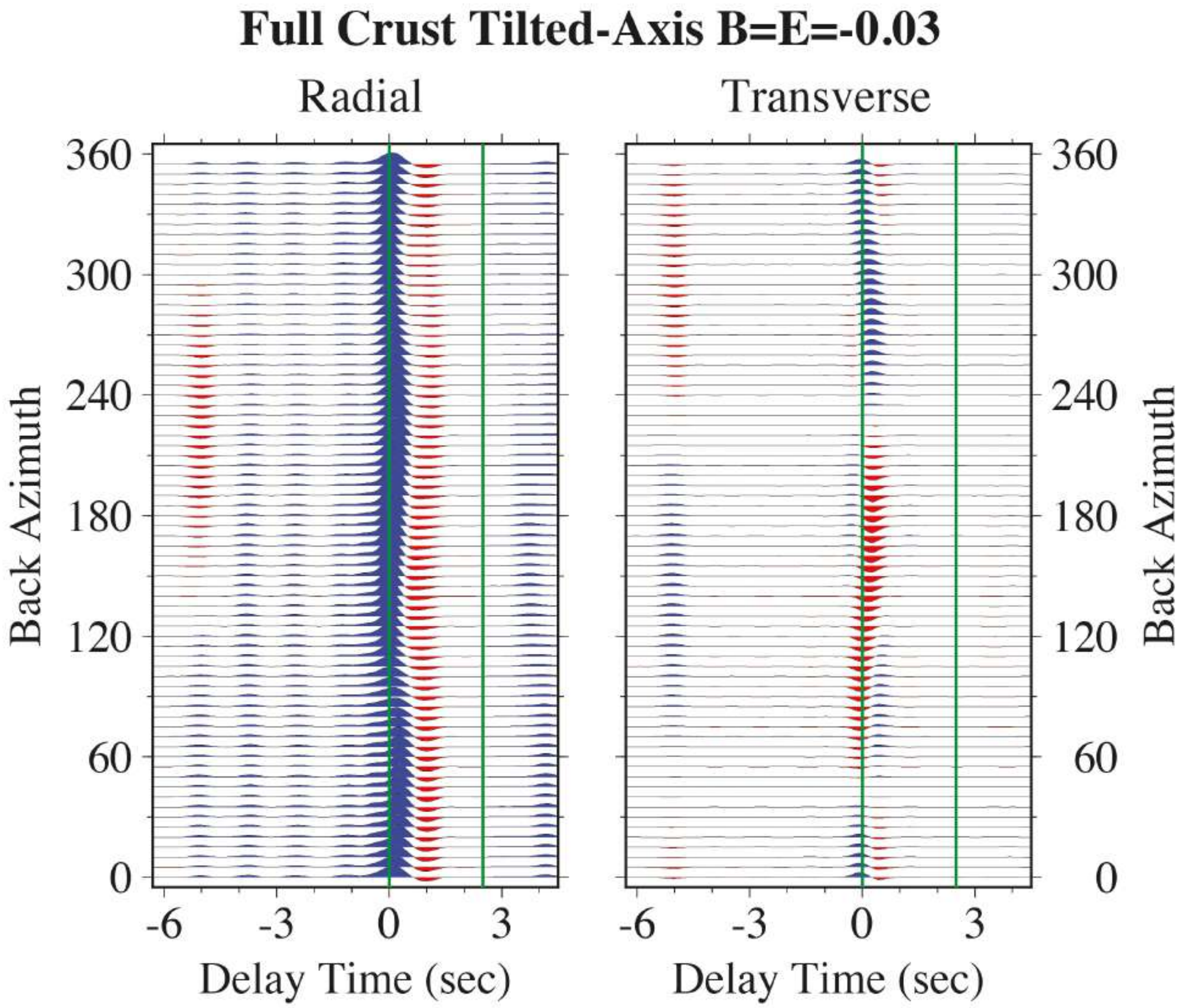

Figure S53. Back-azimuth receiver-function sweeps for synthetic seismograms in a 40-km crust with mixed anisotropy B=E=-0.03 (3% peak-to-peak P and S anisotropy) with a slow symmetry axis with 45° tilt in the full 40-km crust.

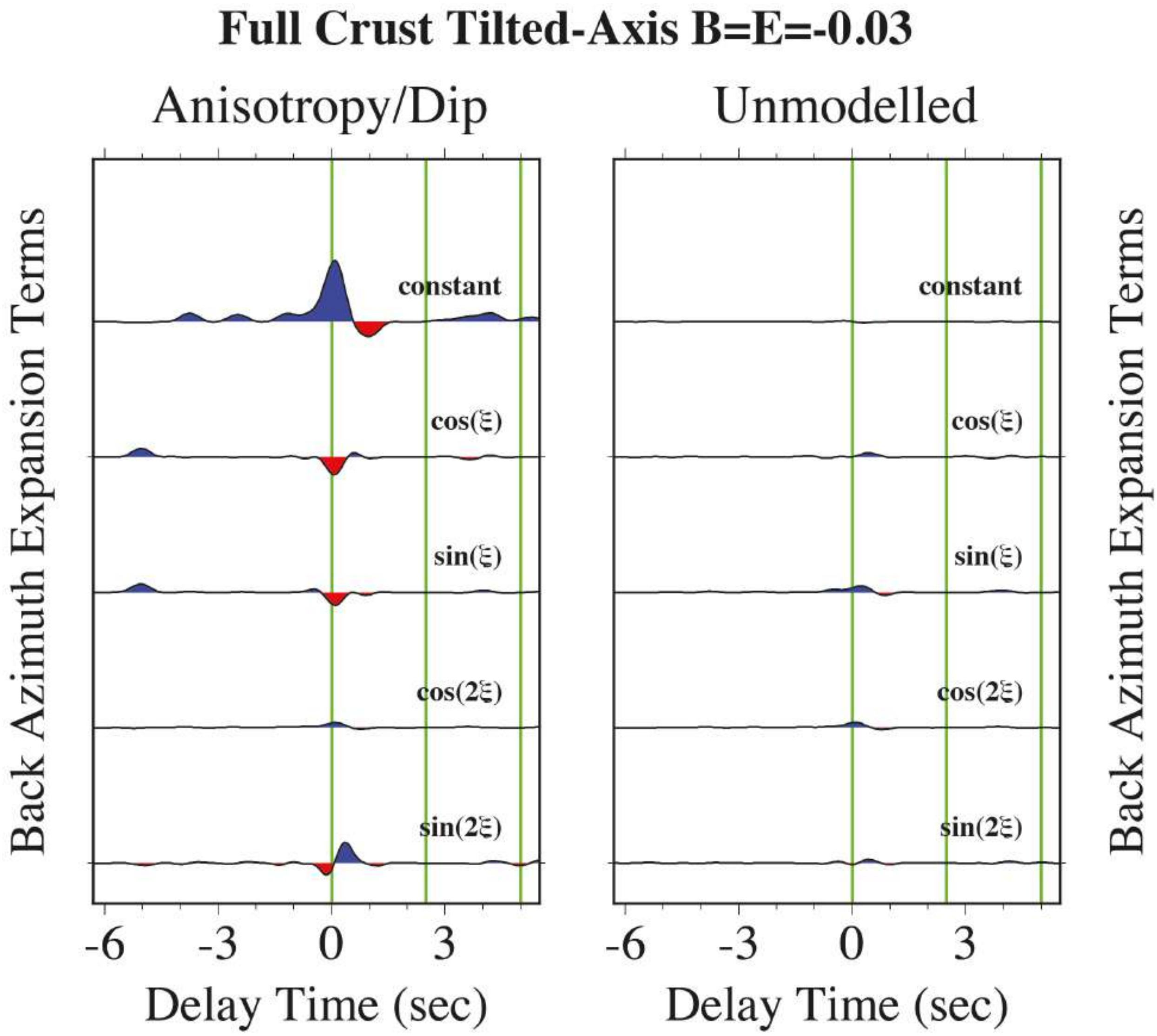

Figure S54. Harmonic terms of back azimuth ξ fit by least-squares in the frequency domain to receiver-functions estimated from synthetic seismograms in a 40-km crust with mixed anisotropy B=E=-0.03 (3% peak-to-peak P and S anisotropy) with a slow symmetry axis with 45° tilt in the full 40-km crust.

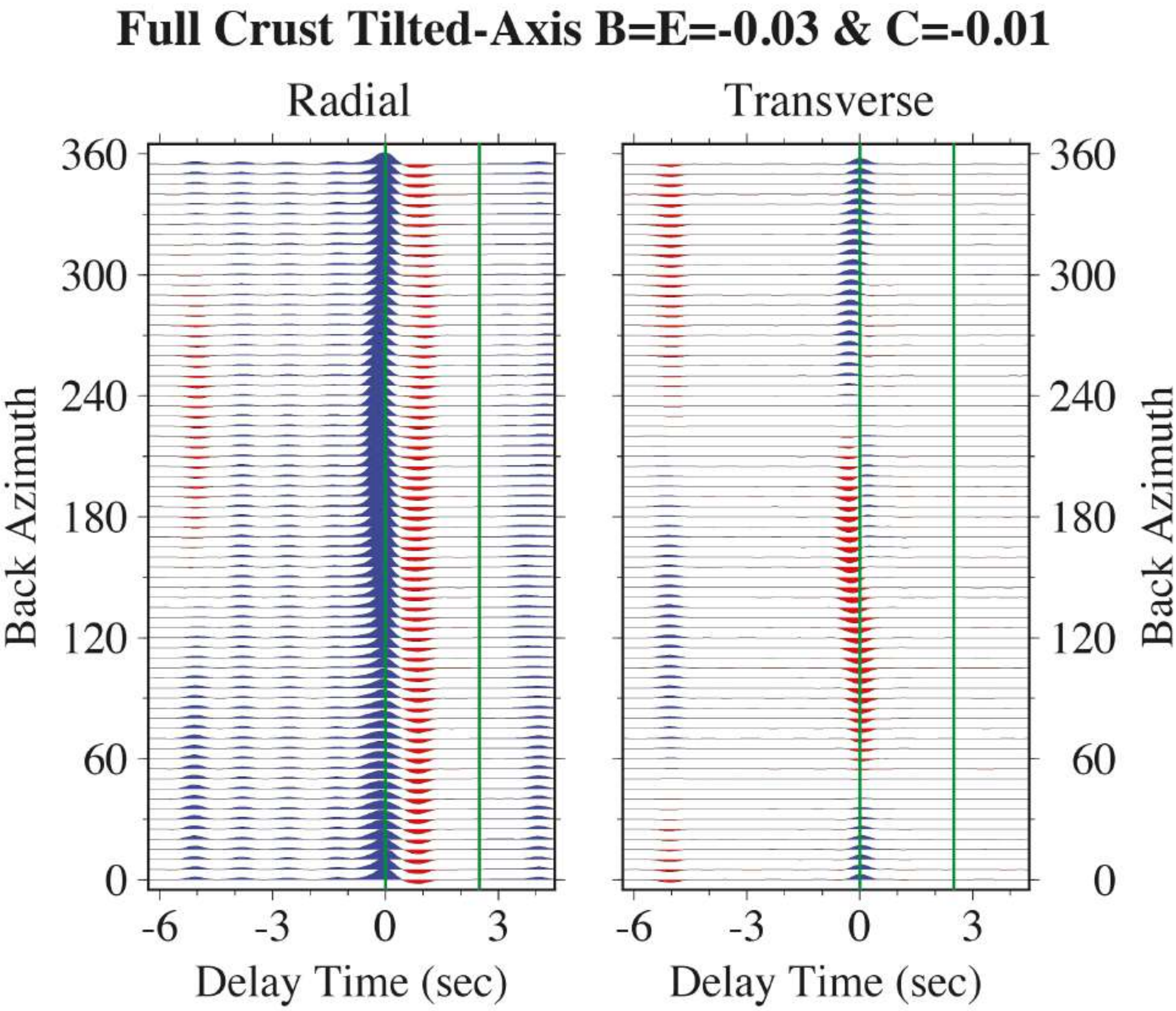

Figure S55. Back-azimuth receiver-function sweeps for synthetic seismograms in a 40-km crust with mixed anisotropy B=E=-0.03 and C=-0.01 with a slow symmetry axis with 45° tilt in the full 40-km crust. This corresponds to 3% peak-to-peak elliptical P and S anisotropy, plus a cos 4ξ wavespeed variation consistent with Brownlee et al (2017).

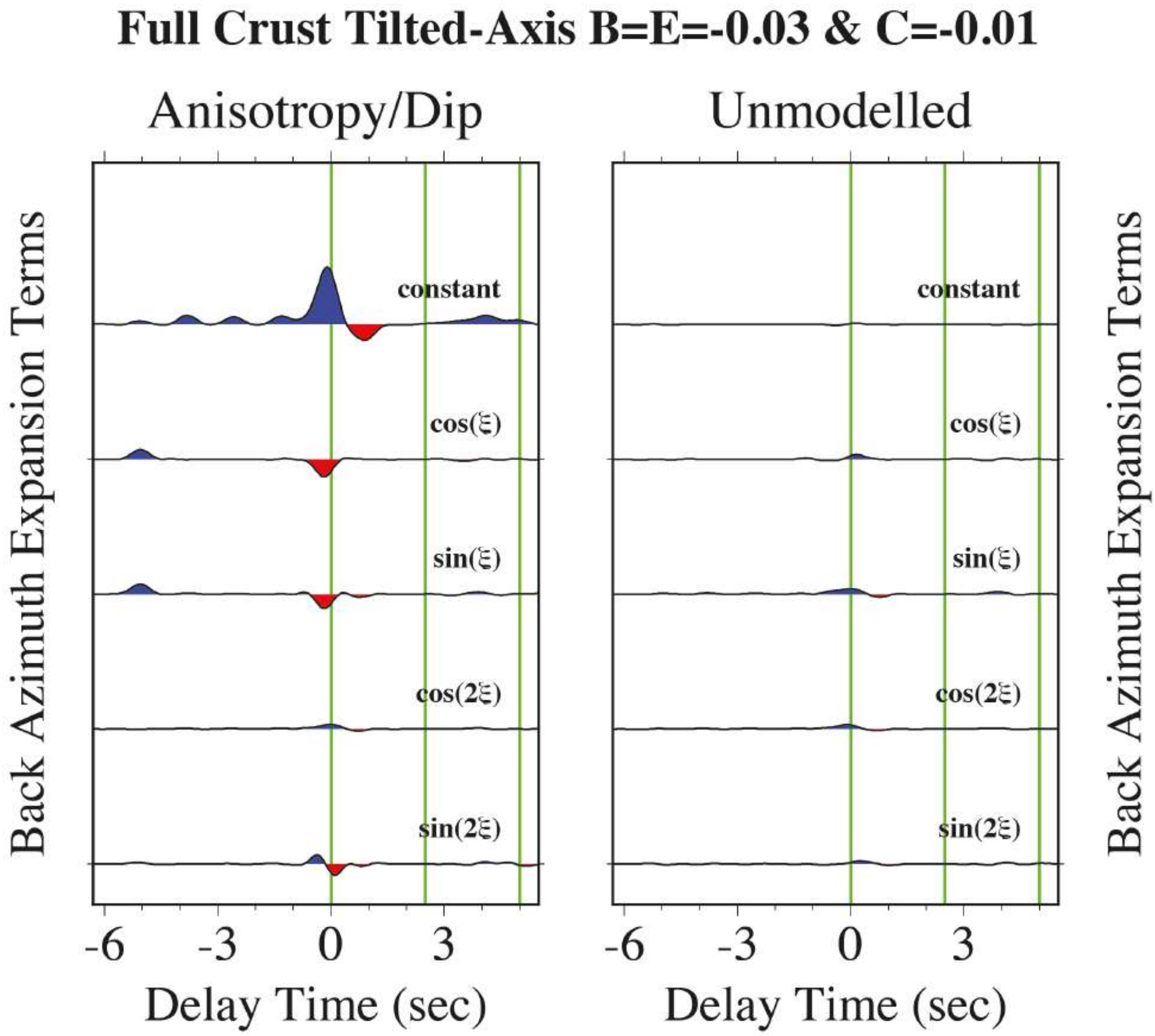

Figure S56. Harmonic terms of back azimuth ξ fit by least-squares in the frequency domain to receiver-functions estimated from synthetic seismograms in a 40-km crust with mixed anisotropy B=E=-0.03 and C=-0.01 with a slow symmetry axis with 45° tilt in the full 40-km crust. This corresponds to 3% peak-to-peak elliptical P and S anisotropy, plus a cos 4ξ wavespeed variation consistent with Brownlee et al (2017).

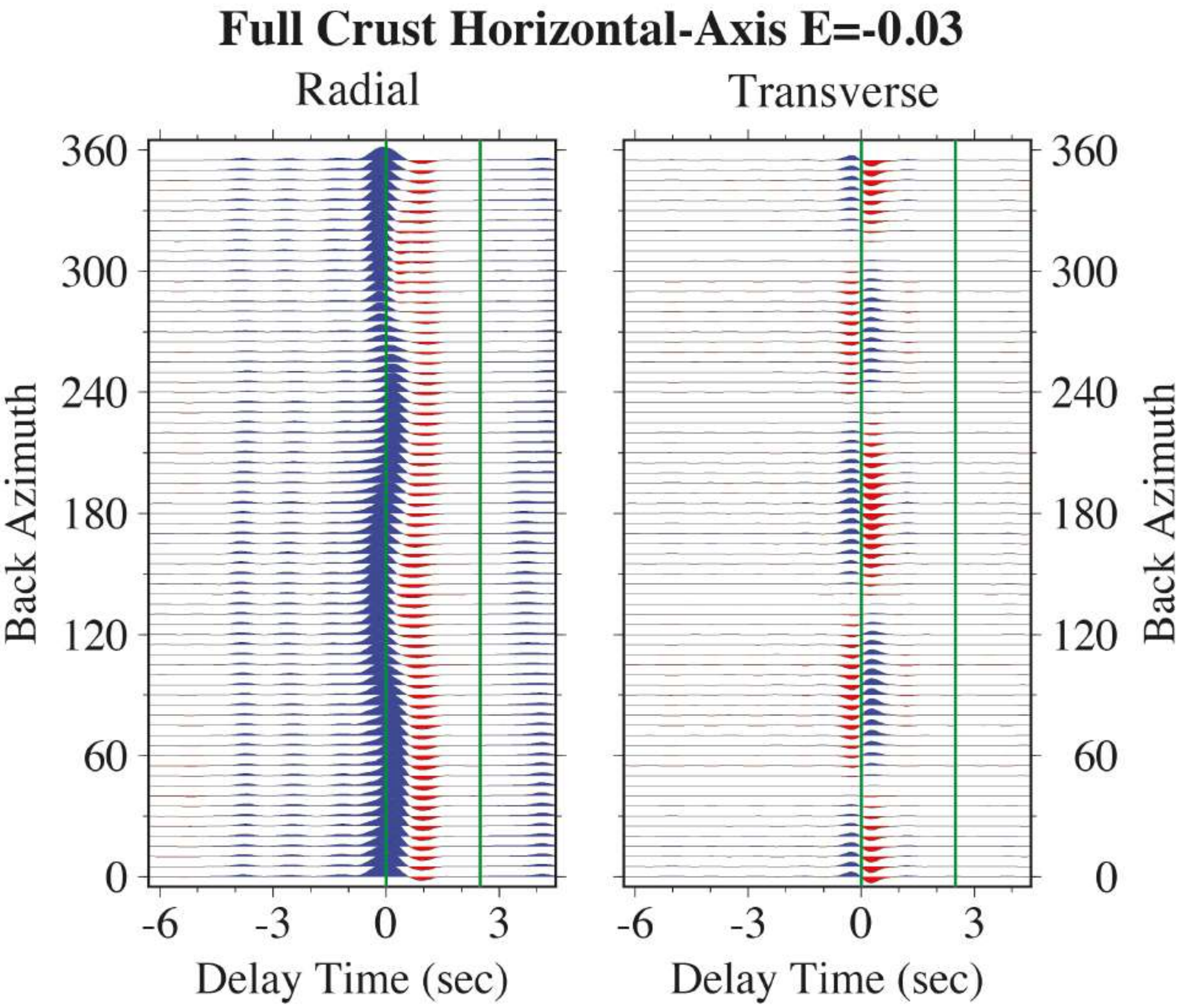

Figure S57. Back-azimuth receiver-function sweeps for synthetic seismograms in a 40-km crust with shear anisotropy E=-0.03 (3% peak-to-peak S anisotropy) with a horizontal slow symmetry axis in the full 40-km crust.

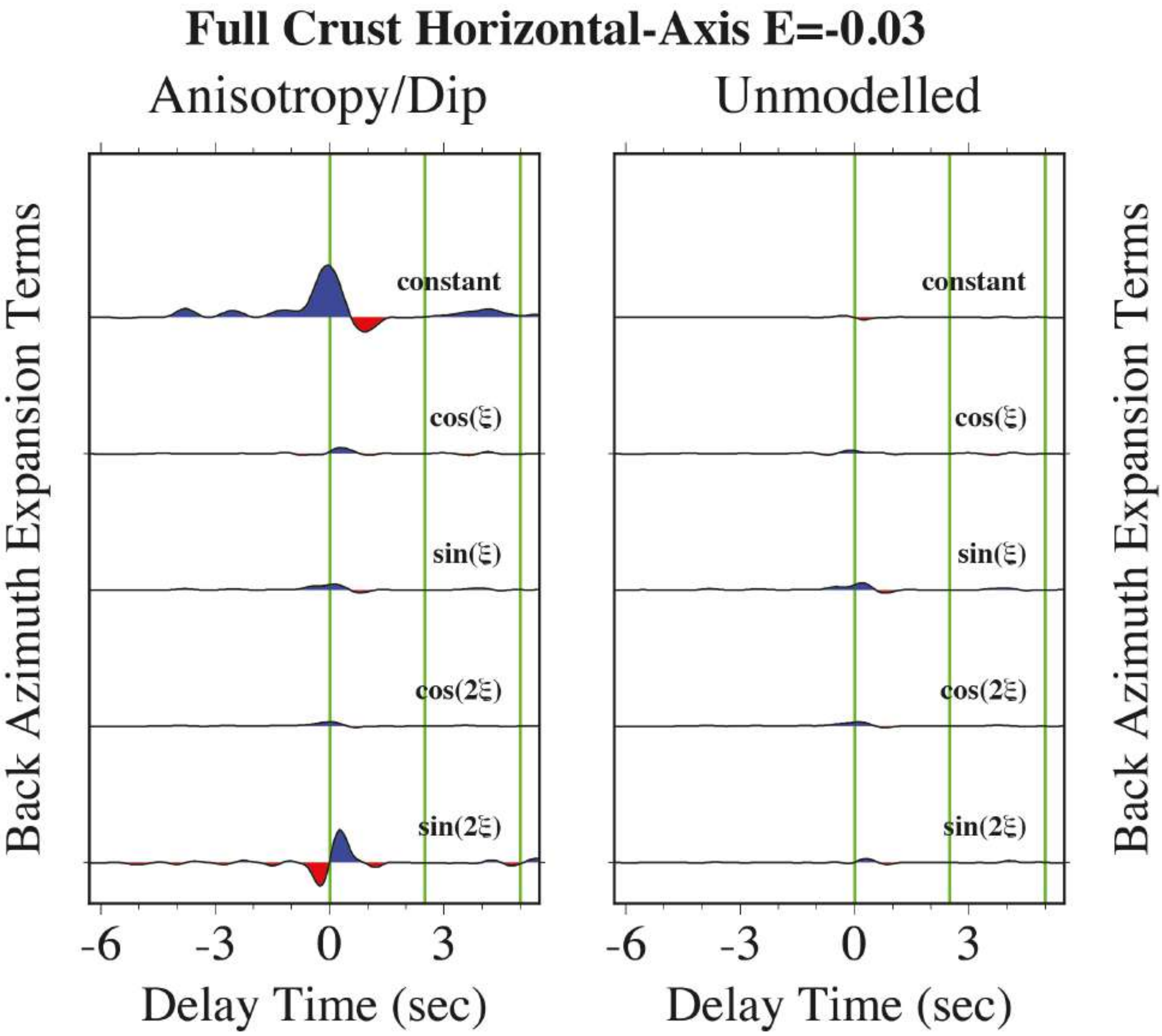

Figure S58. Harmonic terms of back azimuth ξ fit by least-squares in the frequency domain to receiver-functions estimated from synthetic seismograms in a 40-km crust with shear anisotropy E=-0.03 (3% peak-to-peak S anisotropy) with a horizontal slow symmetry axis in the full 40-km crust.

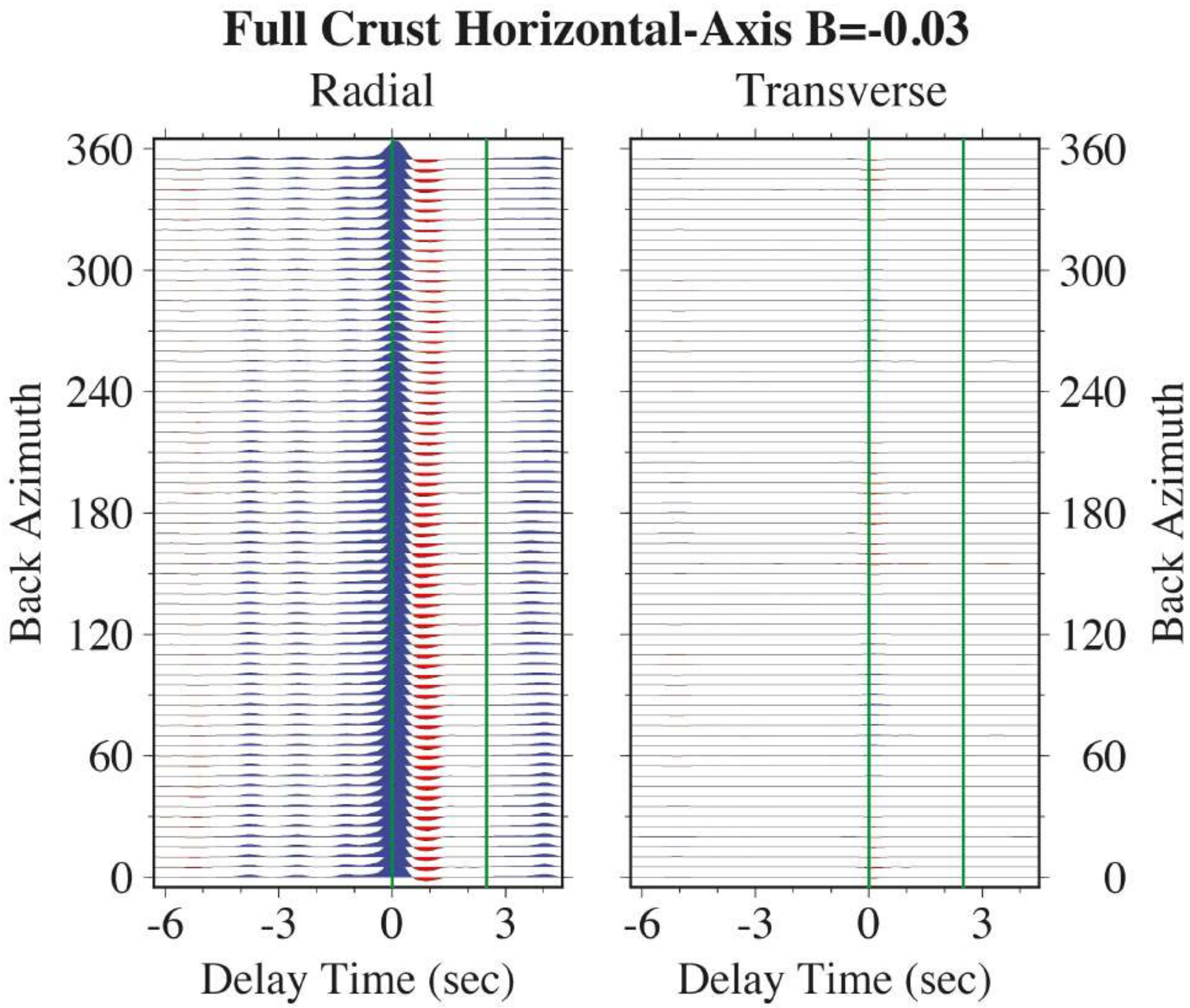

Figure S59. Back-azimuth receiver-function sweeps for synthetic seismograms in a 40-km crust with compressional anisotropy B=-0.03 (3% peak-to-peak P anisotropy) with a horizontal slow symmetry axis in the full 40-km crust.

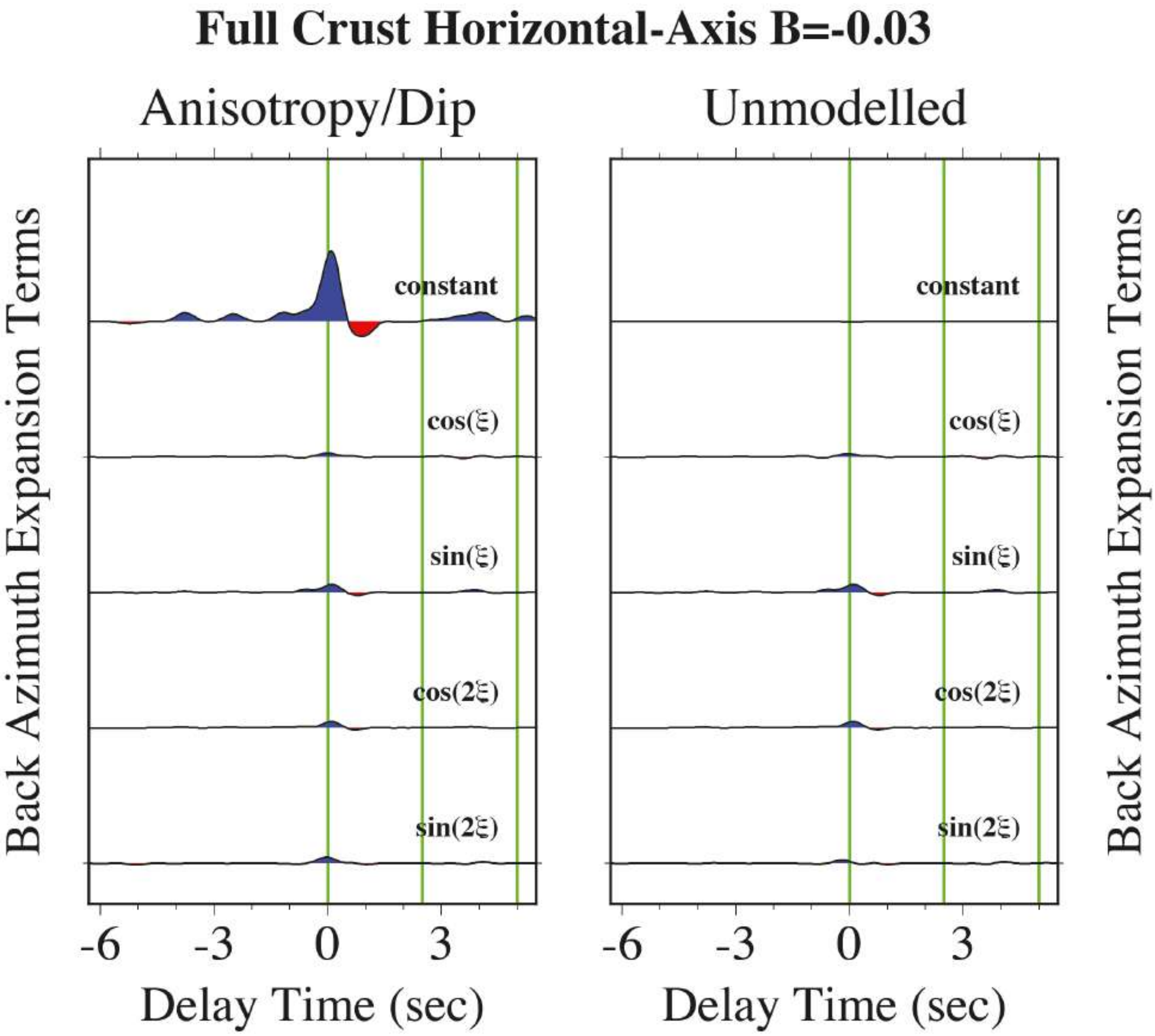

Figure S60. Harmonic terms of back azimuth ξ fit by least-squares in the frequency domain to receiver-functions estimated from synthetic seismograms in a 40-km crust with compressional anisotropy B=-0.03 (3% peak-to-peak P anisotropy) with a horizontal slow symmetry axis in the full 40-km crust.

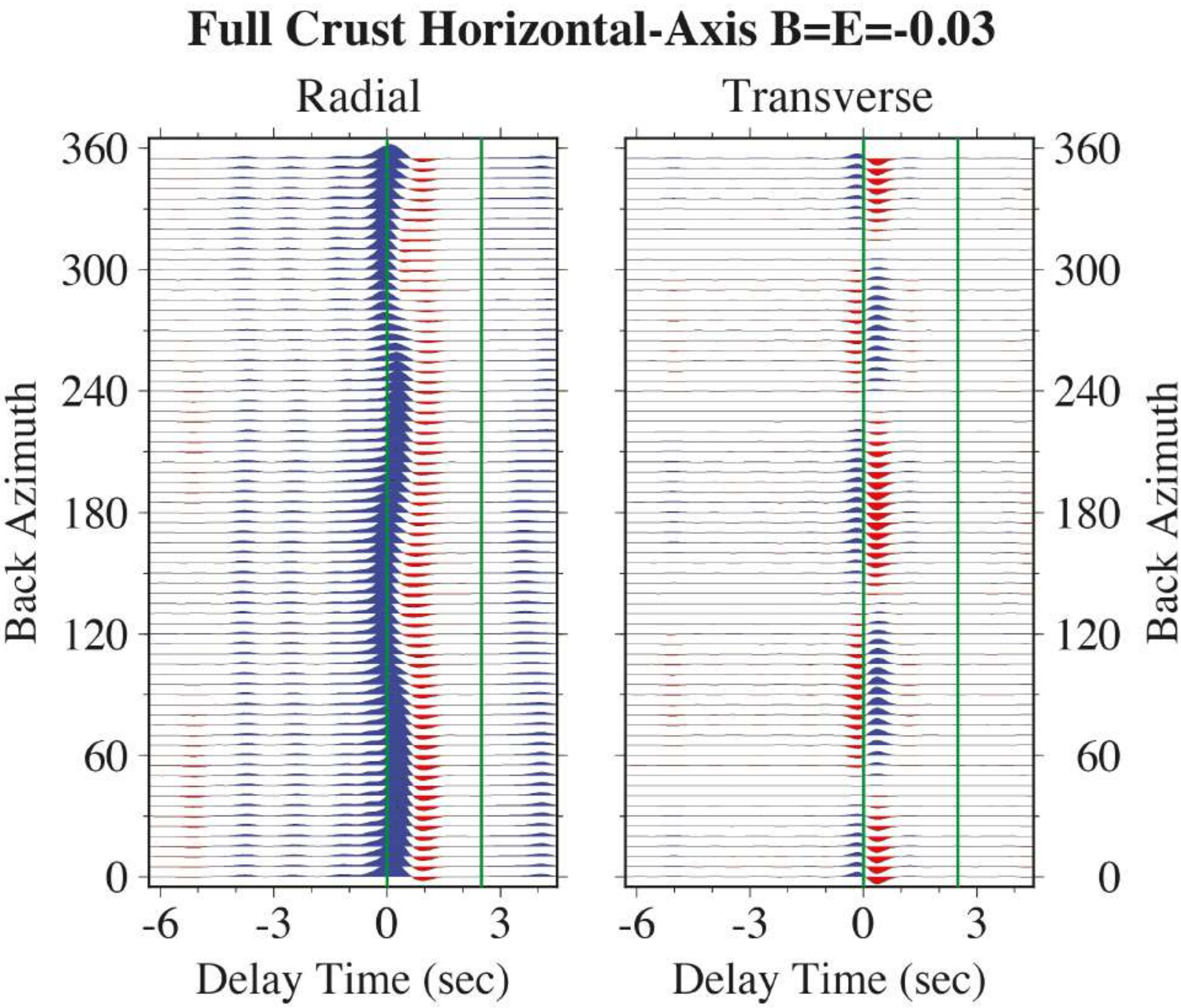

Figure S61. Back-azimuth receiver-function sweeps for synthetic seismograms in a 40-km crust with mixed anisotropy B=E=-0.03 (3% peak-to-peak P and S anisotropy) with a horizontal slow symmetry axis in the full 40-km crust.

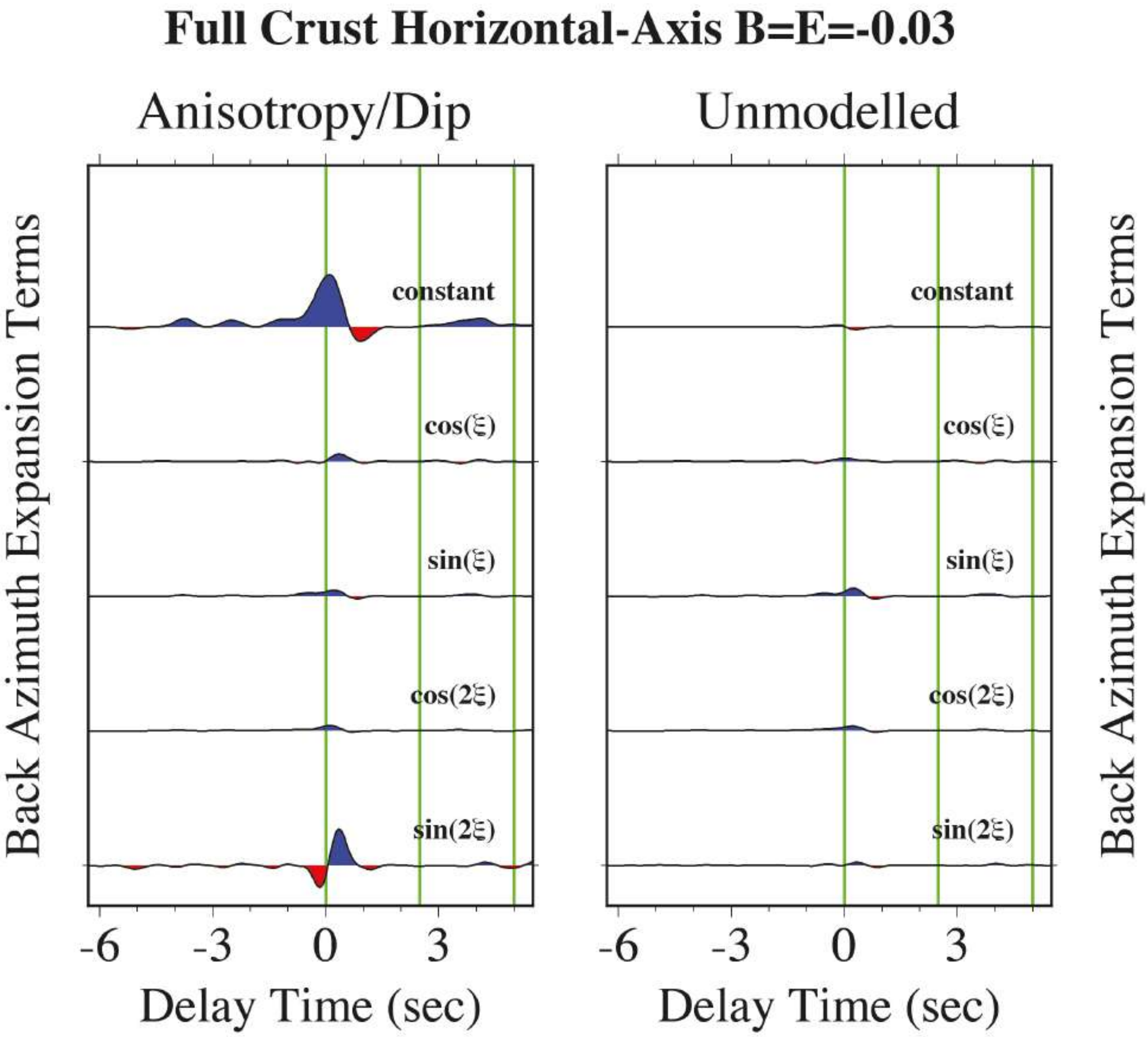

Figure S62. Harmonic terms of back azimuth ξ fit by least-squares in the frequency domain to receiver-functions estimated from synthetic seismograms in a 40-km crust with mixed anisotropy B=E=-0.03 (3% peak-to-peak P and S anisotropy) with a horizontal slow symmetry axis in the full 40-km crust.

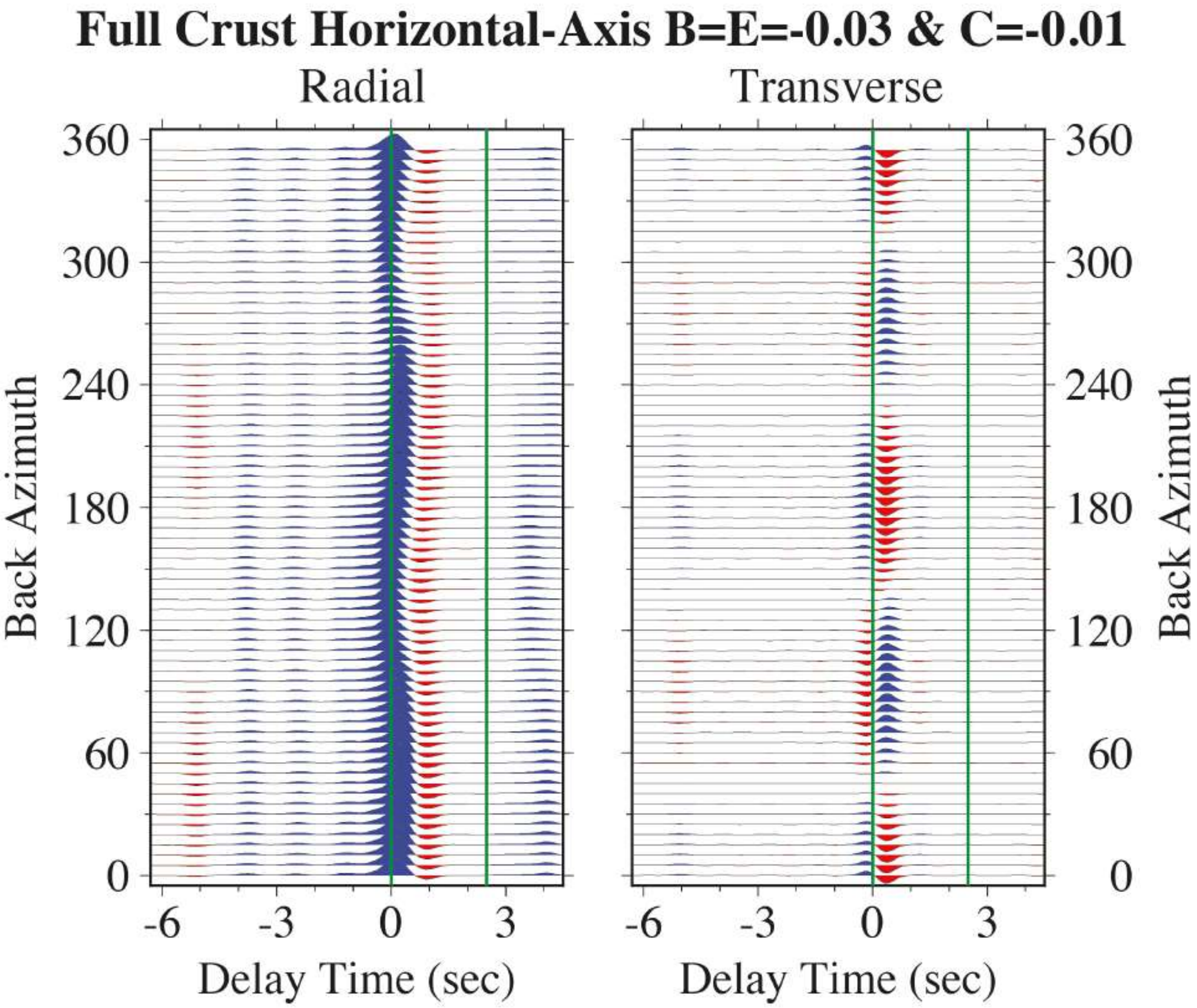

Figure S63. Back-azimuth receiver-function sweeps for synthetic seismograms in a 40-km crust with mixed anisotropy B=E=-0.03 and C=-0.01 with a horizontal slow symmetry axis in the full 40-km crust. This corresponds to 3% peak-to-peak elliptical P and S anisotropy, plus a cos 4ξ wavespeed variation consistent with Brownlee et al (2017).

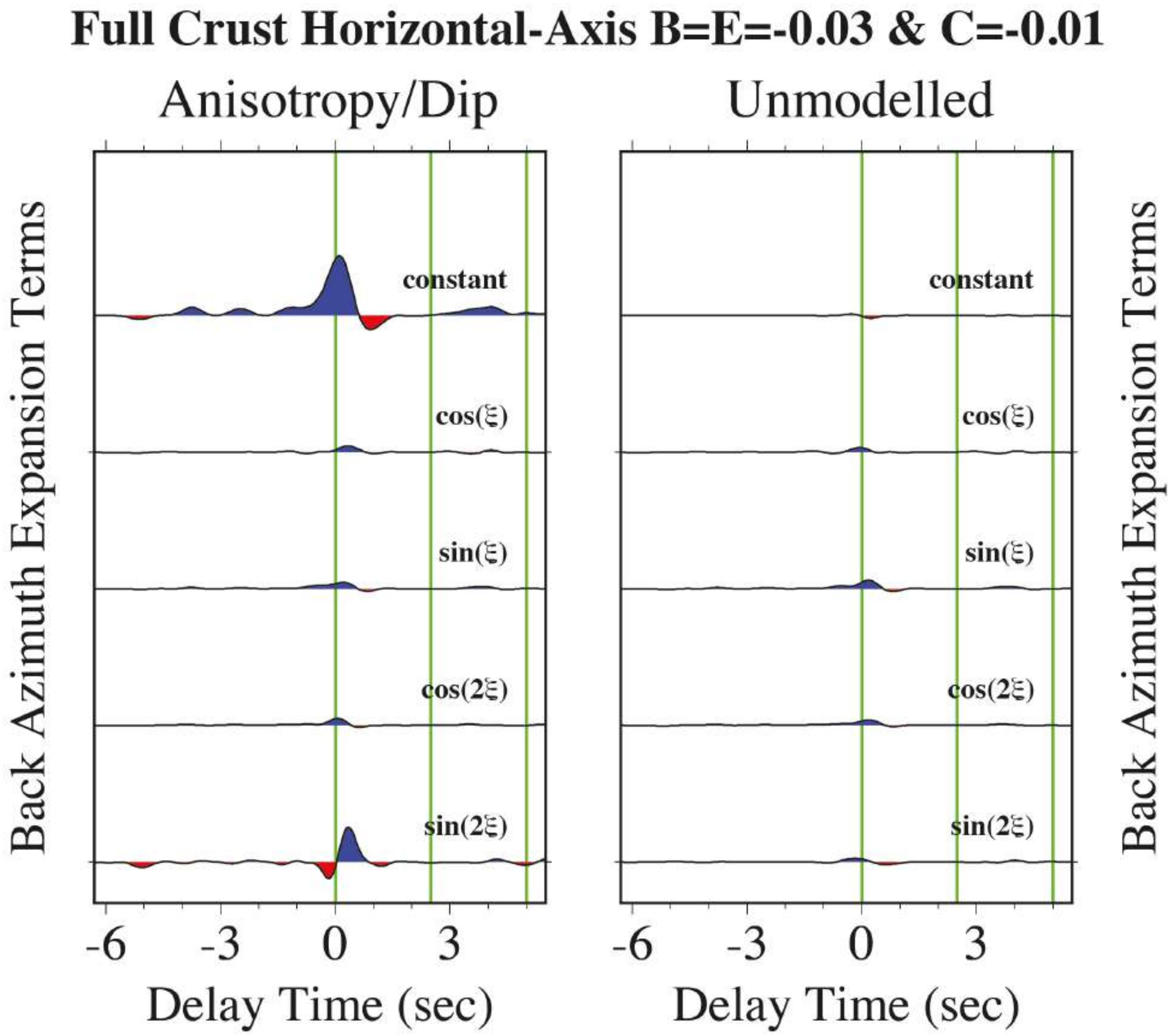

Figure S64. Harmonic terms of back azimuth ξ fit by least-squares in the frequency domain to receiver-functions estimated from synthetic seismograms in a 40-km crust with mixed anisotropy B=E=-0.03 and C=-0.01 with a horizontal slow symmetry axis in the full 40-km crust. This corresponds to 3% peak-to-peak elliptical P and S anisotropy, plus a cos 4ξ wavespeed variation consistent with Brownlee et al (2017).

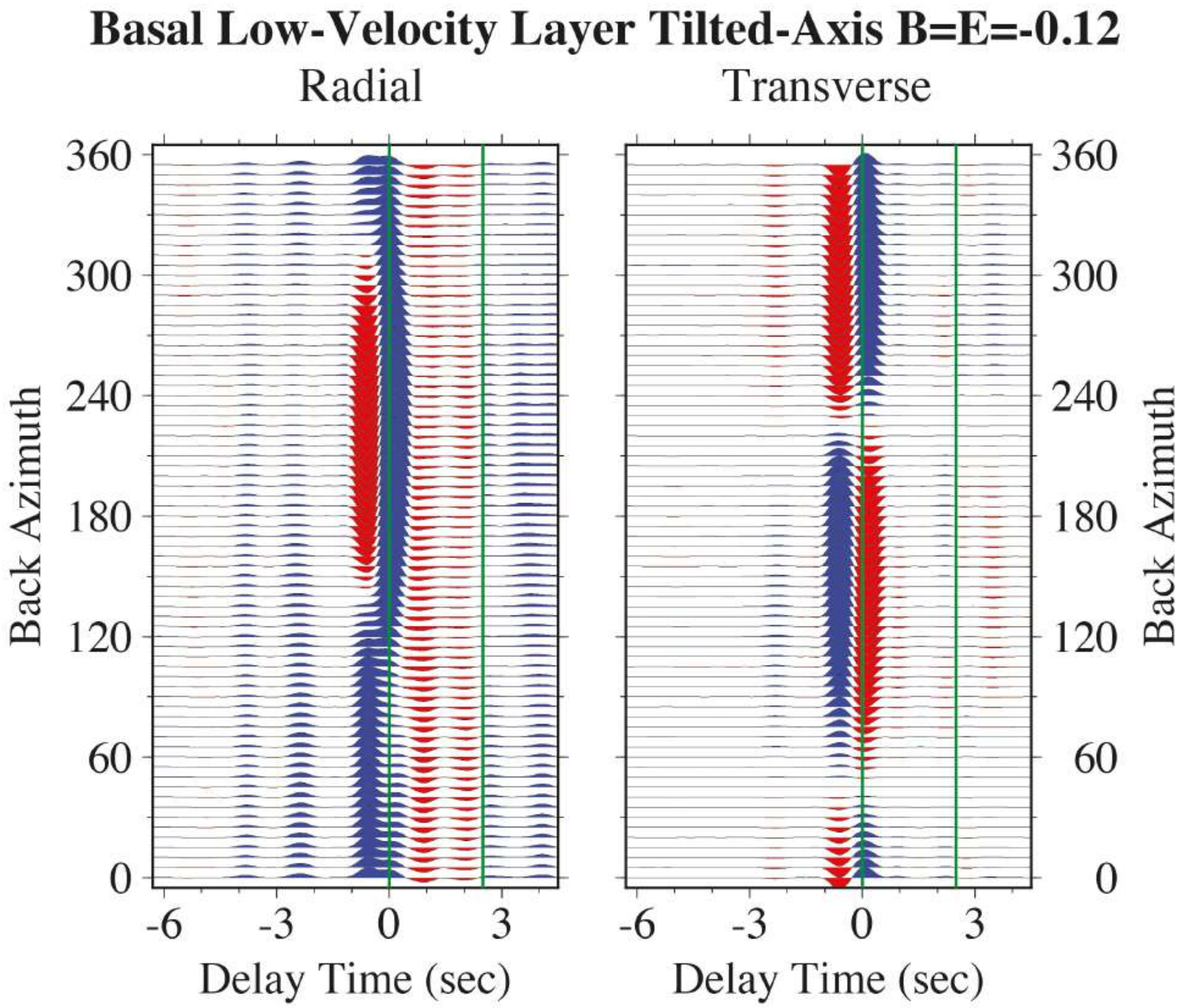

Figure S65. Back-azimuth receiver-function sweeps for synthetic seismograms in a 40-km crust with mixed anisotropy B=E=-0.12 (12% peak-to-peak P and S anisotropy) with a slow symmetry axis with 45° tilt in a basal low-velocity layer at 35-40-km depth, see Figure 11.

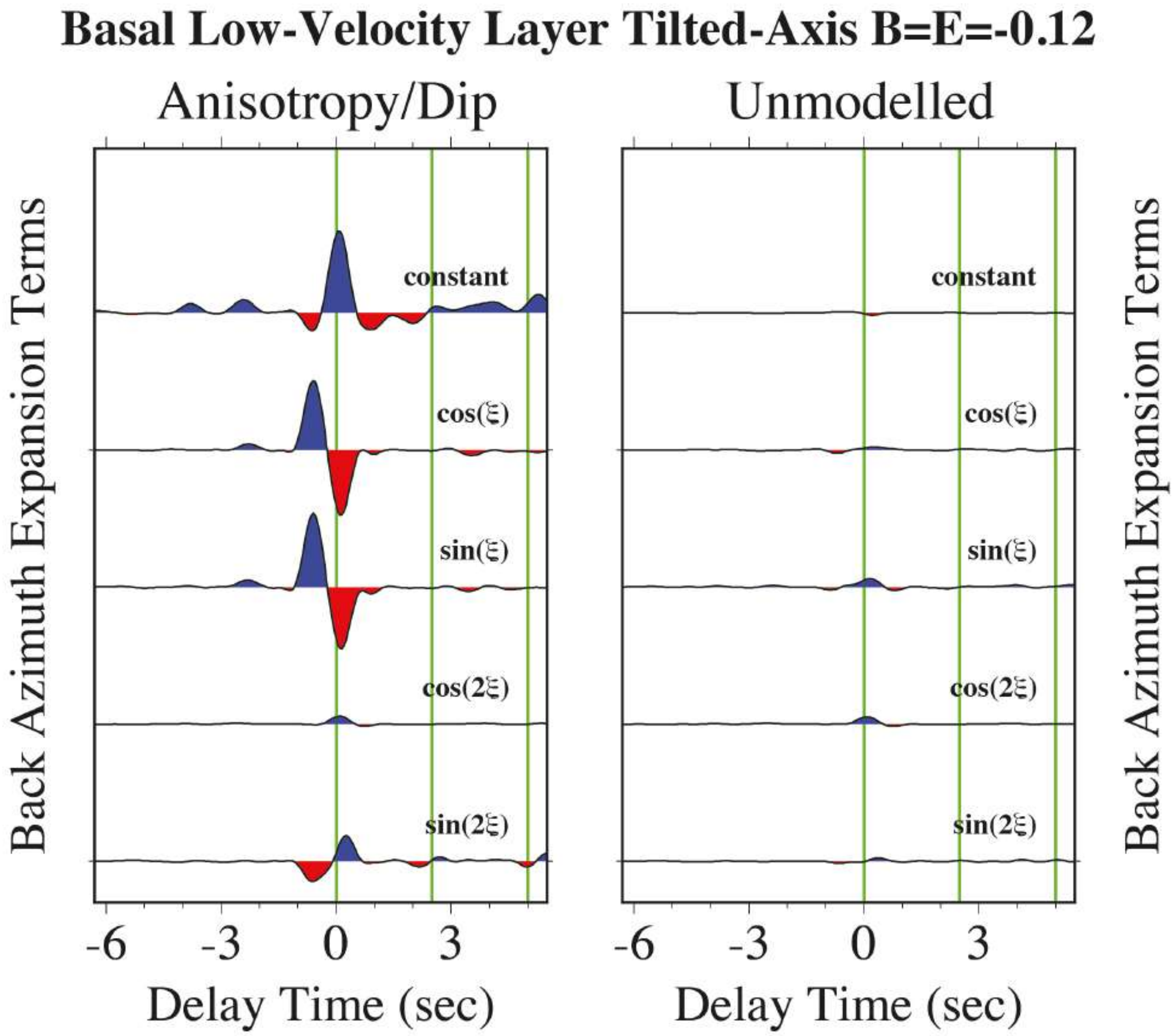

Figure S66. Harmonic terms of back azimuth ξ fit by least-squares in the frequency domain to receiver-functions estimated from synthetic seismograms in a 40-km crust with mixed anisotropy B=E=-0.12 (12% peak-to-peak P and S anisotropy) with a slow symmetry axis with 45° tilt in a basal low-velocity layer at 35-40-km depth, see Figure 11.

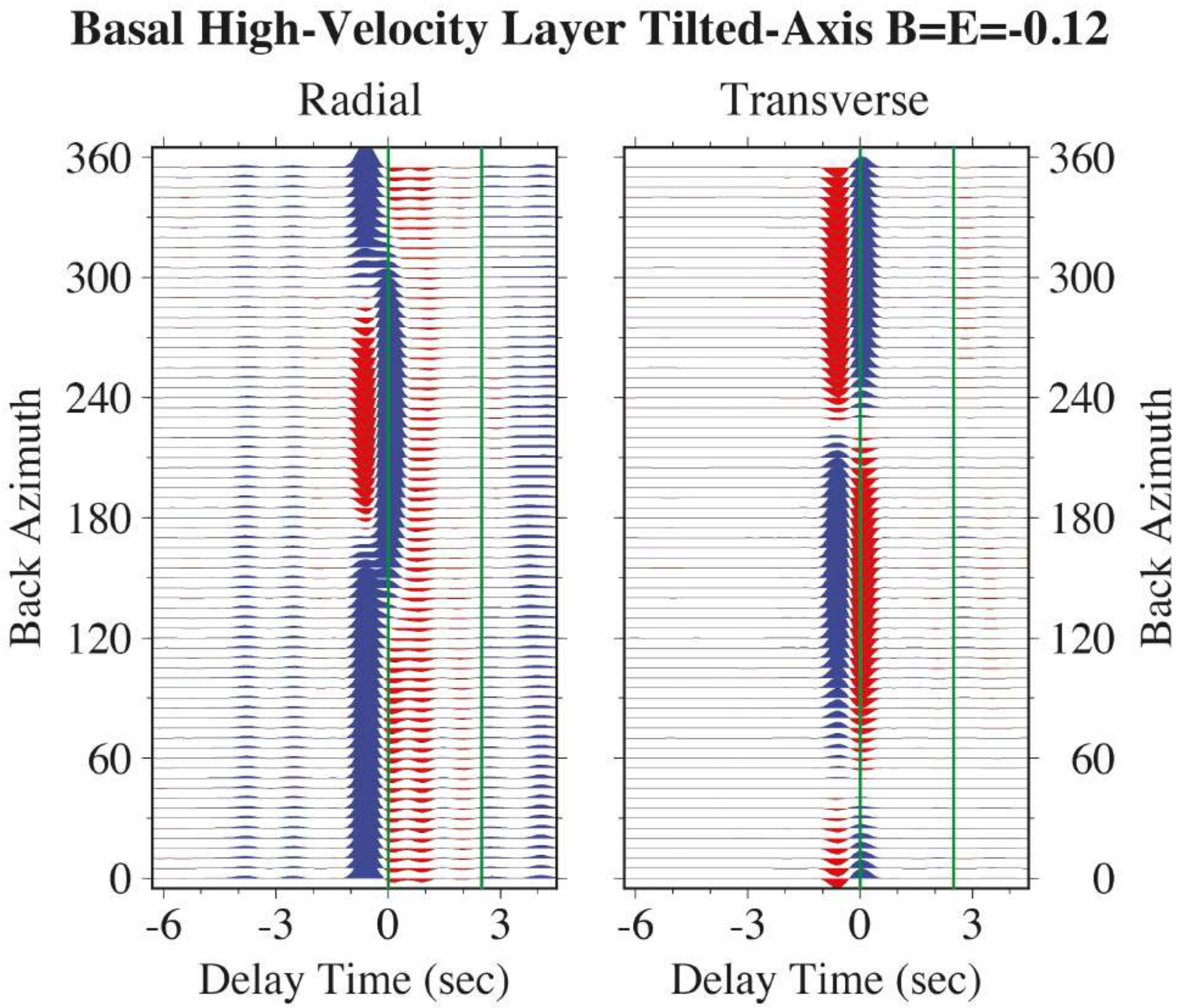

Figure S67. Back-azimuth receiver-function sweeps for synthetic seismograms in a 40-km crust with mixed anisotropy B=E=-0.12 (12% peak-to-peak P and S anisotropy) with a slow symmetry axis with 45° tilt in a basal high-velocity layer at 35-40-km depth, see Figure 11.

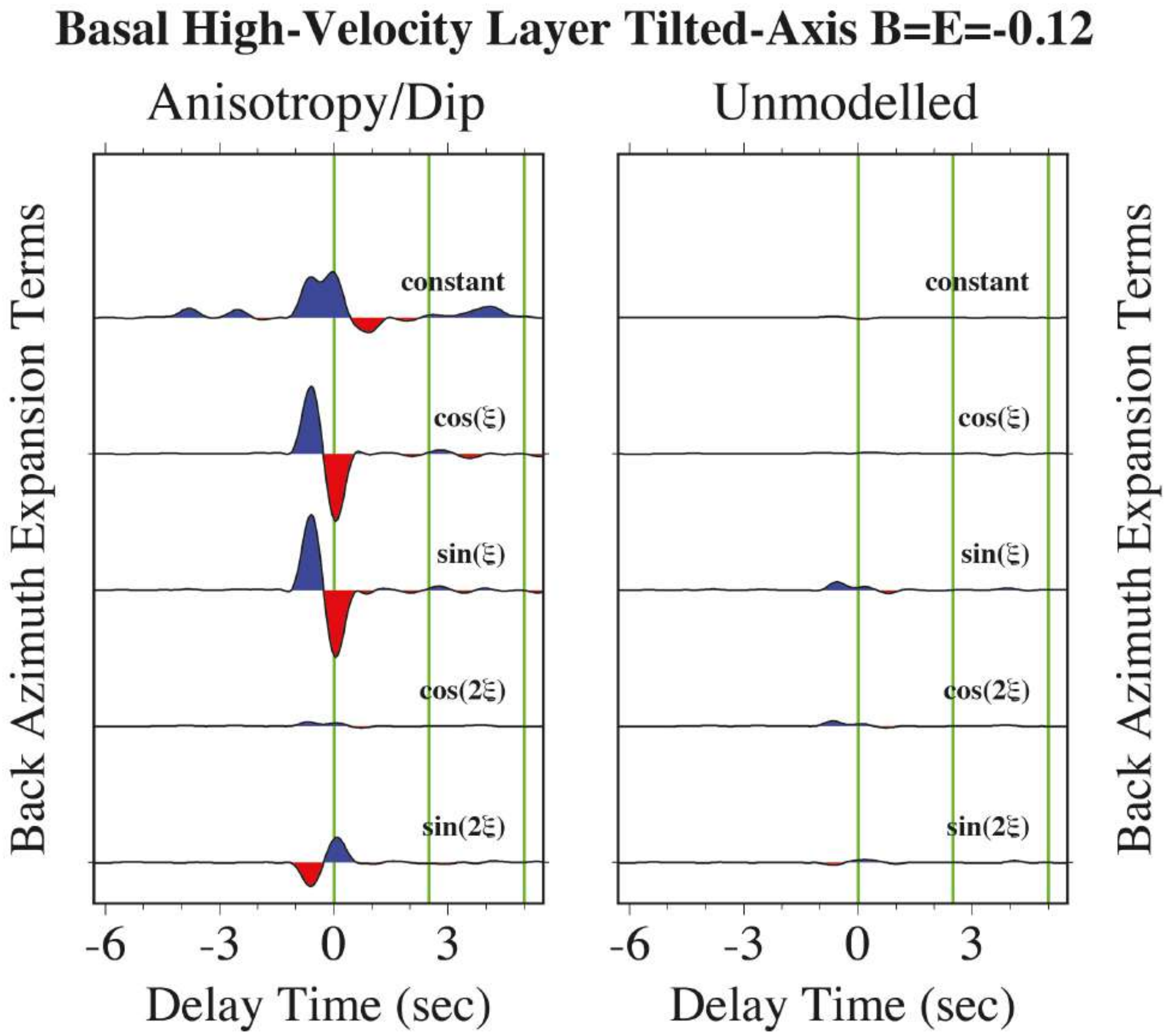

Figure S68. Harmonic terms of back azimuth ξ fit by least-squares in the frequency domain to receiver-functions estimated from synthetic seismograms in a 40-km crust with mixed anisotropy B=E=-0.12 (12% peak-to-peak P and S anisotropy) with a slow symmetry axis with 45° tilt in a basal high-velocity layer at 35-40-km depth, see Figure 11.

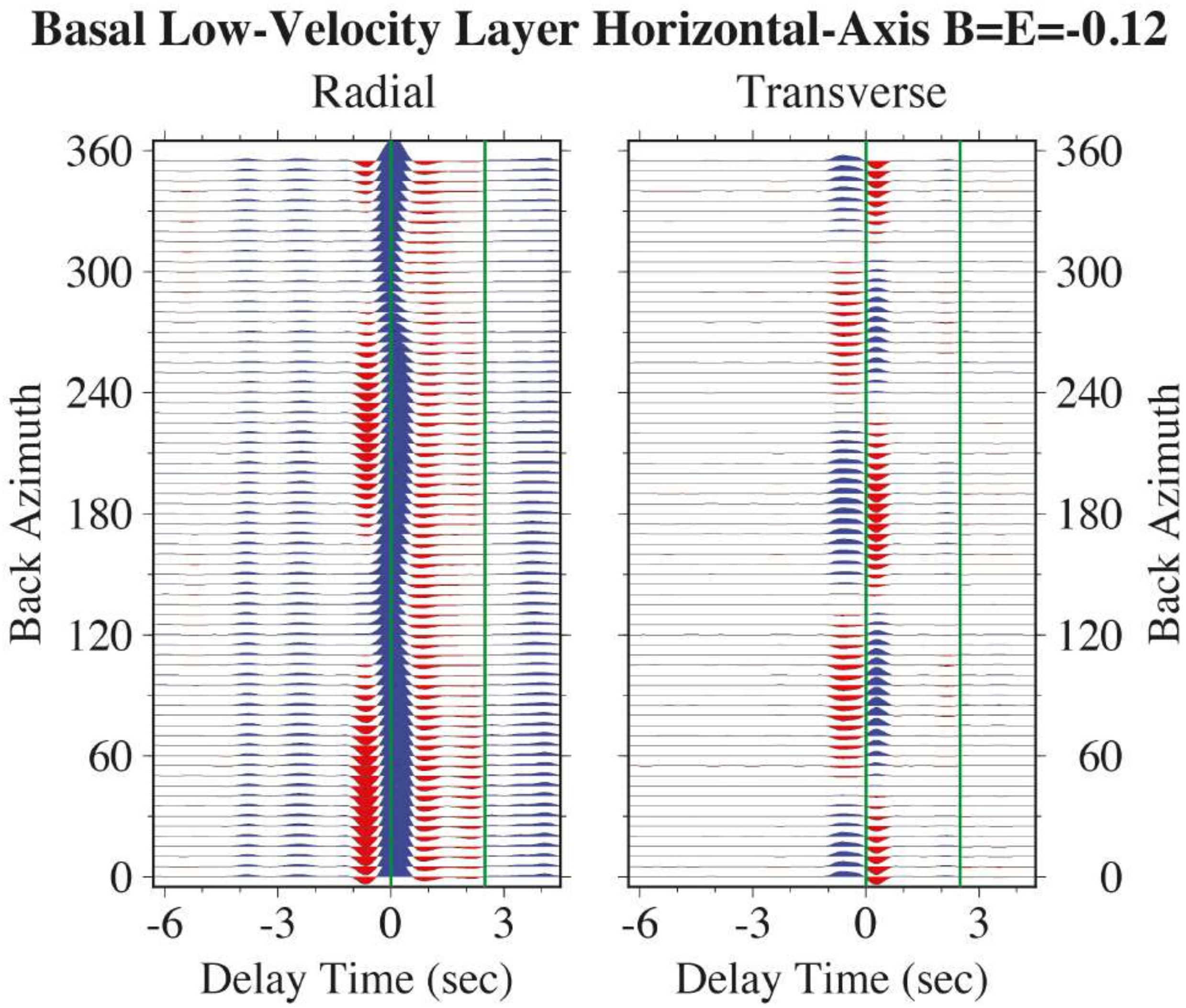

Figure S69. Back-azimuth receiver-function sweeps for synthetic seismograms in a 40-km crust with mixed anisotropy B=E=-0.12 (12% peak-to-peak P and S anisotropy) with a horizontal slow symmetry axis in a basal low-velocity layer at 35-40-km depth, see Figure 11.

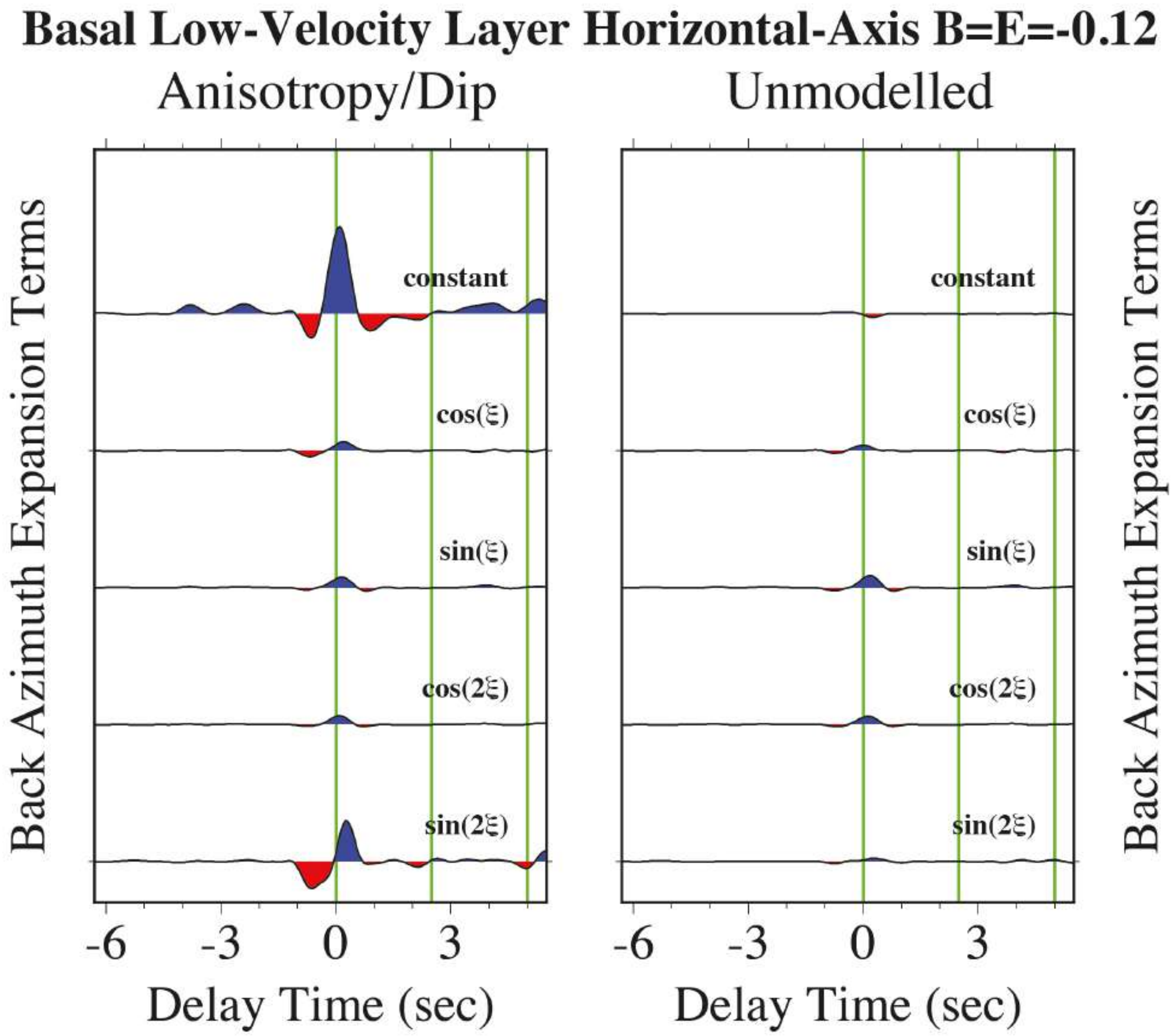

Figure S70. Harmonic terms of back azimuth ξ fit by least-squares in the frequency domain to receiver-functions estimated from synthetic seismograms in a 40-km crust with mixed anisotropy B=E=-0.12 (12% peak-to-peak P and S anisotropy) with a horizontal slow symmetry axis in a basal low-velocity layer at 35-40-km depth, see Figure 11.

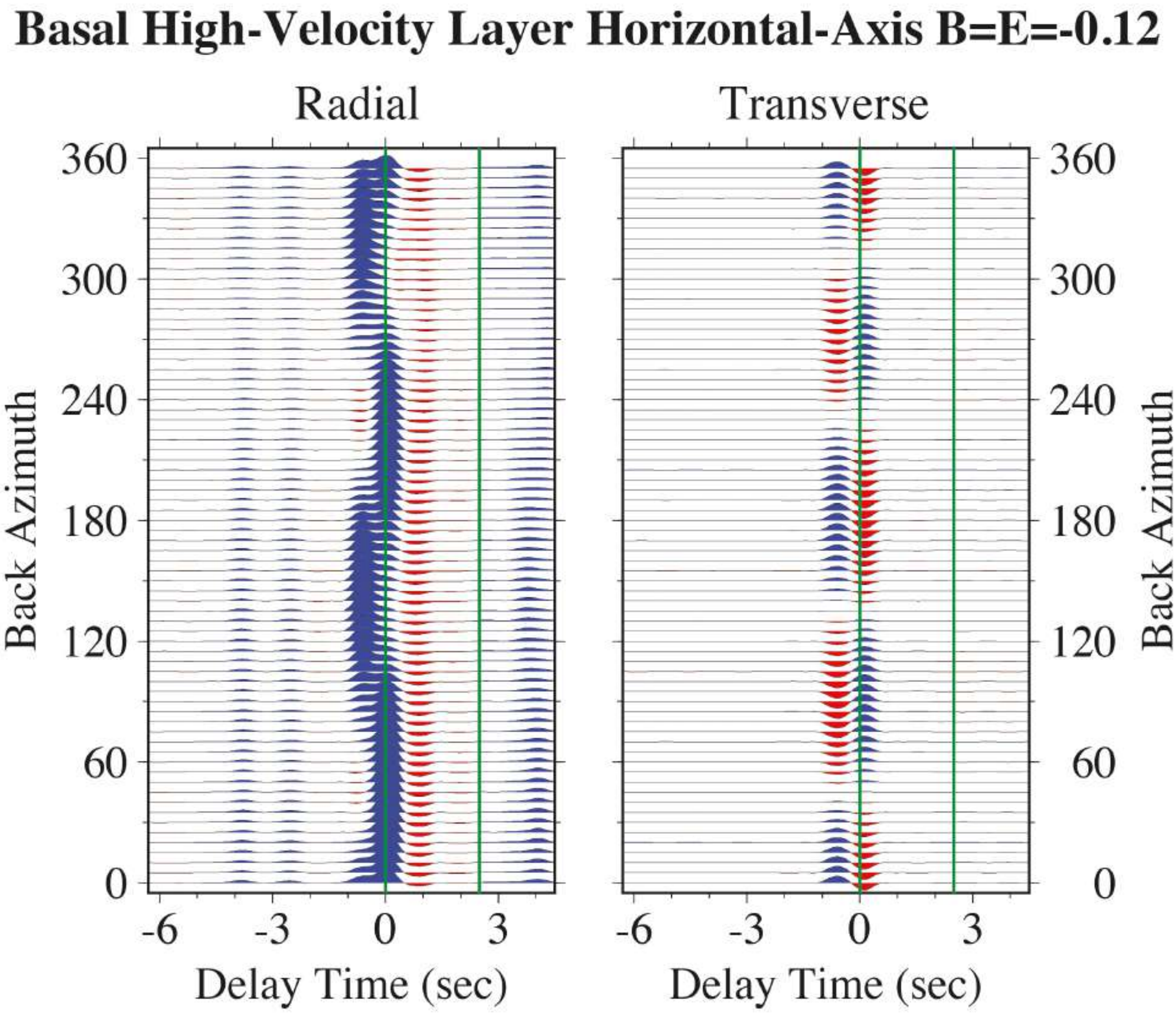

Figure S71. Back-azimuth receiver-function sweeps for synthetic seismograms in a 40-km crust with mixed anisotropy B=E=-0.12 (12% peak-to-peak P and S anisotropy) with a horizontal slow symmetry axis in a basal high-velocity layer at 35-40-km depth, see Figure 11.

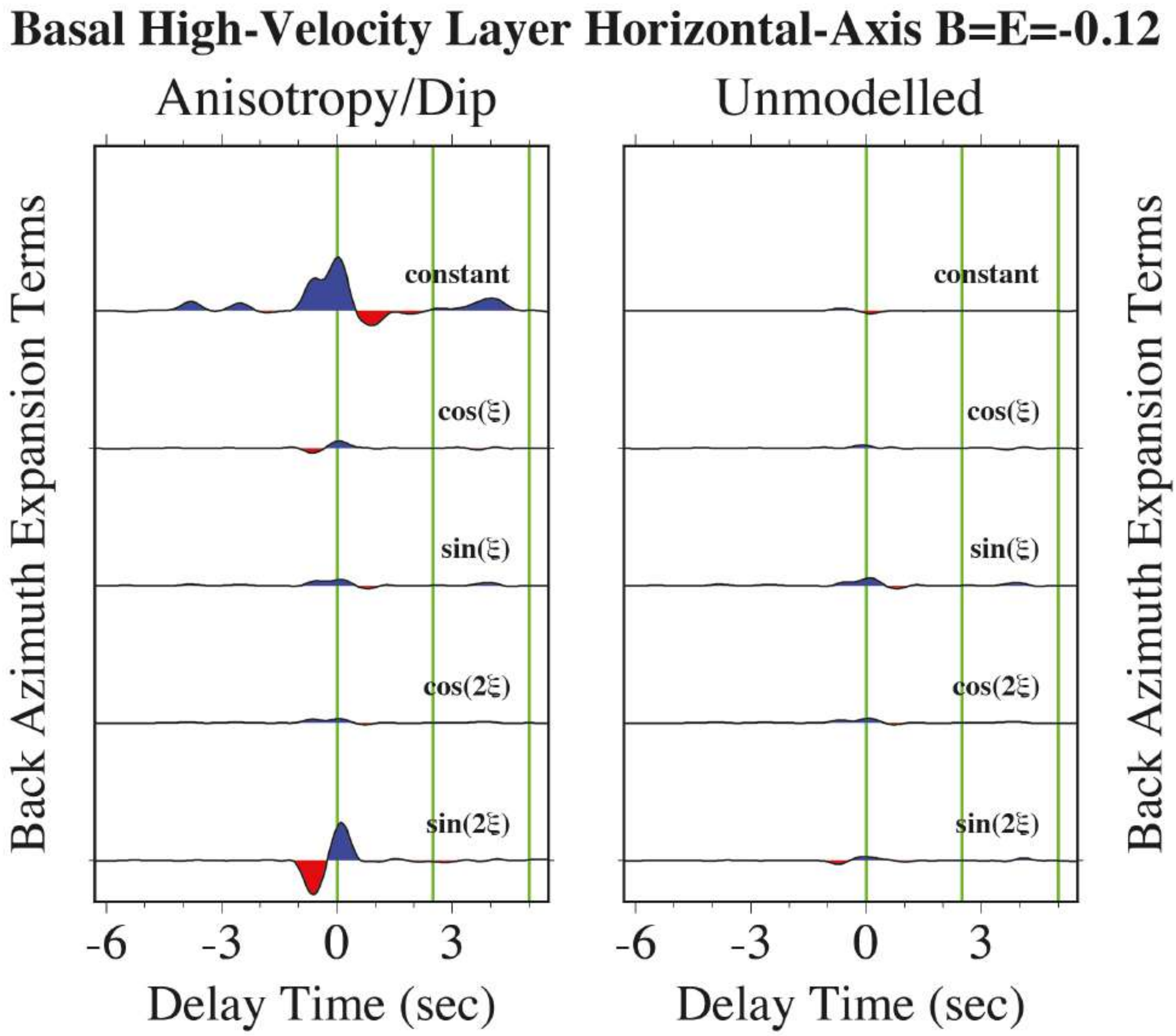

Figure S72. Harmonic terms of back azimuth ξ fit by least-squares in the frequency domain to receiver-functions estimated from synthetic seismograms in a 40-km crust with mixed anisotropy B=E=-0.12 (12% peak-to-peak P and S anisotropy) with a horizontal slow symmetry axis in a basal high-velocity layer at 35-40-km depth, see Figure 11.